SVEUČILIŠTE U ZAGREBU

PRIRODOSLOVNO-MATEMATIČKI FAKULTET

GEOFIZIČKI ODSJEK

AMELA JERIČEVIĆ

PARAMETERIZATION OF VERTICAL DIFFUSION IN AN ATMOSPHERIC CHEMICAL MODEL

DOKTORSKA DISERTACIJA

DOCTORAL THESIS

ZAGREB, 2009.

SVEUČILIŠTE U ZAGREBU
PRIRODOSLOVNO-MATEMATIČKI FAKULTET
GEOFIZIČKI ODSJEK

Amela Jeričević

Parameterization of vertical diffusion in an atmospheric chemical model

Doktorska disertacija
predložena Geofizičkom odsjeku
Prirodoslovno-matematičkog fakulteta Sveučilišta u Zagrebu
radi stjecanja akademskog stupnja
doktora prirodnih znanosti fizike

Doctoral Thesis
Submitted to the Department of Geophysics
Faculty of Science, University of Zagreb
for the academic degree of
Doctor of natural sciences (Physics)

Zagreb, 2009.

This Thesis is elaborated at Meteorological and Hydrological Service, Croatia, supervised by Prof. dr. sc. Branko Grisogono.

The last three years have been very active working on my PhD in collaboration with colleagues from the Norwegian Meteorological Institute in the framework of the EMEP4HR project. It was a lot of work, expectations and goals were very high and there was a moment when I thought that it would be impossible to fulfil all the requirements. Luckily, I have managed it. I need to thank for that to my supervisor Branko Grisogono firstly on his management skills inserted into coordination of my scientific work, on his shared knowledge, but most of all I have to thank him for having a lot of understanding, patience and being very supportive. Sonja Vidič is responsible for implementation of the international project and I am thankful for her vision and all the positive energy involved in the construction of a strong working framework. This journey was accompanied by my colleague Lukša Kraljević who I admire for his skills and dedication to the working tasks, but above all for being opened for many discussions. Hilde from the Met. No. is thanked for shared knowledge about the atmospheric chemical modelling, for correcting many of my misconceptions and for preparation of a wonderful Norwegian meal. Work with Željko on LES was interesting and opened a field for future work that I am looking forward to. Dave Simpson is thanked for a constructive criticism and intensive collaboration and above all for willingness to take an important part in the realisation of my PhD. Leonor Tarrason is an inspirational person and she took an important role in my work. Zvjezdana Bencetić Klaić was also involved as a co supervisor and I am thankful for collaboration on different papers. Domagoj is thanked for shared knowledge about statistics (and for the sailing adventure).

Nothing of this would be possible without the endless support of my family. My dearest Zvone, Dino and Marin.

Contents

1. Introduction

1.1 Overview

Air quality models are nowadays recognized as an important tool for air quality assessment. Although measurements are the basis of air quality assessment, there are several advantages provided by numerical models: high spatial and temporal resolution of simulated data, forecasting of air quality as a result of changes in emissions or/and meteorological conditions and a better understanding of the physical processes affecting the fate of pollutants in the atmosphere. For nearly 30 years, the European Monitoring and Evaluation Programme (EMEP) under the Convention on Long-Range Transboundary Air Pollution (LRTAP), has been responsible for development of air quality modelling systems to support the design of the environmental control strategies in Europe. The Unified EMEP model (Simpson et al., 2003) was developed and used to simulate transboundary transport of air pollution on the European scale. Recently, special applications of the model have been developed at higher resolutions and coupled with different meteorological drivers: EMEP4UK (e.g. Vieno et al., 2009; Vieno et al., submitted), and EMEP4HR (Jeričević et al., 2007; Kraljević et al., 2008). Development of the EMEP model includes detailed meteorological effects that become progressively more important on the finer spatial scale, such as turbulence and convection generated by a complex terrain. Turbulence parameterizations, particularly schemes for calculation of vertical diffusion coefficients $K(z)$, need to be tested as a first step of the EMEP model development on a finer horizontal scale.

Previous studies have already shown that the parameterizations of $K(z)$ have significant impacts on simulated chemical concentrations (e.g. Nowacki et al., 1996; Biswas and Rao, 2000; Oliviè et al., 2004). Different parameterizations for $K(z)$, depending on the stability in the atmospheric boundary layer (ABL), have been proposed (e.g. O'Brien, 1970; Deardorff, 1972; Louis, 1979; Holtslag and Moeng, 1991; Holtslag and Boville, 1993; Grisogono, 1995). O'Brien suggested a simple parameterization $K(z)$ scheme used in many air quality models ranging from simple 1D models (e.g. Lee and Larsen, 1997) towards application as in complex chemical models e.g. Comprehensive Air Quality Model with Extensions (CAMx, http://www.camx.com/; ENVIRON, 1998; Zhang et al., 2004), and the EMEP model (Fagerli and Eliassen, 2002). In CAMx there are a few $K(z)$ parameterization schemes, with the O'Brien scheme as one of the options. Presently, in the EMEP model the O'Brien scheme is used for the convective boundary layer (CBL), while in the stable boundary layer (SBL) conditions $K(z)$ based on Monin - Obukhov (M-O; Monin and Obukhov, 1954) similarity theory is applied. In this work the operational $K(z)$ scheme has been called OLD scheme. There are many studies which show that the surface-layer formulations based on the M-O theory are often not applicable in the statically stable conditions (e.g. Mahrt, 1999; Pahlow et al., 2001; Poulos and Burns, 2003; Mauritsen et al., 2007; Grisogono et al., 2007). A new proposed scheme, called Grisogono, is implemented in the model and it is not based on the M-O similarity theory. The Grisogono scheme uses a exponentially decaying profile, generalizing the O'Brien third-order polynomial $K(z)$ into an analytic function which depends on only two parameters (Grisogono and Oerlemans, 2001 and 2002). It has already been shown on Large Eddy Simulation (LES) and the experimental data sets that the Grisogono method performs better than the O'Brien's polynomial, especially in stable conditions (Jeričević and Večenaj, 2009).

Special emphasis is given to the ability of the ABL height scheme to capture the vertical transport and dispersion of atmospheric air pollution. A significant influence of the ABL height (H) on various pollutants has often been found e.g. on the surface nitrogen oxide (NO_x) and the particulate matter (PM) concentrations in urban and suburban areas e.g. Schäfer et al., (2006), while Athanassiadis et al., (2002) show that an accurate H determination is needed to properly simulate pollutant levels with grid-based photochemical models. Furthermore, H is explicitly included in the both EMEP $K(z)$ parameterizations. Therefore it is important to evaluate the EMEP model ability to simulate the spatial and temporal variability of H. The operational (e.g. Jakobsen et al., 1995; Seibert et al., 2000) and a new ABL height scheme based on the bulk Richardson number (Ri_B) are evaluated. The Ri_B method is a standard and widely used approach to derive H from the numerical weather prediction (NWP) models, as well as from the radiosounding data (e.g. Mahrt, 1981; Troen and Mahrt, 1986, Sørensen et al., 1996; Fay et al., 1997; Seibert et al. 2000; Zilitinkevich and Calanca, 2000; Zilitinkevich and Baklanov, 2002; Gryning and Batchvarova, 2002; Jeričević, 2005; Jeričević and Grisogono, 2006).

This work provides an evaluation of the $K(z)$ schemes on the LES data prior to the application in the EMEP model. Following, the operational version of the EMEP model and the version with new parameterization schemes (i.e. $K(z)$ and ABL schemes) are verified by comparing one full year of the modelled data against the corresponding set of observed daily surface NO_2, SO_2 and

SO_4^{2-} concentrations from different EMEP stations in Europe (Jeričević et al., 2009). Furthermore, simulations of the Radon 222 (^{222}Rn) concentrations are performed during years 2005 and 2006 in order to evaluate the vertical mixing schemes, the performance of the EMEP model and to investigate the local and non-local effects of different $K(z)$ schemes (Jeričević et al., in preparation). The simulated hourly ^{222}Rn concentrations are compared to the available ^{222}Rn measurements in Europe, i.e. the Cabauw tower in Netherlands, the Angus tower in Scotland, Freiburg and Schauinsland in Germany and Krakow in Poland. Since radionuclide ^{222}Rn has a half-life of 3.8 days and it is emitted primarily from the continents at a fairly constant emission rate of about 1 atom cm^{-2} s^{-1} (Liu et al., 1984; Conen and Robertson, 2002) , it is ideal to study the model sub-grid mixing schemes, numerical advection schemes or to compare different models. A considerable number of global and regional studies have been devoted to the simulation of ^{222}Rn for different purposes (e.g. Allen et. al., 1996; Lee and Larsen, 1997; Petersen et. al. 1998; Dentener et. al. 1999; Oliviè et al., 2004; Josse et al., 2004; Galmarini, 2006; Vinuesa and Galmarini, 2007). In addition to the non-local schemes, the O'Brien and Grisogono, a new scheme which is a local and based on total turbulent energy (TTE) closure (e.g., Mauritsen et. al, 2007) has been implemented in the EMEP model and evaluated (Jeričević et al., in preparation). Based on all those evaluations, uncertainties (both in the measurements and in the model) are established. Pronounced differences between the performances of the three model versions and impacts on the simulated concentrations are investigated and recommendations for future work are provided.

1.2 Air quality modelling in Croatia

Development of the air quality modelling in Croatia started at the Croatian Meteorological and Hydrological Service (MHSC) during 1980's with the application of the dispersion models based on the Gaussian plume model (Šinik, 1981; Vidič, 1981, 1989; Šinik et al., 1984). Gaussian models were used in many environmental impact studies conducted at MHSC as well as for research purposes (Špoler and Jeričević, 2005). Furthermore lagrangian box model has been used at the Andrija Mohorovičić Geophysical Institute (AMGI) in several studies of long-range transport of sulphur (Klaić, 1990; 1996; 2003; Klaić and Beširević, 1998). The first version of Atmospheric Lagrangian Particle Stochastic (ALPS) model was created as an exercise during a graduate course at the AMGI, under the guidance of Prof. D. Koračin (Belušić et al., 2004; Kos et al., 2004). The ALPS is a Lagrangian random particle model that is based on statistical approach by modelling the randomness of the trajectories of fluid elements. The aim of that research was to introduce students to the problem of numerical modelling by combining education and research. ALPS was created using a basic algorithm of Langevin equation models as presented in Koračin et al. (1998, 1999). The challenge was in finding solutions for using available meteorological model data, choosing turbulence representation, dealing with interpolation within the grid, reflection at the boundaries, etc. Trajectory simulations have also been used for different scientific research purposes (e.g., Klaić and Cvitan 1993; Peljto and Klaić, 1999-2000; Bešlić et al., 2008). However, systematic development of air quality modelling in Croatia is conducted within the Environmental Modelling and Evaluation Programme for Croatia (EMEP4HR) project. The EMEP4HR project is a joint project of Norwegian and Croatian meteorological services, University of Zagreb and Energy Research and Environmental Protection Institute (EKONERG) that started in 2006, and is due to last until 2010. In particular, the main objectives of this project involve:

- the development of high resolution emission inventories of air pollutants in Croatia and in selected urban areas,
- the implementation and further development of a mesoscale version of the Eulerian EMEP Unified chemical transport model coupled with the Aire Limitée Adaptation dynamique Développement InterNational (ALADIN), numerical weather prediction model (Geleyn et al., 1992), and the Weather Research and Forecasting (WRF) model (Skamarock et al., 2005),
- the development of a new capability for the assessment of urban air quality in main Croatian cities,
- the evaluation and testing of the new modelling capability according to international standards.

The project will allow for a stable long-term development of Croatia's scientific capacity to support the design of environmental protection strategies. Applications of the EMEP and EMEP4HR model have already been provided in the Rijeka area, the most industrially developed part of Croatia, during the severe SO_2 episode (Prtenjak et al., 2009).

The goal of this work is to improve the understanding of turbulent processes and their effects in the atmospheric chemical models by validating the performance of various vertical diffusion parameterization schemes, as well as the boundary layer height schemes against different data sets.

2. Model and data description

2.1 FLOSSII and CASES-99 data

Composite vertical profiles for the two datasets, Fluxes over Snow-covered Surfaces II (FLOSSII) and Cooperative Atmosphere – surface Exchange Study - 1999 (CASES-99), analyzed by Mahrt and Vickers (2006), were used. In FLOSSII, which took place from 1 December 2002 to 31 March 2003 in the North Park Basin of north-west Colorado, U.S.A. the 30-m tower provided seven levels of nocturnal eddy-correlation data over a grass surface, sometimes partially or completely snow covered. In CASES-99 one month of eddy-correlation data from a 60-m tower with seven levels of eddy-correlation data over grassland in south central Kansas, U.S.A was also analyzed. In their work authors categorize eddy diffusivities computed from class-averaged heat flux and along-wind momentum flux, and corresponding vertical gradients, according to weak and strong turbulence classes. Both classes correspond to stable stratification with different turbulence intensity; from very weak turbulence to the stronger turbulence stable cases. Threshold values for definition of cases were imposed on the fine-scale velocity variance averaged over one hour and than averaged over the tower layer for FLOSII and CASES - 99 (Table I; Mahrt and Vickers, 2006). For illustration in e.g. for FLOSII threshold value of one-hour average of the vertical velocity variance ($\overline{w'w'}$) in weak class was $\overline{w'w'}$ = 0.09 m^2 s^{-2}, while for the strong class $\overline{w'w'}$ = 22 m^2 s^{-2}. For further information see Mahrt and Vickers (2006). Here only vertical eddy diffusivity profiles of strong turbulence class determined from measurements, (K_{meas}) were used. Very weak conditions with intermittent turbulence are not considered, and our emphasis is on eddy diffusivities for strong turbulence classes corresponding to stable, nocturnal conditions.

2.2 LES model

Since measurements cover only the lowest 30 m of the ABL in FLOSSII and 60 m in CASES - 99, for a thorough study it was necessary to include data covering the full vertical extension of the ABL. LES data have been found to be very useful in numerous studies of the ABL (e.g. Deardorff 1970; Wyngaard and Brost, 1984; Andrèn et al., 1994; Kosovic and Curry; 2000; Ding et al., 2001; Zilitinkevich and Esau, 2003; Mauritsen et al., 2007).

Here LES data from DATABASE64 (e.g. Esau and Zilitinkevich, 2006) including a wide range of neutral and stably stratified cases are used to evaluate two different methods for the vertical diffusion calculation. DATABASE64 was chosen since it contains numerous idealized LES cases, which is an advantage compared to e.g. those from the first GEWEX Atmospheric Boundary Layer Study (GABLS, where GEWEX is the Global Energy and Water Cycle Experiment). The first GABLS intercomparison (Kosovic and Curry, 2000) considers a particular idealized case only; this case corresponds to the long-lived stable class in DATABASE64.

Special classification of neutral and stable conditions according to the buoyancy (Brunt-Väisälä) frequency, $N = \left(\frac{g}{\theta_0} \frac{\partial \theta}{\partial z} \right)^{1/2}$, (g, θ_0, θ and z are acceleration due to gravity, a reference potential temperature, potential temperature and altitude, respectively), and surface heat fluxes is shown in Table 1, and in this study we have analyzed conventionally neutral, nocturnal and long-lived stable classes. Modelled normalized profiles of mean wind, potential temperature and turbulent fluxes for each class are represented in Fig. 1.

Table 1. Overview of boundary-layer classes, number of cases (No), ranges of the bulk Richardson number (Ri_B) in the class and boundary-layer depths (H_{LES}), buoyancy or Brunt-Väisälä frequency (N) and $w\theta_0$ is initial surface heat flux.

Class	$w\theta_0$	N	No.	R_B	H_{LES}
Conventionally neutral	0	> 0	39	0.005 – 3.59	128 – 1652
Nocturnal	< 0	0	31	0.05 – 3.38	46 – 1875
Long-lived	< 0	> 0	15	0.35 – 7.6	16 - 507

In all cases the initial temperature profile (neutral or with constant stratification), the constant background geostrophic wind, the surface roughness length and surface heat flux were defined. The conventionally neutral class has zero surface heat flux with the ABL growing against a stably stratified atmosphere. As a consequence the lower part of the ABL is well mixed, and the top is capped by a stably stratified elevated inversion. This case is representative of windy situations when the surface heat flux is negligible. The nocturnal boundary layer develops in a near neutral atmosphere, with heat loss at the surface, and occurs during night time over land with a near-neutral residual layer present as a remnant of the daytime convective boundary layer. For the long-lived stable class, surface cooling predominates with a background stable stratification, and can be found at high latitudes over land during wintertime.

Each simulation was run for 15 hours to achieve a quasy steady state, but it was not used if the chosen LES domain was smaller than 1.5 times the height of the ABL.

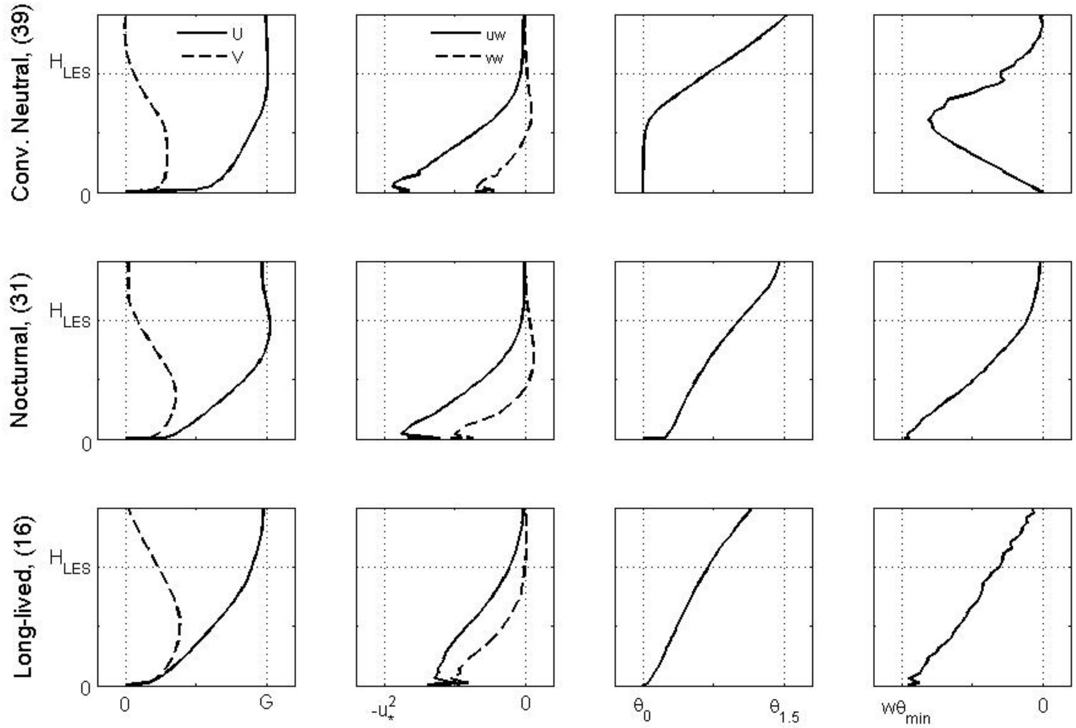

Figure 1. Normalized average profiles from LES. The vertical normalization was done with the boundary-layer height derived from LES; boundary-layer depth (H_{LES}), G is the geostrophic wind, u_*^2 is the LES total surface stress, θ_0 is the LES total surface potential temperature, $\theta_{1.5}$ is the LES potential temperature at $1.5H_{LES}$ and $w\theta_{\min}$ is the minimum potential temperature flux in the LES. Numbers in brackets of vertical axes represent the number of cases corresponding to the each analyzed stability. The columns represent wind components, momentum fluxes, potential temperature and heat flux respectively.

2.3 The EMEP model

The Unified EMEP model (http://www.emep.int/) was developed at the Norwegian Meteorological Institute under the EMEP programme. The model is a development of the earlier EMEP models (Berge and Jakobsen, 1998; Jonson et al., 1998), and is fully documented in Simpson et al. (2003) and Fagerli et al. (2004). The model has been extensively validated against measurements (Fagerli et al., 2003, Simpson et al., 2006a,b, Jonson et al., 2006, Tsyro et al., 2007, Simpson et al., 2007, Fagerli et al., 2007, Fagerli and Aas, 2008). It simulates the atmospheric transport and deposition of acidifying and eutrophying compounds, as well as photo-oxidants and particulate matter over Europe. The model domain covers Europe and the Atlantic Ocean with the grid size 50 km × 50 km while in the vertical there are 20 terrain-following layers reaching up to 100 hPa. The Unified EMEP models uses the 3-hourly meteorological data from PARallel Limited Area Model with the Polar Stereographic map projection (PARLAM-PS), which is a dedicated version of the HIgh Resolution Limited Area Model (HIRLAM) model for use within the EMEP. In this work the Unified EMEP model version rv2_6_1 was used.

2.4. Measurements used for verification of the EMEP model performance

Different data sets have been used here to evaluate the EMEP model performance: (i) observed daily surface concentrations of NO_2, SO_2 and SO_4^{2-} at different EMEP stations in Europe during year 2001 (Fig. 2), (ii) radiosounding measurements from various European cities in January and July 2001 (Table 2) and (iii) wind and temperature profiles from the Cabauw tower, the Netherlands, also in the year 2001.

The selected pollutants are among the most important acidifying and eutrophying pollutants contributing to air pollution and atmospheric chemistry. Sulphate is a secondary pollutant, an oxidant of SO_2, which contributes to acid rain formation. Since atmospheric lifetimes of SO_2 and NO_2 are 1 to 3 days and their oxidation product's lifetime is generally even longer (Seinfeld and Pandis, 1998), they are subjected to the atmospheric transport and mixing processes, and therefore suitable for validation of vertical diffusion scheme efficiency. Furthermore, NO_2, SO_2 and SO_4^{2-} are monitored at the majority of EMEP stations, with a good spatial and time resolution.

2.4.1 Measurements from the EMEP stations

This study has used the measurements at the EMEP stations (http://www.emep.int/) for the model evaluation. They are well documented, quality controlled and they mostly represent background conditions over a larger area. In order to obtain data that are characteristic for long-range transport, it is important that a station is representative of the EMEP 50 x 50 km^2 grid square averages. It should be emphasised that the recommendation for the EMEP sites not to be influenced by local pollution implies that their location is chosen to ensure the representativeness of the lower concentrations in the grid, not the grid average. Also, the measurements are not of equal quality at all stations and to some extent it may be explained by different measurement methods (e.g. Fagerli et al., 2003).

The analyzed stations within the EMEP domain are shown in Figure 2. Most of the stations are below 300 m (blue dots). Nevertheless, many stations in the Central European area are located between 600 m and 1000 m, while in the Alps area stations are often above 1000 m.

Jungfraujoch (CH01) in Switzerland is above 3000 m and Chopok (SK02) in Slovakia is above 2000 m. Mountain stations are not very well represented in models with coarse horizontal resolution, having too low altitude in the model and consequently surface concentrations are too high compared to measurements. The orography misrepresentation is a known modelling problem (e.g. Žagar and Rakovec, 1999; Ivatek Šahdan and Tudor, 2004), which is a result of orography averaging due to an insufficient horizontal resolution in models.

A list of all EMEP stations with more details on the measuring programme and available data can be found at: http://tarantula.nilu.no/projects/ccc/network/index.html. The number of used stations varied from element to element i.e. the measured daily SO_2 was available at 68 stations, NO_2 at 43 stations and SO_4^{2-} at 58 stations.

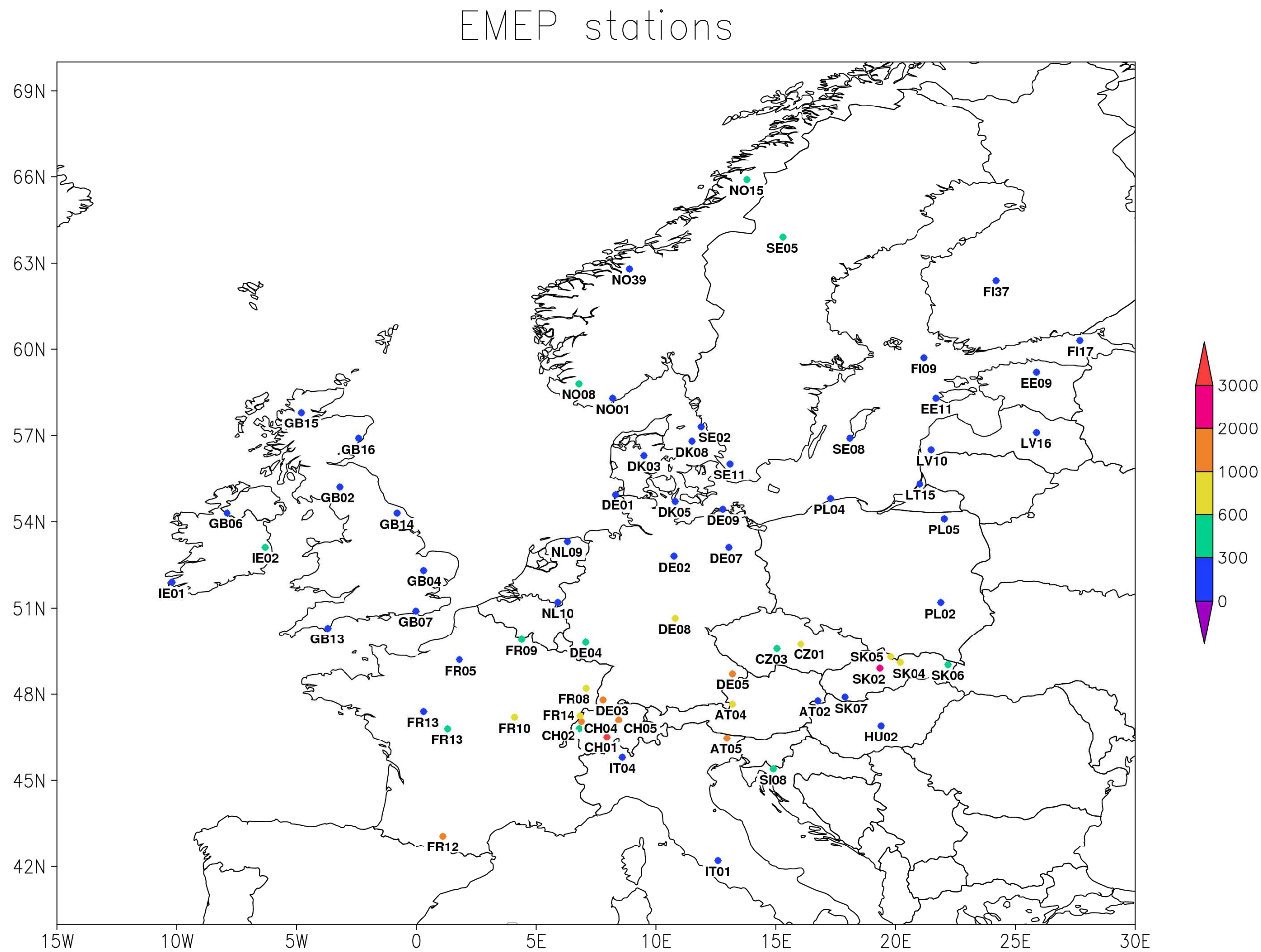

Figure 2. Stations used for evaluation of the EMEP model performance. Station altitude is represented with different colours ranging from less than 300 m (blue) to higher than 3000 m (red).

2.4.2 Measurements from the radiosounding stations

Radiosoundings are often used in order to operationally determine and verify *H* values (e.g. Seibert et al., 2000). Nevertheless, these measurements are usually only taken twice a day at 00 and 12 UTC and consequently the soundings can only be used as an overall reference. The data possess reasonably good spatial distribution over Europe and they are commonly available and quality controlled. In this work, the evaluation was performed using the data obtained from 24 different measuring stations in Europe (Table 2) during January and July in 2001.

Table 2. List of radiosounding stations over Europe used for validation of the ABL height, *H*, in the EMEP model in January and July 2001. Station name, coordinates, country, station altitude (m) and observational terms according to UTC are given.

Station	Coordinates	Country	Altitude(m)	UTC
Gothenburg	57.67 N, 12.32 E	Sweden	164	00 and 12
Orland	63.70N, 9.6 E	Norway	10	00 and 12
Stavanger	63.70 N, 9.6 E	Norway	37	00 and 12
Oslo	60.2 N, 11.08 E	Norway	201	06
Torshaven	62.20N, 6.77 E	Denmark	56	00 and 12
Hillsborough	54.8, 6 N.17 W	UK	38	00, 06, 12
Hearstmonceux	50.9 N,0.32 E	UK	0	00 and 12
Lisbon	38,77N, 9.13 W	Portugal	105	00 and 12
Zagreb	45.82 N,16.03 E	Croatia	128	00 and 12
Payerne	46.82 N,6.95 E	Switzerland	491	00 and 12
Meiningen	50.57 N,10.37 E	Germany	453	00 and 12
Vienna	48.25 N,16.87 E	Austria	200	00 and 12
Trappes	48.77 N, 2.02 E	France	168	00 and 12
Legionowo	52.4 N,20.97 E	Poland	96	00 and 12
Uccle	50.8 N,4.35 E	Belgium	104	00 and 12
Izmir	30.43 W, 27.17 E	Turkey	29	00 and 12
La Coruna	43.73 N, 8.42 W	Spain	67	00 and 12
Madrid	40.45 N, 3.55 W	Spain	633	00 and 12
Practica di Mare	41.46 N,12.43 W	Italy	32	00, 06, 12 and 18
Wroclaw	51.13 N,16.98 E	Poland	122	00 and 12
Copenhagen	55.77 N, 12.53 E	Denmark	42	00 and 12
Prague	50 N, 14.45 E	Czech	303	00, 06, 12
Milan	45,43 N,9.28 E	Italy	103	00, 06, 12

2.4.3 Cabauw measurements

The Cabauw tower (Fig. 3) is located in the western part of the Netherlands (51°58′N, 4°56′E) with flat surroundings e.g. van Ulden and Wieringa (1995). Temperature and wind averages are computed over 10-min intervals. Wind speed and wind direction are measured at six levels: 10, 20, 40, 80, 140 and 200 m while temperature is measured at one additional level, at 1.5 m. Pressure is measured at 1.5 m height only. A hydrostatic balance is assumed in order to derive potential temperature needed for the Ri_B. Pressure on upper levels is integrated from the surface pressure at 1.5 m using the trapezoidal rule. The Cabauw observations have been used in other studies to validate the land surface parameterization schemes e.g. Beljaars and Bosveld (1997), Chen et al. (1997) and Ek and Holtslag (2005).

The measurements from the Cabauw tower have a high resolution in time and their vertical distribution is dense enough to reconstruct physical processes in the surface layer (occasionally even higher) thus providing the possibility to investigate and analyze the ABL structure near the surface into greater details than with 'standard' measurements.

Figure 3. The Cabauw tower, the Netherlands (51°58′N, 4°56′E).

2.4.4 Radon data

Radon is a radioactive gas and isotopes, different forms of the same element, occur in the three naturally-occurring decay chains headed by uranium-238, uranium-235 and thorium-232. These radionuclides are found naturally in trace amounts in most rocks and soils; the most abundant isotope of uranium (over 99 %) is uranium-238 which includes radon-222 in its decay chain. The higher abundance of radon-222, coupled with a relatively long half-life of 3.8 days, means it is the most important radon isotope as far as risks to human health are concerned. The other two isotopes, radon-219 and radon-220, have half-lives of 3.9 seconds and 54 seconds and are less able to escape from the ground before undergoing further radioactive decay into solid elements. Attention is therefore focussed on radon-222, which will be referred to as radon, ^{222}Rn. Radon is measured in Becquerel's* per cubic meter of air (Bq m^{-3}).

Radon is one of a group of elements, called the noble gases, that also includes helium (He) and neon (Ne). These elements do not readily react to form chemical compounds and are simple gases under most conditions. However, radon undergoes radioactive decay by alpha-particle emission to form a short-lived isotope of polonium, which is very toxic. Several further short-lived decay products are formed in a series of decays by alpha and beta-particle emission before a long-lived isotope, lead-210 – half-life 22 years, is reached. It is the short-lived decay products of radon that are responsible for its serious health effects.

^{222}Rn is emitted at relatively uniform rate from the soil on the continents. It is relatively insoluble in water, inert and not efficiently removed by rain. It is assumed that the average flux from the soil lies somewhere between 0.8 and 1.3 atom cm^{-2} s^{-1} (Dentener et al., 1999). Oceans are also sources for ^{222}Rn, but their flux is estimated to be 100 times weaker than the continental sources. In the EMEP model emissions of ^{222}Rn are 1 atom cm^{-2} s^{-1} uniformly distributed over the continent.

2.4.4.1 Measurements of ^{222}Rn

In this work ^{222}Rn observations from four stations are used for evaluation of the EMEP model performance. Hourly measurements of ^{222}Rn at Freiburg (47° 55′ N, 7° 54′ E) and Schauinsland (47° 59′ N, 7° 51′ E) in year 2005 are used.

*Becquerel is the SI derived unit of radioactivity (symbol Bq). One Bq is defined as the activity of a quantity of radioactive material in which one nucleus decays per second. It is therefore equivalent to s^{-1}.

Freiburg and Schauinsland are stations in Germany located at heights 300 and 1205 m above sea respectively. Schauinsland is located approximately 12 km south of Freiburg. The model horizontal resolution is 50 km x 50 km, both stations are at the same grid point since the local orography is not resolved in the model. Therefore, different heights were assumed for intercomparison, surface value for Freiburg and model level approximately 1000 m from surface is taken as a representative for Schauinsland.

Measurements of ^{222}Rn at 20 m and 200 m heights are performed at the Cabauw tower in the Netherlands (56° 33′ N, 2° 59′ E) and hourly observations for the year 2006 are used. Site is described in subsection 2.4.3.

Measurements of ^{222}Rn at 50 m height are performed at the Angus tower in Scotland (56° 33′ N, 2° 59′ W) and hourly observations for the year 2006 are used. Surroundings are flat and the tower is shown in Fig. 4.

Measurements of ^{222}Rn are also performed in Krakow, Poland (50° 04′ N, 19° 54′ E) and hourly observations for the year 2006 are used in this work.

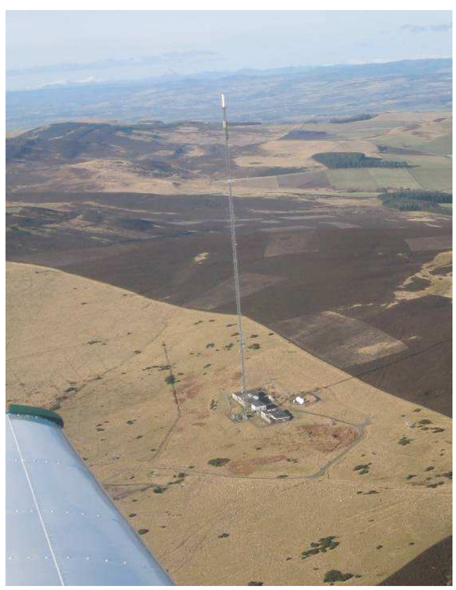

Figure 4. ^{222}Rn measuring site at Angus tower in Scotland (56°33′ N, 2°59′ W) where measurements at 50 m height are performed.

3. Methods

3.1 Description of *K*(*z*) parameterization schemes

O'Brien (1970) developed a method for the calculation of the eddy diffusion coefficient, $K(z)$ which has been widely used in many practical applications. In this so called 1st order closure approach, $K(z)$ is calculated from the following cubic polynomial, which requires four independent parameters for its evaluation:

$$K(z) = K_H + \left[(z-H)^2/(\Delta z)^2\right] \times \\ \left\{K_{H_S} - K_H + (z - H_S)\left[\partial K_{H_S}/\partial z + 2(K_{H_S} - K_H)/(H - H_S)\right]\right\} \quad (1)$$

where K_H is a $K(z)$ value at the top of the ABL, i.e. $K(z = H)$ and K_{H_S} is a $K(z)$ value at the top of the surface-layer (H_S). It is assumed that $\partial K(z)/\partial z$ =0, at $z = H$. In practical applications $\partial K_{H_S}/\partial z$ is determined from:

$$\frac{\partial K_{H_S}}{\partial z} \approx \frac{K_{H_S} - K_1}{H_s - z_1} \quad (2)$$

where z_1 is the lowest modelling level and correspondingly $K_1 = K(z_1)$. It is supposed that variations of $K(z)$ at height H are infinitesimally small, so that $\partial K_H/\partial z$ = 0. From $\partial K_{H_S}/\partial z > 0$ follows that K in Eq. (1) must increase monotonically with height in the constant-flux layer, and that the maximum value of $K(z)$, ($K_{\max}$), must occur between H_S and H. In the constant-flux layer O'Brien (1970) assumed $K(z) = ku_* z/(1+\phi(z))$, and derived equation for $K_{\max}$ from Eq. (1) taking into account that the ABL height is much higher than the height of the surface-layer; $H >> H_s$, and also that the strength of vertical diffusion at the top of surface-layer is significantly higher than that at the ABL top; $K_{H_S} >> K_H$

Finally, after some calculation the following equation is found:

$$K_{\max} \approx \frac{4}{27}(K_{H_s} + H\frac{\partial K_{H_S}}{\partial z}), \tag{3}$$

at $z = 1/3H$. It should be noted here that the O'Brien polynomial depends on the model vertical resolution, i.e. the number of model levels for which $K(z)$ is calculated. Therefore, the O'Brien method is physically plausible or even reasonable in unstable conditions, when condition $H >> H_s$ is satisfied. In cases of near-neutral and especially (very) stable conditions when H is not much higher than H_s the applicability of the O'Brien method in numerical models is questionable. Nevertheless, it is often used and even recommended in neutral and stable conditions (e.g., Stull, 1988; Pielke, 2002). Consequently, we introduce a exponential method where the O'Brien third-order polynomial $K(z)$ is generalized into a exponential function (e.g. Grisogono and Oerlemans, 2002):

$$K(z) = (K_{\max} e^{1/2} / h) z \exp(-0.5(z/h)^2) \tag{4}$$

where h is the height of the $K_{\max}$. Comparing Eq. 1, (O'Brien), with Eq. 4, (Grisogono), one notes that an advantage of (4) in respect to (1) is that it needs only two input parameters, $K_{\max}$ and h. A schematic representation of all input parameters for the O'Brien as well as for the Grisogono approach is given in Fig. 5.

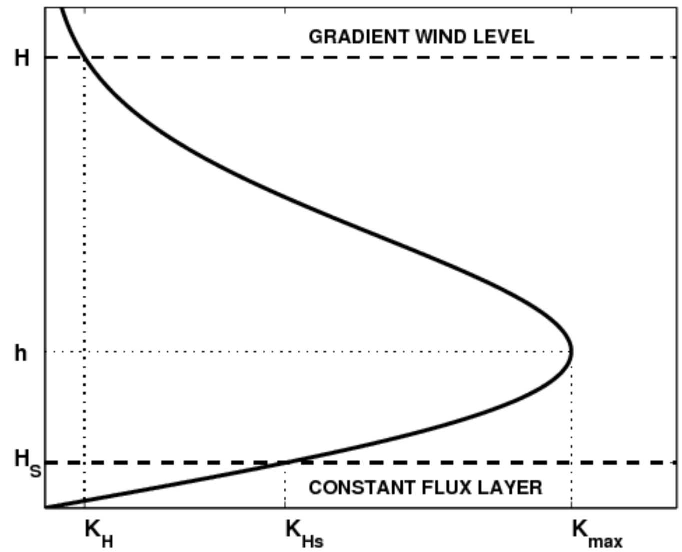

Figure 5. Schematic representation of input variables needed for the O'Brien polynomial: K_H, K_{H_S}, H, and H_S, and the variables needed in the Grisogono approach: h and K_{max}.

3.1.1 Practical determination of the input parameters

All input parameters for the O'Brien and Grisogono methods used on different data and models are summarized in Table 3. Input parameters for the O'Brien approach (K_H, K_{H_S}, H, and H_S) used in Eq. (1) and for the Grisogono approach ($K_{\max}$, h) used in Eq. (4) applied to FLOSSII and CASES-99 are determined from experimentally defined profiles (K_{meas}) from Figures 6 and 7 in Mahrt and Vickers (2006). Values of H_S are at the top of K_{meas} linear profile starting from the surface, while $H = 10 \cdot H_S$, assuming that the height of the surface-layer is about 10 % of the ABL height (e.g. Stull, 1988). In this study eddy diffusivity at the top of the ABL is set to 0.1 m^2 s^{-1}, i.e. K_A = 0.1 m^2 s^{-1}.

Table 3. Description of the input parameters used for $K(z)$ determination using the O'Brien and Grisogono methods based on FLOSSII, CASES - 99, LES and EMEP data.

	FLOSSII and CASES-99	LES	EMEP
	O'Brien		
H (m)	$10H_s$	Height of which $TKE = 0.02TKE_{\max}$	(i) operational ABL scheme (ii) Ri_B scheme
H_s (m)	Height of which K_{meas} linear profile terminates	$0.1H$	$0.4H$
K_H (m ^{2}s $^{-1}$)	0.1	0.1	0.001
K_{H_S} (m ^{2}s $^{-1}$)	$K_{meas}(H_S)$	$kH_S u_* / \phi_m(z/L)$	$kH_S u_* / \phi_m(z/L)$
	Grisogono		
h	Height of which K_{meas} reaches the maximum	$H/C(h)$	$H/3$
$K_{\max}$	Maximum value of K_{meas}	$C(K)Hu_*$	$0.1Hu_*$

The K_{H_S} is at height H_S while $K_{\max}$ and h needed for the Grisogono profiles calculation are also taken from measurements as the maximum value of K_{meas} and its height.

From the LES data H is determined from profiles of turbulent kinetic energy (TKE) calculated from the LES, while H_S and K_H are defined in the same way as in the FLOSSII and CASES - 99 cases.

The value of K_{H_S} is calculated using stability functions $\phi_m(z/L)$ according to e.g. Stull (1988):

$$K_{H_S} = \frac{kzu_*}{\phi_m(z/L)} \tag{5}$$

where the Obukhov length (L), and the friction velocity (u_*) are taken from the LES. Next, ϕ_m is defined for stable conditions as:

$$\phi_m = 1 + 4.7(z/L) \tag{6a}$$

and for unstable conditions as,

$$\phi_m = (1 - 15z/L)^{-1/4}. \tag{6b}$$

From the LES data, input parameters needed in Eq. (4), i.e. the maximum value of the vertical diffusion coefficient, $K_{\max}$, and its height h are calculated according to:

$$K_{\max} = C(K)Hu_*, \tag{7}$$

$$h = H/C(h), \tag{8}$$

where the $C(K)$ and $C(h)$ represent constants empirically estimated here from the LES data. Definition of $K_{\max}$, Eq. (7), includes non-local effects through the ABL depth which is an integral atmospheric property, while local turbulence property is included in the friction velocity u_*. The ABL height is an integral property that relates surface processes to upper processes in the ABL and thus embeds non-local effects. The surface is assumed to be the main source of turbulence, with the fluxes mainly driven by the surface heat and friction. Furthermore, the ABL height is a good stability parameter since it acquires smaller values from only a few meters to few hundreds in stable conditions to few thousand meters in unstable conditions.

For every LES run $K_{\max}$ and h are determined from the LES $K(z)$ profiles and from the profiles determined with the Grisogono method with predefined initial constant values, $C_0(K)$ and $C_0(h)$, providing the basis for the calculation of ratios $K_{\max}(LES)/K_{\max}(Grisogono)$. Averaged ratios were used to find an optimal coefficient needed in Eqs. (7) and (8):

$$C(K) = \frac{1}{N}\sum_{n=1}^{N}\left(\frac{K\max(LES)}{K\max(Grisogono)}\right)_n C_0(K) \tag{9}$$

where the index n denotes the number of the LES runs n = 1,…,86. Coefficients calculated with this procedure are represented in Table 4. Based on the coefficients calculated from the LES data in stable conditions, the maximum value of eddy diffusivity for momentum, (K_m), is greater than that of heat, (K_h), by a factor of two.

Table 4. Initial and calibrated constants used for determination of input parameters $K_{\max}$ and h used for the calculation of K_m and K_h with the Grisogono method.

	$C_0(K)$	$C(K)$	$C_0(h)$	$C(h)$
K_m (m ^{2} s $^{-1}$)	0.125	0.13	2	1.52
K_h (m ^{2} s $^{-1}$)	0.125	0.06	2	3.73

As previously mentioned the operational method in the EMEP model i.e. the OLD method is the combination of the local Blackadar method that is applied in stable conditions and non-local O'Brien scheme applied in unstable conditions.

In the EMEP model $K(z)$ is initially calculated from the surface to the top of the domain with the local scheme proposed by Blackadar (1979):

$$K(z) = \begin{cases} 1.1(Ri_C - Ri)l^2 \left|\Delta V_H / \Delta z\right| / Ri_C & Ri \le Ri_C \\ 0.001 & Ri > Ri_C \end{cases} \quad (10)$$

where l is the turbulent mixing length (m), V_H is horizontal wind speed, , Δz is the model layer thickness, $\left|\Delta V_H / \Delta z\right|$ is the absolute value of wind shear in the vertical. The turbulent mixing length, l, is parameterized according to:

$$\begin{aligned} l &= k \cdot z & z &\le z_m \\ l &= k \cdot z_m & z &> z_m \end{aligned} \quad (11)$$

where z is the height above the ground and $z_m = 200$ m. The R_i is the gradient Richardson number defined as:

$$Ri = \frac{g}{\theta} \frac{\Delta\theta / \Delta z}{\left(\Delta V_H / \Delta z\right)^2} = \frac{g \Delta z \Delta\theta}{\theta \left(\Delta V_H\right)^2} = \frac{gz\left(\theta(z) - \theta(z-1)\right)}{\theta(z)\left(V_H(z) - V_H(z-1)\right)^2}, \quad (12)$$

where θ is a potential temperature, $\Delta\theta$ is the potential temperature difference in the model layer, and Ri_C is the critical Richardson number calculated from the McNider and Pielke (1981) equation:

$$Ri_C = A\left(\frac{\Delta z}{\Delta z_0}\right)^B, \quad (13)$$

where $A = 0.115$, B = 0.175 and $\Delta z_0 = 0.01$ m.

Final Ri_C value is: $Ri_C = MAX\left(0.25, 11.5(\Delta z)^{0.175}\right)$. Obviously with $\Delta z \to 0$, $Ri_C \to 0.25$.

In unstable ABL, $K(z)$ is calculated with the O'Brien scheme, Eq. (1), with K_B determined in the EMEP from Eq. (5), formulation based on M-O similarity theory for the surface layer (e.g. Stull, 1988).

Universal functions Φ used in the EMEP are those recommended by Garratt (1992) in unstable case:

$$\Phi = \left(1 - 16\frac{z}{L}\right)^{-1/2}, \tag{14a}$$

and in stable case:

$$\Phi = 1 + 5\frac{z}{L} \qquad\qquad z/L < 1. \tag{14b}$$

The L is given by the near-surface turbulent fluxes of momentum, τ (N m^{-2}), and sensible heat flux, Q_h (W m^{-2}), which are taken from the NWP PARLAM-PS model:

$$L = -\frac{\theta_S \cdot u_*^3 \cdot \rho \cdot C_p}{k \cdot g \cdot Q_h}, \tag{15}$$

$$u_*^{\,2} = \frac{\tau}{\rho}, \tag{16}$$

where θ_S is a surface potential temperature, g is acceleration of gravity (9.8 m s^{-1}) and C_p is a specific heat capacity of dry air at constant pressure (1005 J kg^{-1} K^{-1}).

In the EMEP model input parameters in the Grisogono scheme are evaluated from Eqs. (7) and (8) with empirical constants $C(K)$ = 0.1 and $C(h)$ = 3 estimated based on the LES data (Jeričević and Večenaj, 2009). By inserting equations (7) and (8) into (4) a new simplified form is derived:

$$K(z) = Cu_* z \exp\left(-4.5\left(z/H\right)^2\right) \tag{17}$$

where $C \approx 0.493$ is a new derived constant.

Both methods, the O'Brien and Grisogono, are non-local approaches and mainly depend on the position and intensity of $K_{\max}$. In the Grisogono approach, the value of $K_{\max}$ explicitly includes u_* and H, utilized from the meteorological driver and its accuracy is constrained with the NWP model performance. On the other hand, the O'Brien scheme represents $K(z)$ as a polynomial function that depends on parameters K_H, K_{H_S}, H and H_S. Note that these parameters (e.g. H_S) are not easy to resolve and describe especially in statically stable conditions (e.g. Zilitinkevich and Calanca, 2000; Jeričević and Grisogono, 2006; Mahrt, 2007).

3.2 Description of boundary layer parameterization schemes

The ABL height is an important parameter, which limits the modelled vertical extent of turbulent mixing in the atmosphere starting from the surface. The operational method for the calculation of H in the EMEP model determines H from the NWP PARLAM-PS output (Jakobsen et al., 1995; Simpson et al., 2003). In stable conditions H is calculated as the height where $K(z) < 1$ m^2 s^{-1}, with $K(z)$ profiles calculated with the local Blackadar method Eq. (10) and vertically linearly smoothed over few adjacent layers. In unstable conditions hourly Q_h is distributed vertically via dry adiabatic adjustment and H is the height of the corresponding adiabatic layer. Finally, H in is determined from: $H = MAX(H_{stable}, H_{unstable})$.

The proposed commonly used Ri_B method is based on the assumption that continuous turbulence vanishes beyond Ri_{BC}, some previously defined critical value of Ri_B. The height at which Ri_B reaches Ri_{BC}, is considered as H. It is defined as:

$$Ri_B = \frac{g(z-z_1)}{\overline{\theta(z)}} \frac{\theta(z)-\theta_1}{(\Delta u(z))^2 + (\Delta v(z))^2}, \tag{18}$$

$$(\Delta u(z))^2 = (u(z)-u(z_1))^2 = (u(z)-0)^2 = u(z)^2 \tag{19}$$

$$(\Delta v(z))^2 = (v(z)-v(z_1))^2 = (v(z)-0)^2 = v(z)^2 \tag{20}$$

Here θ_1 is a potential temperature at the lowest model level, z_1, and $\overline{\theta}$ (z) is an average potential temperature between heights z and z_1. H is the height of the level where Ri_{BC}=0.25 is reached. However, the supposed existence of Ri_{BC} has recently been criticised (Zilitinkevich and Baklanov, 2002; Jeričević and Grisogono, 2006; Mauritsen et al., 2007; Zilitinkevich et al., 2008; Grisogono and Belušić, 2008) and the development of the $K(z)$ schemes based on higher order closure is a subject of current and future research. The main advantages of this method over the operational approach are that Ri_B includes the two major turbulence generators in the atmosphere: thermal and mechanical sources of turbulence and it is applicable in stable and unstable atmospheric conditions. Eq. (18) describes H as an integral atmospheric property that relates surface processes to upper processes in the ABL and thus comprises non-local effects. The main weakness of the operational ABL height method in stable conditions is dependence on the $K(z)$ profiles calculated with the Blackadar approach (Eq. 10). The operational method in stable conditions is based on the Ri number and also includes both sources of turbulence; however it can be oversensitive to the local turbulence and may underestimate the ABL height. In unstable conditions the accuracy of the operational method depends on surface parameters obtained from the NWP model e.g. Q_h, and vertical distribution of Q_h via dry adiabatic adjustment, while effects of the mean wind shear are not included.

3.3 Total turbulent energy scheme

Here description of a new $K(z)$ scheme, so called the total turbulent energy (TTE) scheme, based on a higher-order closure for neutral and stratified atmospheric conditions, is given. The TTE is the sum of the turbulent kinetic energy (TKE) and turbulent potential energy which is proportional to the potential temperature variance. In unstable conditions the closure deploys only the TKE.

Higher-order closures are common approach to the turbulence closure problem in which additional prognostic equations are applied. We start with the mean state as:

$$\frac{DU}{Dt} = -\frac{\partial \overline{uw}}{\partial z} - f(V_g - V), \tag{21}$$

$$\frac{DV}{Dt} = -\frac{\partial \overline{vw}}{\partial z} + f(U_g - U), \tag{22}$$

$$\frac{D\theta}{Dt} = -\frac{\partial \overline{w\theta}}{Dz}, \tag{23}$$

where $\overline{uw}$ and $\overline{vw}$ are the vertical momentum fluxes, $\overline{w\theta}$ is the vertical potential temperature flux, f is the Coriolis parameter, D/Dt denotes the total derivative and U_g and V_g are the zonal and meridional components of the background geostrophic wind vector. Upper case letters denotes means, while lower case letters are turbulent departures from the mean.

In a higher-order closure, usually a prognostic TKE, E_k, equation is applied:

$$\frac{DE_k}{Dt} = \vec{\tau} \cdot \vec{S} + \beta \overline{w\theta} - \varepsilon - \frac{\partial F_k}{\partial z}, \tag{24}$$

where ε is the dissipation rate, $\beta = g/\Theta$ is the buoyancy parameter, $\vec{\tau} = -(\overline{uw}, \overline{vw})$ is the turbulent stress vector, $\vec{S} = \left(\frac{\partial \vec{U}}{\partial z}, \frac{\partial \vec{V}}{\partial z}\right)$ is the shear vector and $F_k = \overline{E_k w} + \overline{pw}/\rho$ is the third-order vertical flux of E_k.

Turbulent potential energy (E_p) is proportional to the density variations in the fluid, which can be expressed via the potential temperature variance (e.g. Zilitinkevich et al., 2008):

$$E_p = \frac{1}{2}\sigma_\theta^2 \frac{\beta^2}{|N^2|} \tag{25}$$

where σ_θ^2 is the potential temperature variance and $N^2 = \beta\, \partial\theta/\partial z$ is the squared buoyancy (Brunt-Väisälä) frequency again.

Here we consider the TTE (E):

$$E = E_k + E_p \tag{26}$$

After some algebra, prognostic equation for the E can be found:

$$\frac{DE}{Dt} = \vec{\tau} \cdot \vec{S} - \gamma - \frac{\partial F_E}{\partial z} + \begin{cases} 0 & \text{for } N^2 \geq 0 \\ 2\beta\overline{w\theta} & \text{for } N^2 < 0 \end{cases} \tag{27}$$

where γ is the dissipation rate of E and F_E is the third-order flux defined as $F_E = F_k + F_\theta\, \beta^2 / |N^2|$, where F_θ is the third-order vertical flux of σ_θ^2 defined as $F_\theta = \overline{\sigma_\theta^2 w}/2$.

According to TTE scheme vertical diffusion coefficient can be found from:

$$K(z) \approx \frac{2 f_\theta^2 E_k l}{C_\phi \sqrt{E}} \tag{28}$$

where f_θ is the non-dimensional heat flux, *l* is the dissipation length scale and C_ϕ is the empirical constant determined based on the LES data (Mauritsen et al., 2007). Fully derived Eq. (27) can be found in Appendix 2 in paper of Mauritsen et al., (2007). In this work simple stability functions subjectively fitted to the observations are used for calculation of non-dimensional fluxes for heat (f_θ) and momentum (f_τ):

$$f_\theta = \frac{\overline{w\theta}}{\sqrt{E_k \sigma_\theta^2}} = -0.145(1+4R_i)^{-1} \tag{29}$$

$$f_\tau = \frac{|\tau|}{E_k} = 0.17(0.25 + 0.75(1+4Ri)^{-1}) \tag{30}$$

where *Ri* is the gradient Richardson number as in Eq. (11). Dissipation length scale is approximated by a multi-limit formulation as follows:

$$\frac{1}{l} = \frac{1}{kz} + \frac{f}{C_f\sqrt{\tau}} + \frac{N}{C_N\sqrt{\tau}}, \tag{31}$$

where C_f and C_N are determined based on the LES data (Mauritsen et al., 2007). Eq. (30) takes into account the distance from the ground, the Coriolis effect and static stability. Future work will include the wind shear, $\vec{S}$, explicitly in Eq. (31), similar to Grisogono and Belušić (2008).
Ratio E_p/E_k is determined by assuming steady-state and neglecting vertical energy transport in different atmospheric stability conditions from the equation:

$$\frac{E_p}{E_k} = \frac{\beta\left|\overline{w\theta}\right|}{\vec{\tau}\cdot\vec{S} + \beta\overline{w\theta}} \tag{32}$$

In unstable conditions when $Ri \rightarrow -\infty$, i.e. $\left|\vec{\tau} \cdot \vec{S}\right| << \beta \left|\overline{w\theta}\right|$ it is $E_p / E_k \rightarrow 1$. In the neutral limit, when $Ri \rightarrow 0$, we have $\left|\vec{\tau} \cdot \vec{S}\right| >> \beta \left|\overline{w\theta}\right|$, we have $E_p / E_k \approx Ri / P_r(0)$ where $P_r = K_m / K_h$ is the turbulent Prandtl number and $P_r(0) = \frac{f_\tau^2}{2 f_\theta^2}$. In stable conditions when $Ri \rightarrow +\infty$ the main source of E is shear-production. Therefore it is not possible that the buoyancy redistribution term exceeds the shear production. Taking the limit $\beta \left|\overline{w\theta}\right| \rightarrow \left|\vec{\tau} \cdot \vec{S}\right|$ it is found $E_p / E_k \approx 1/2$.

According to Stull (1988), for near-neutral and stable atmospheric conditions TKE can be calculated as follows:

$$E_k = \frac{1}{2} u_*^2 \left(A \left(1 - \frac{z}{z_i}\right)^2 + \left(1 - \frac{z}{z_i}\right)^{1/2} \right) \tag{33}$$

where z_i is the boundary layer height and $A = 9$ is an empirical constant.

In unstable atmospheric conditions TKE is calculated from:

$$E_k = \frac{1}{2} \left(B u_*^2 1 + 1.8 w_*^2 \left(\frac{z}{z_i}\right)^{2/3} \left(1 - 0.8 \frac{z}{z_i}\right)^2 \right) \tag{34}$$

where w_* is convective velocity scale, and $B = 8$ is an empirical constant. It is convenient to define a velocity scale by combining surface buoyancy flux and the ABL height by obtaining the free convection scaling vertical velocity, e.g. Stull (1988):

$$w_* = \left(\frac{gz}{\theta} (\overline{w\theta_0}) \right)^{1/3} \tag{35}$$

This scale is magnitude of the vertical velocity fluctuations in thermals and can assume values of about 1 – 2 m s^{-1}.

3.4 Statistical methods for the model evaluation

It is important to properly evaluate air quality models in order to demonstrate their fidelity in simulating the phenomena of interest. Before beginning the calculation of various statistical performance measures it is extremely useful to perform exploratory data analysis by simply plotting the data in different ways. In this work data analysis of the ^{222}Rn data are started with plotting of scatter plots and probability density function plots. To create the cumulative density function plots first rank observed and predicted data separately from lowest to highest. Therefore 3rd lowest observed data will be plotted against the 3rd lowest modelled data and calculate an empirical probability density function. The scatter plots and the cumulative density function plots give an overall assessment of model performance

In order to evaluate the predictions of a model with observations according to e.g. Wilmot (1982) and Chang and Hanna (2004) following statistical performance measures are used: the correlation coefficient (*r*), bias (*BIAS*), mean absolute error (*MAE*), mean square error (*MSE*), root mean square error (*RMSE*), fractional bias (*FB*), the normalized mean square error (*NMSE*) and the index of agreement (*d*).

$$r = \frac{n\sum O_i M_i - \sum O_i \sum M_i}{\sqrt{n\sum O_i^2 - (\sum O_i)^2}\sqrt{n\sum M_i^2 - (\sum M_i)^2}} \tag{36}$$

$$BIAS = \left(\frac{\overline{M} - \overline{O}}{\overline{O}}\right) \times 100\%, \tag{37}$$

$$MAE = \frac{1}{n}\sum_{i=1}^{n}\left|O_i - M_i\right| , \tag{38}$$

$$MSE = \frac{1}{n}\sum_{i=1}^{n}(M_i - O_i)^2 \tag{39}$$

$$RMSE = \sqrt{\frac{1}{n}\sum_{i=1}^{n}(M_i - O_i)^2} \tag{40}$$

$$FB = \frac{(\overline{O} - \overline{M})}{0.5(\overline{O} + \overline{M})}, \tag{41}$$

$$NMSE = \frac{\overline{(O - M)^2}}{\overline{O}\,\overline{M}}, \tag{42}$$

$$d = 1 - \left[\sum_{i=1}^{N}(M_i - O_i)^2 / \sum_{i=1}^{N}\left(\left|M_i^{'}\right| + \left|O_i^{'}\right|\right)^2\right] \qquad 0 \le d \le 1 \tag{43}$$

where

M: model predictions,

O: observations,

overbar ($\overline{O}$) denotes average over the dataset.

$M_i^{'} = M_i - \overline{O}_i$

$O_i^{'} = O_i - \overline{O}_i$

Differences (*D*) between *r* and *BIAS* values calculated with different model versions are defined as:

$$D(X) = X(Grisogono) - X(O'Brien), \tag{44}$$

and relative differences (*RD*) as:

$$RD(X) = (X(Grisogono) - X(O'Brien)) \times 100\% / X(O'Brien), \tag{45}$$

where parameter X can be r or the absolute value of *BIAS*, *ABS (BIAS)*. For $X = r$, $D(r) > 0$ and $RD(r) > 0$ means that the model performs better with the Grisogono $K(z)$ scheme, while for $X =$

$BIAS$, $D\,(BIAS) > 0$ and $RD\,(BIAS) > 0$ denotes that the OLD scheme agrees better with the observations. Similarly $D \approx 0$ and $RD \approx 0$ denotes equally good performance of both schemes.

Since *NMSE* accounts for both systematic and unsystematic or random errors, it is helpful to partition *NMSE* into the component due to systematic errors, *NMSEs*, and the unsystematic component due to random errors, *NMSEu*. It can be shown that

$$NMSE_s = \frac{4FB^2}{4 - FB^2} \ . \tag{46}$$

The above expression gives the minimum *NMSE*, i.e., without any unsystematic errors, for a given value of *FB* (Hanna et al., 1991). The total *NMSE* is:

$$NMSE = NMSE_s + NMSE_u \,. \tag{47}$$

The M*AE* measures average magnitude of the errors. The *RMSE* and *MSE* measure differences between modelled and observed values. It measures accuracy for continuous variables. The *MSE* = 0 means that model predicts observations perfectly, while particular values of the *MSE* are meaningless they may be used for comparative purposes. The unbiased model version with the smallest *MSE* is generally considered as the best. Generally lower values of both, *MAE* and *RMSE* are better.

A perfect model would have *FB* and $NMSE = 0.0$. However due to the influence of random atmospheric processes, there is no such thing as perfect air quality modelling. Note that since FB and *BIAS* measure only the systematic bias of a model, it is possible for a model to have predictions completely out of phase of observations and still have $FB = 0$ or $BIAS = 0$ because of cancelling errors.

Multiple performance measures should be applied and considered in any model evaluation exercise, as each measure has advantages and disadvantages and there is no single measure that is universally applicable to all conditions. The relative advantages of each performance measure are partly determined by the characteristics and distributions of the model predictions and observations. For most atmospheric pollutants concentrations the distribution is close to log-normal. In this case, the linear measures *FB* and *NMSE* may be overly influenced by infrequently occurring high observed and/or predicted concentrations.

FB is a measure of a mean relative bias and indicates only systematic errors, whereas *NMSE* is a measure of mean relative scatter and reflect both systematic and unsystematic (random) errors. By considering two error components, systematic and unsystematic, of *FB* it is possible to overcome the problem of having $F\ = 0$ even if model predictions are completely out of phase.

The correlation coefficient, *r*, reflects the linear relationship between two variables and does not reveal any other non-linear relation (e.g. parabolic) between the data. Also *r* is sensitive to a few aberrant data pairs. In case of generally poor agreement the presence of a good match for a few extreme pairs will greatly improve *r*. Therefore the use of *r* is often discouraged (e.g., Willmott, 1982).

Values of *FB* and *NMSE*, can be further interpreted in terms of measure that is more easily comprehended, such as the equivalent ratio of *M* to *O*.

For example, Eq. (41) can be expressed as:

$$\frac{\vec{C}_p}{\overline{C}_o} = \frac{1 - \frac{1}{2} FB}{1 + \frac{1}{2} FB}. \tag{48}$$

Therefore, $F\ = 0.67$ would imply a factor of two mean underprediction, and *FB* = -0.67 would imply a factor of two mean overprediction.

To interpret *NMSE*, assume that the mean of the observed concentrations equals the mean of the predicted concentrations. Then *NMSE*=1.0 implies that *RMSE* is equal to the mean. As *NMSE* becomes much larger than 1.0, it can be inferred that the distribution is not normal but is closer to log-normal (e.g., many low values and a few large values).

The index of agreement (*d*) is intended to be a descriptive measure, and it is both a relative and bounded measure which can be widely applied in order to make cross-comparisons between models.

In order to find the best parameterization schemes in models conclusions should be made on intercomparison between the various evaluations parameters. The best scheme is the one which gives the best model results. The best model performance has the highest *r* and *d*, the lowest

BIAS, *MAE*, *MSE*, *RMSE*, *FB* and total *NMSE*, while better parameterization scheme should lower the NMSEs values.

3.4.1 Significance tests

Standard significance Fishers z-test (e.g. Pavlić, 1988) is conducted on correlation coefficients (r) determined between the measurements and the modelled data in order to find whether the change in r reflects the change of stochastic relation between the two data sets.
Hypothesis H_0: $r_1 = r_2$, and H_1: $r_1 \neq r_2$, have been tested, where r_1 and r_2 are the correlation coefficients determined between the observations and the modelled data calculated with the two different $K(z)$ schemes, the OLD and Grisogono. For the 95 % confidence interval hypothesis H_0 is accepted if condition $|z| = \frac{|z_1 - z_2|}{\sigma_{z_1 - z_2}} \leq 2$ is satisfied. Variables z_1, z_2 and $\sigma_{z_1 - z_2}$ are determined from the following equations:

$$z_{1,2} = \frac{1}{2} \ln \frac{1 + r_{1,2}}{1 - r_{1,2}} \tag{49}$$

$$\sigma^2_{z_1 - z_2} = \frac{1}{n_1 - 3} + \frac{1}{n_2 - 3} \tag{50}$$

where n_1 and n_2 are the sizes of analyzed data sets.

However, the appropriateness of this procedure is questioned since initial assumptions for its application are not completely satisfied, i.e. mutual independence of the observation and the modelled data, and the distribution of the quantity following a normal distribution. The z-test has been used in practice, nevertheless it is found to be quite insensitive to establish whether two correlations have different strengths. Furthermore, it is based on the assumption that data from two samples are normally-distributed, while SO_2, SO_4^{2-} and NO_2 are found to be log-normally distributed. In this test, as in many other standard statistical tests, an assumption of mutual independence is made. However, daily concentrations are not completely independent since they are time-correlated with the persistence of meteorological events (Fox, 1980; Chang and Hanna, 2003). Time correlation in data sets may affect significance tests in many different ways making estimation of degrees of freedom needed for level of significance determination impossible. Willmott (1982) argued that it is inappropriate to report r as statistically significant, not only because the magnitude of r and its associated significance level are not necessarily related to accuracy and rarely conform to the assumptions that are prerequisite to the appropriate application of inferential statistics, as it was also stated here.

4. Results

4.1 FLOSSII and CASES-99

The O'Brien polynomial approach and the Grisogono analytical approach are compared in order to evaluate their performance in stable and near-neutral conditions. Vertical profiles of $K(z)$ have been analyzed for two different datasets: FLOSSII and CASES-99 observations.

Vertical profiles of K_m and K_h are calculated with Eqs. (1) and (4) for the strong turbulence class from FLOSSII and from CASES - 99, see Fig. 6. These calculated profiles are compared with K_{meas}. The O'Brien method, Eq. (1), overestimates the height of K_m for FLOSSII (Fig. 6a) and the maximum value of K_h for CASES - 99 (Fig. 6d), while Grisogono Eq. (4) agrees well with the K_{meas}. An overestimation of h or $K_{\max}$ with Eq. (1) is a consequence of a misrepresentation of surface-layer parameters used in the O'Brien approach. While the height of $K_{\max}$ calculated with the O'Brien method agrees with the CASES - 99 measurements, magnitude of $K_{\max}$ was overestimated (Fig. 6c). For the same data the maximum of K_h was well represented with the O'Brien approach, although its height was somewhat underestimated (Fig. 6d).

The misrepresentation of h and $K_{\max}$ with the O'Brien method may lead to either an overestimation or underestimation of simulated concentrations when Eq. (1) is applied in various air quality models. Note that profiles of K_h and K_m determined from the FLOSSII and CASES -

99 data are different while both the O'Brien and Grisogono methods are non-local and mainly depend on magnitude and height of $K_{\max}$.

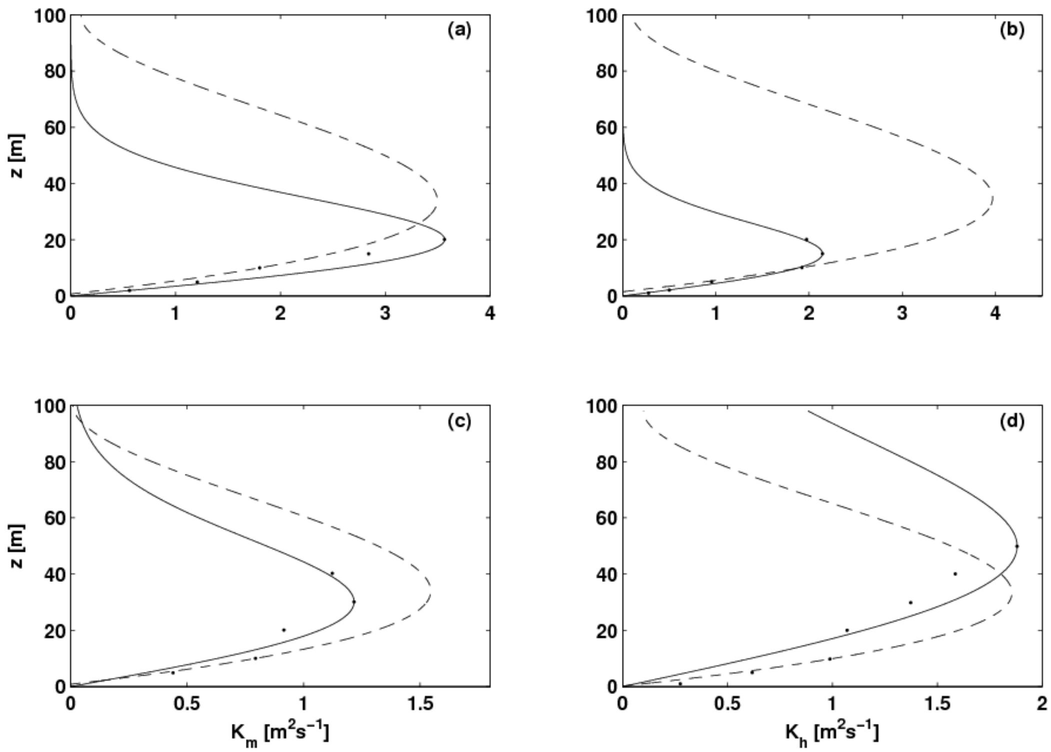

Figure 6. Vertical profiles of eddy diffusivity estimated from the composite vertical structure for the stratified strong turbulence class for FLOSSII: momentum (a) and heat flux (b), and CASES-99: momentum (c) and heat flux (d). Dashed line is O'Brien third-order polynomial Eq. (1), solid line is Grisogono Eq. (4) and the dots represent the measurements digitalized from Figures 6 and 7 in Mahrt and Vickers (2006).

4.2 Results deploying the LES data

Around 90 large-eddy simulations, including a wide range of neutral and stably stratified cases, are used to evaluate two different methods for vertical diffusion calculation. In Fig. 7 an intercomparison of different vertical diffusion schemes against six randomly chosen LES $K(z)$

profiles in conventionally neutral conditions is shown. In the shear driven ABL, K_m is the stronger and dominant factor compared to K_h which experiences lower magnitudes and a higher spread in values. Better agreement of the Grisogono method is apparent while the O'Brien profiles tend to underestimate K_m (Figs. 7a, 7b and 7c) and overestimate K_h (Fig. 7d, 7e and 7f). Note the good agreement for the $K(z) < K_{\max}$, i.e. in the surface-layer, for both methods. The overestimation of K_h with the O'Brien method is in agreement with the results for FLOSSII in Fig. 6b.

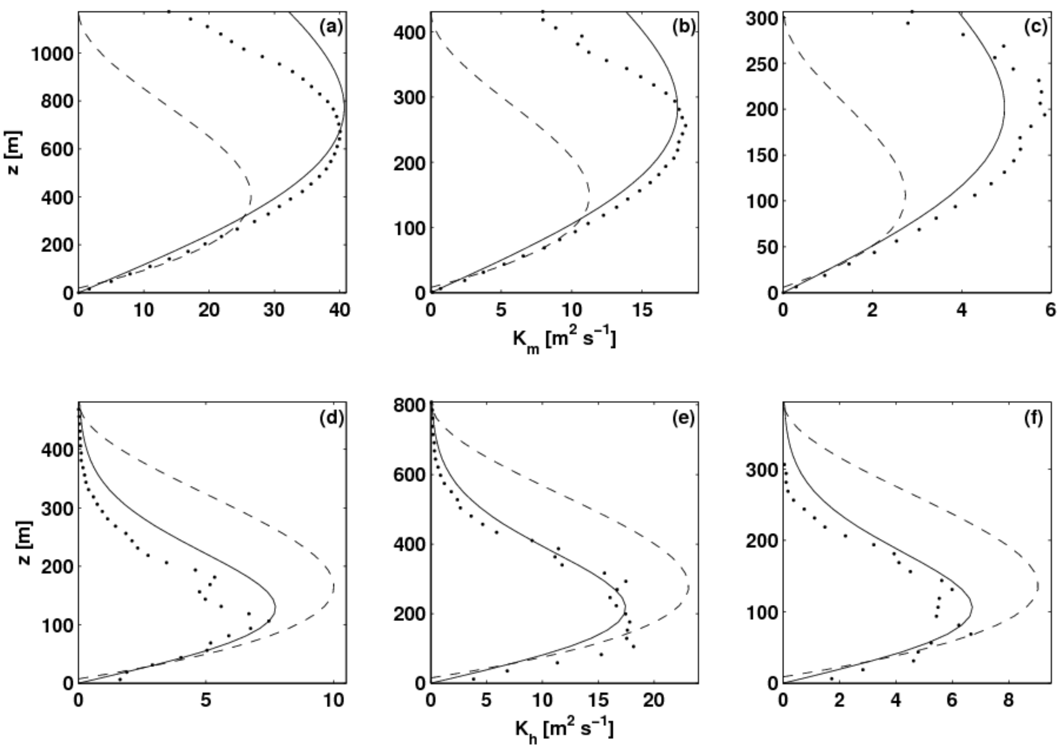

Figure 7. Vertical profiles of eddy diffusivity in selected runs (number of selected runs/number of total conventionally neutral runs = 6/39) (a), (b) and (c) and eddy conductivity (d), (e), (f) profiles calculated with O'Brien (dashed) and Grisogono method (solid) against $K(z)$ from the LES data (dots) for conventionally neutral conditions.

Figure 8 represents nocturnal stable conditions, where the O'Brien polynomial function tends to underestimate the LES data for K_m (Fig. 8a, 8b and 8c) by under-predicting the mechanical mixing in the surface-layer. In cases of weaker turbulence with $K_{\max}$ between 1 and 3 m^2 s^{-1}, K_h calculated with the O'Brien method is underestimated (Fig. 8d and 8e) while it is overestimated in stronger turbulence cases (Fig. 7d, 7e and 7f). Although the O'Brien and Grisogono methods agree better for K_h especially for the stronger turbulence cases, Grisogono method prevails.

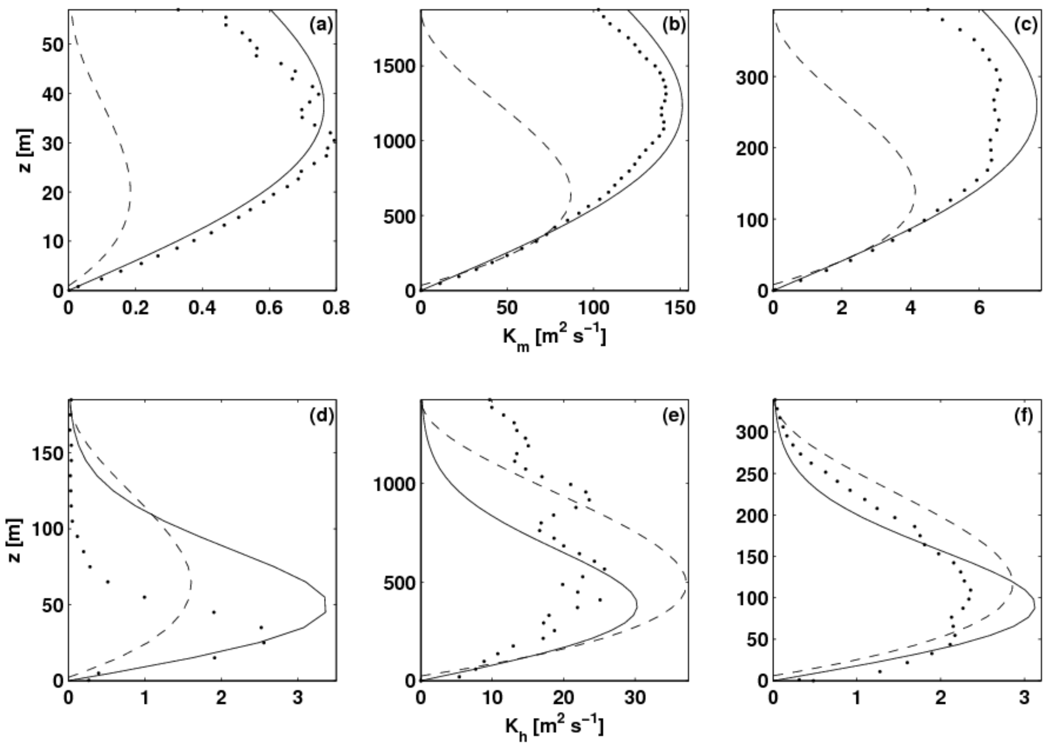

Figure 8. Same as in Fig. 7 but for the nocturnal stable conditions runs (number of selected runs/number of total nocturnal stable conditions runs = 6/31).

In the case of strong stability, Fig. 9, the results are similar for K_m. Both methods overpredict K_h compared to the LES data (Fig. 9d, 9e and 9f), probably because K_h in these conditions is very small and cannot be described with 'standard' parameterization methods; moreover, the overall scatter is high: turbulence is intermittent; vertical fluctuations are pronounced and K_h does not have a continuous vertical distribution. Similar results are found in Mahrt and Vickers (2006) for extremely weak mixing in stable conditions in FLOSSII. In the latter situation, typical K theory most probably fails due to intermittency, nonstationarity and measurement problems.

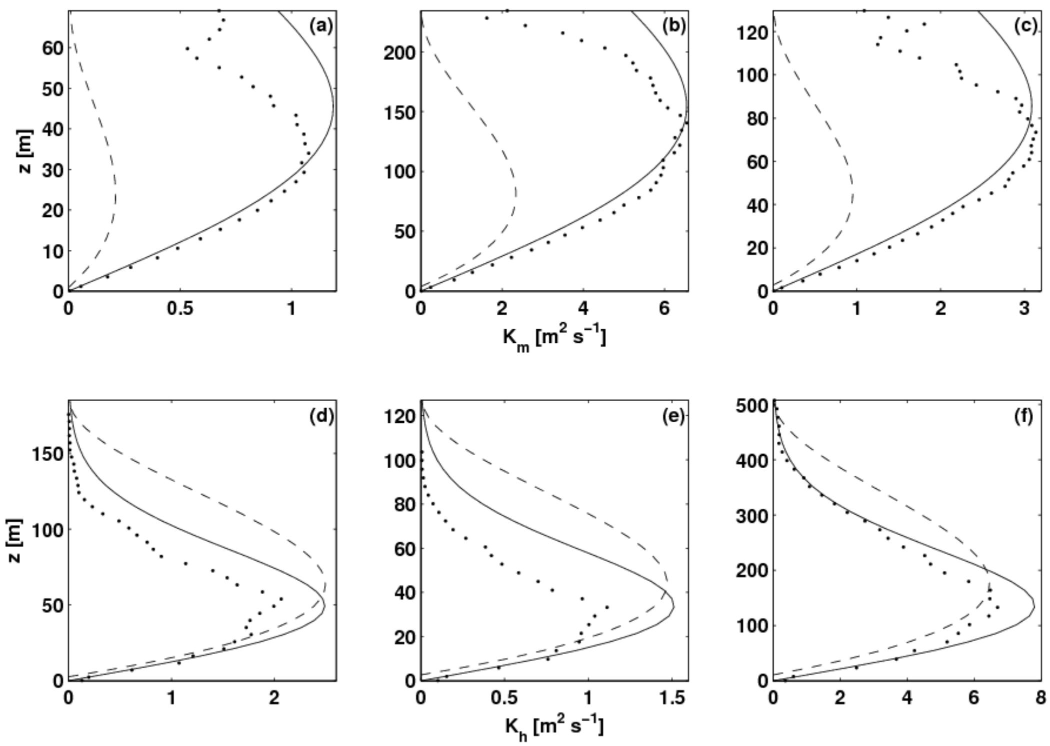

Figure 9. Same as in Fig. 7 but for the long-lived stable conditions runs (number of selected runs/number of long-lived stable runs = 6/15).

4.3 Verification of the *K*(*z*) schemes in the EMEP model

As it was previously explained in Sec. 2.4.1 the EMEP recommends that measuring stations are located away from large local emission sources. Not all the measurements are being representative for the evaluation of turbulence parameterization schemes in models. If the station is affected by local sources, irregular variability is observed in concentrations, which is not modelled, and underestimation as well as overestimation of the measurements may occur. Based on the operational EMEP model evaluation in the year 2001, discrepancies between the model and measurements are identified. Discrepancies with factor of 2 or more between the model and measurements are found on different stations which can be categorized as: (i) stations where peak events or episodes occurred in the measurements influenced by local emission sources, and stations in the vicinity of large emission sources (shipping area in the North Sea) and (ii) mountain stations.

An underestimation of NO_2 with *BIAS* < -30 %, is found at some stations in Ireland, Switzerland, Poland and Italy (not shown). For example, Payerne (CH02) in Switzerland is located relatively near the motorway, and therefore the corresponding measured $c(NO_2)$ had significantly higher values than the other EMEP stations in that region. An overestimation of $c(NO_2)$ is detected at Scandinavian stations, NO01, SE02 and DK08 located at the entrance to the Baltic Sea, where emissions from the shipping in the model are significant. A few other stations in the shipping area also had a notably high *BIAS* for SO_2, those are: DK03, DK05, DK08, EE11, IE02, GB07 and SE02. Since shipping emission paths are not sufficiently resolved due to the coarse horizontal resolution in the model, higher concentrations are horizontally diffused over larger areas (including analyzed stations, where obviously these high concentrations were not observed). Generally, stations in the North Sea shipping area are probably overestimated with the EMEP model due to the coarse model horizontal resolution but it might be due to other reasons e.g. emissions, meteorology, chemistry, etc. Stations with the highest discrepancies were excluded from the annual *r* and *BIAS* estimation. Changes in *r* and *BIAS* values, obtained by varying two different *K*(*z*) schemes in the model, are analyzed at all available stations in the EMEP domain (Figs. 13, 14, 15 and 16). Stations with the highest uncertainties were excluded from the yearly *r* and *BIAS* estimation (Fig. 17).

4.3.1 Evaluation of the operational EMEP model performance in the year 2001

The operational EMEP model performance has been regularly assessed by comparison with observations of air and precipitation data complied in the EMEP network. Results of the model evaluations have been published in the official reports (http://www.emep.int/publications.html). The operational model set-up is evaluated based on *r* and *BIAS* values between the observed daily surface NO_2, SO_2 and SO_4^{2-} concentrations ($c(NO_2)$, $c(SO_2)$, $c(SO_4^{2-})$) and the corresponding modelled values in the year 2001 for different EMEP stations (Fig. 2). Evaluation shows a good agreement with measurements and the correlation coefficient $0.5 \le r\,(NO_2) \le 0.75$ is found on 56 % stations, $0.5 \le r\,(SO_2) \le 0.77$ is on 43 % stations, and $0.5 \le r\,(SO_4^{2-}) \le 0.87$ is on 86 % stations. It should be pointed out that $r\,(SO_4^{2-})$ is the highest among all analyzed species with $r\,(SO_4^{2-}) > 0.7$ on 31 % stations. Based on one year of data it is found that the model underestimates the measured $c(NO_2)$ with $BIAS\,(NO_2) \approx$ -20 %. Since main emission source of NO_2 is traffic, it is likely that some stations are influenced by the local sources and may not be considered as a representative background stations. For the SO_2 generally an overestimation is found with the EMEP model on 71 % stations with $BIAS(SO_2) \approx 30\%$, while the model generally underestimates sulphate with $BIAS(SO_4^{2-}) \approx -12\%$. The overestimation of SO_2 and the underestimation of sulphate indicate that other processes responsible for sulphate formation in the model should be investigated as well as meteorology, particularly precipitation and moisture provided by the NWP model. The analyzed year was not exceptional regarding meteorological conditions and the EMEP model performance is in agreement with the previous evaluation results (Fagerli et al., 2003).

4.3.2 Time series

The annual time series of the observed and modelled $c(NO_2)$ during year 2001 are represented in Fig. 10 for two selected stations: a) Westerland/Wenningstedt (DE01) with $r > 0.7$ and b) Svratouch (CZ01) with $r \approx 0.1$. Although the agreement between the modelled and the observed $c(NO_2)$ in other periods is good, the summer peaks at e.g. CZ01 are not captured by the model, which leads to lower values of *r*. Note that the both applied $K(z)$ schemes have similar performance during the peak events.

Further, peaks in $c(SO_2)$ and $c(SO_4^{2-})$ that are not captured in the model are also observed during the year. The time series of $c(SO_2)$ in year 2001 are shown in Fig. 11 for two selected stations: a) Illmitz (AT02) with $r > 0.75$ and b) Vorhegg (AT05) with $r = 0.25$. Lower *r* at AT05 is likely to be a consequence of discrepancies between the model and the observations during the peaks events. For SO_4^{2-} only a few stations have lower *r* values also with stronger local influence. The time series of $c(SO_4^{2-})$ are shown in Figure 12 for a) Neuglobsow (DE07) with $r \approx 0.8$ and b) Peyrusse Vielle (FR13) with $r \approx 0.25$.

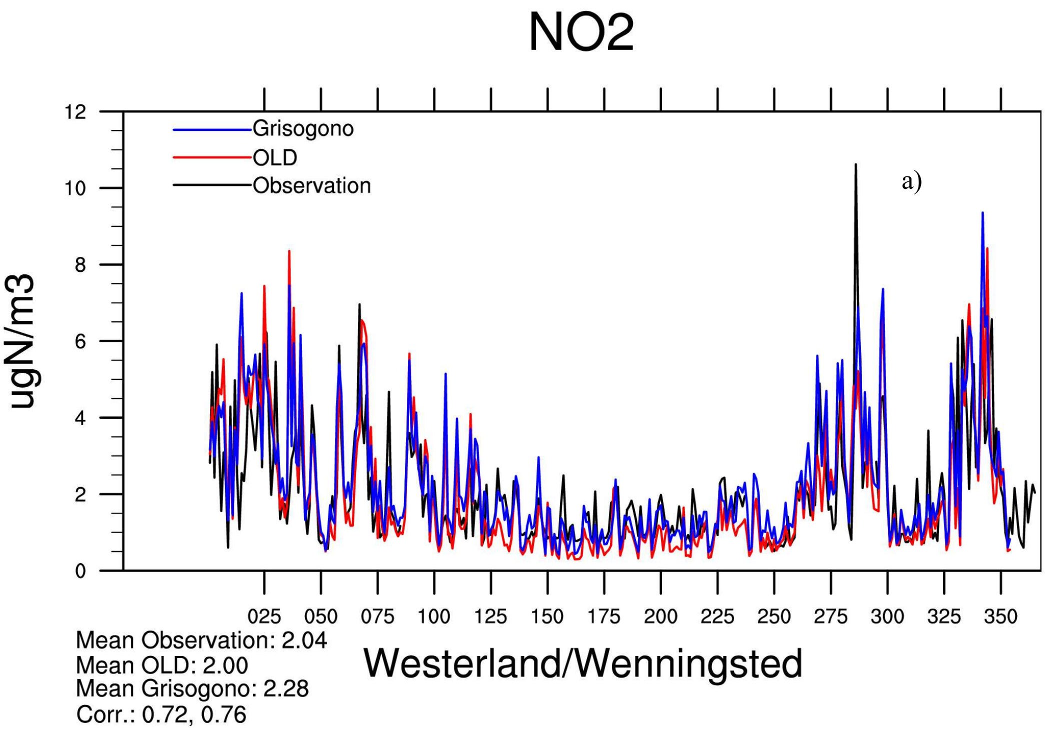

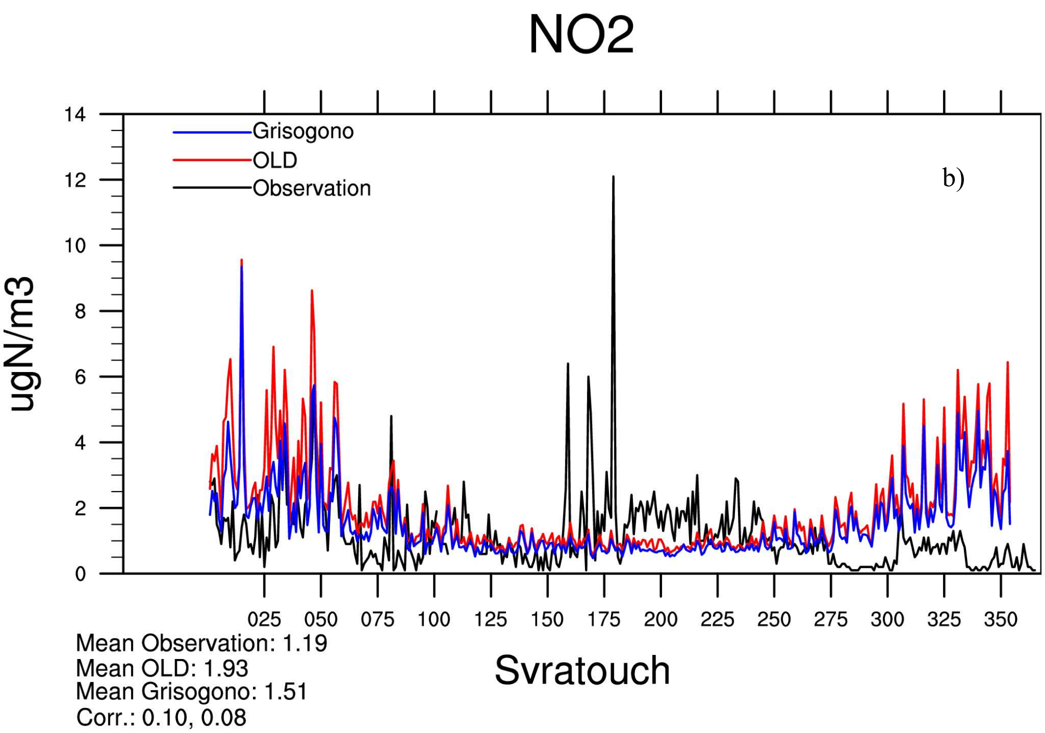

Fig 10. Time series of the measured (black line) and the modelled daily surface NO_2 concentrations (μg (N) m^{-3}) for: a) Westerland (DE01) and b) Svratouch (CZ01) in year 2001. Modelled results are obtained with two different vertical diffusion schemes: O'Brien (red line) and Grisogono (blue line). Time is given on x-axes in Julian days.

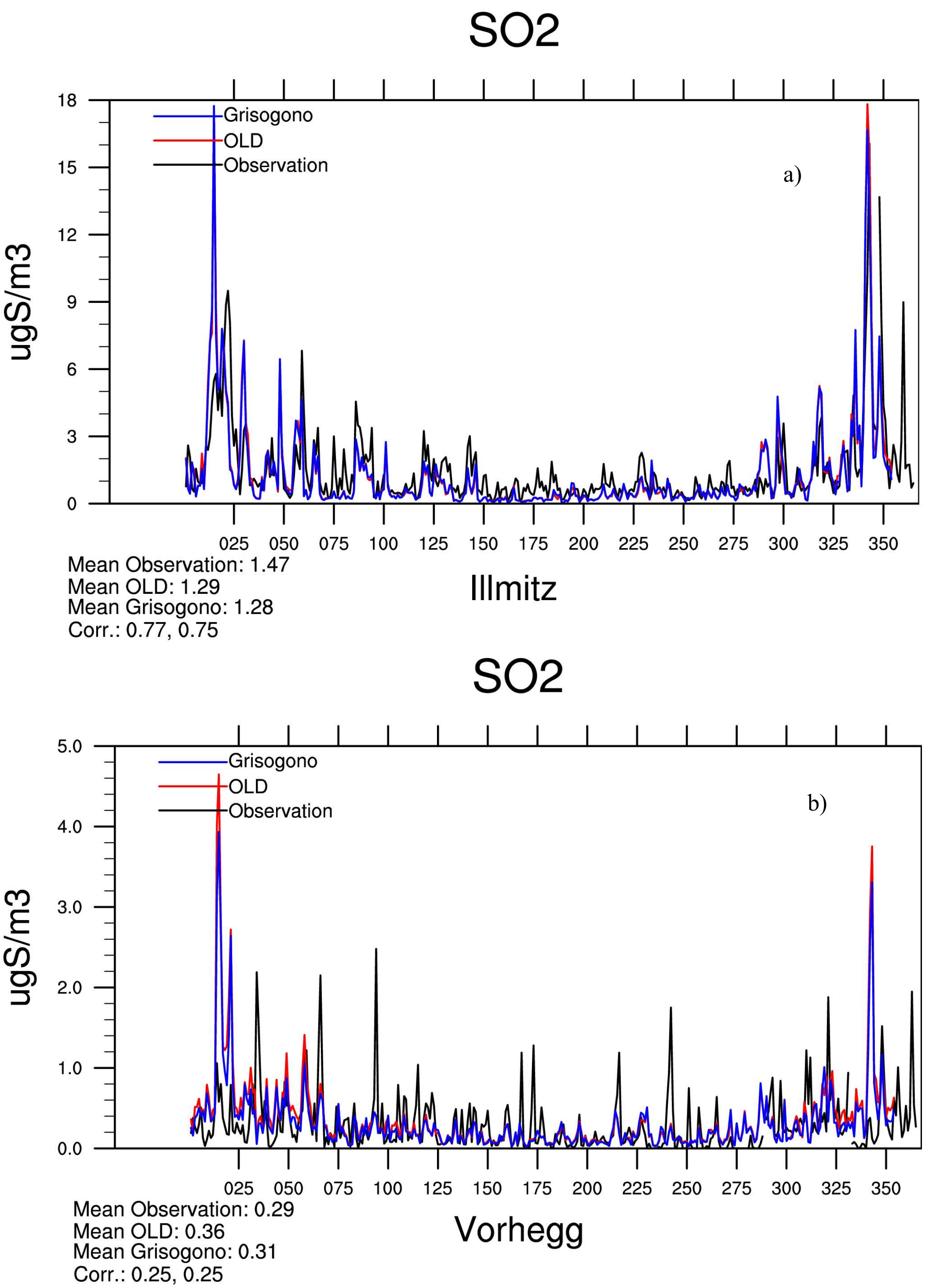

Fig 11. Same as Fig. 10 but for SO_2 (μg (S) m^{-3}) on the stations: a) Ilmitz (AT02) and b) Vorhegg (AT05).

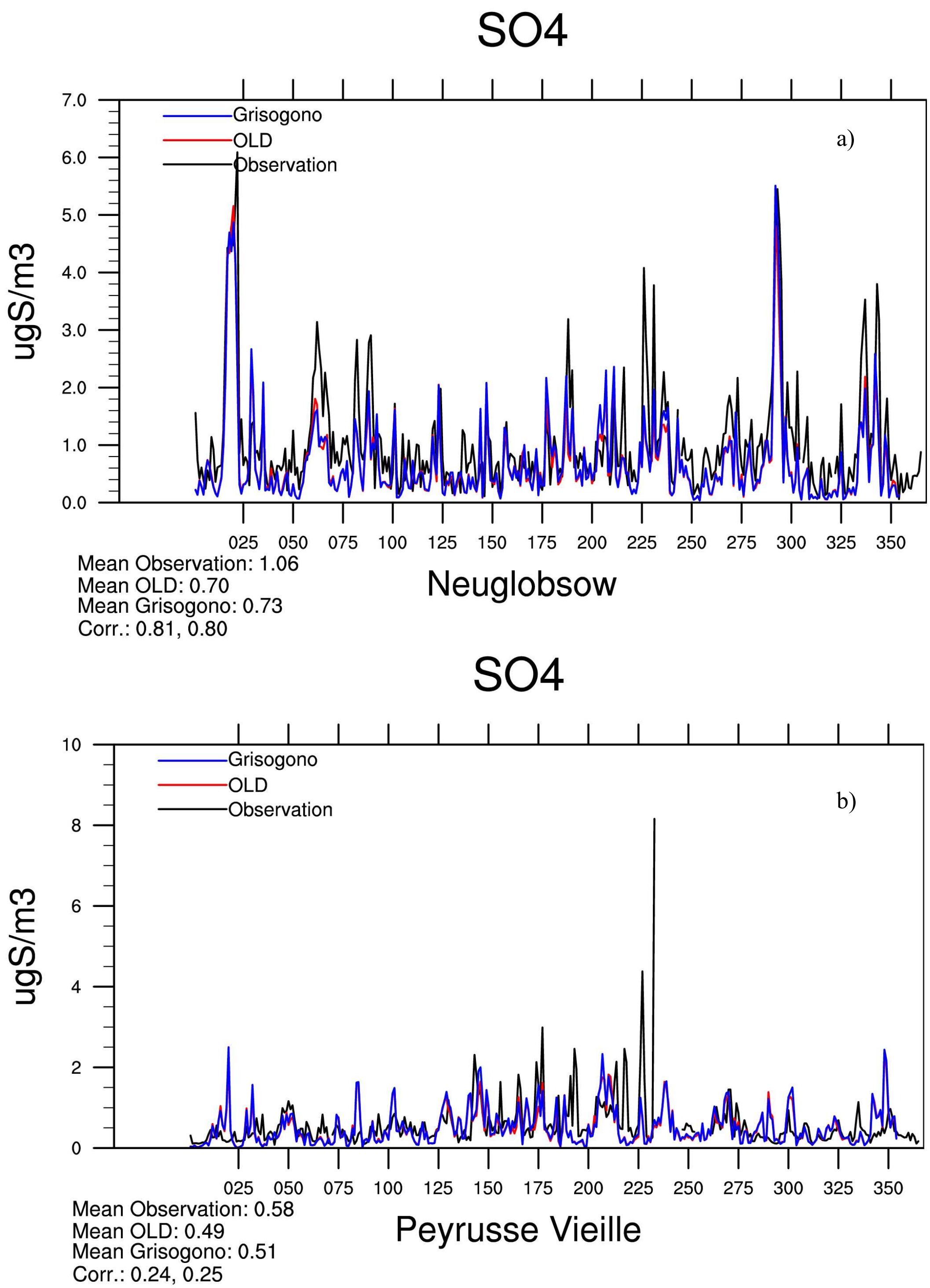

Fig 12. Same as Fig. 10 but for SO_4^{-2} (μg (S) m^{-3}) on the stations: a) Neuglobsow (DE07) and b) Peyrusse Vielle (FR13).

4.3.2 Evaluation of the Grisogono *K*(*z*) scheme

In order to quantify changes with the new *K*(*z*) scheme, *RD*(*r*) is given for NO_2 in Fig. 13a. The modelled absolute values and *BIAS* are very sensitive to the balance between the different processes in the model. Therefore, a smaller *BIAS* between the model and measurements does not necessarily mean that the new scheme is better than the old; it only means that average concentrations determined with the new scheme are closer to the average of the observed concentrations. However, the *BIAS* can give insight into the general effect of the new scheme on the modelled values. For instance, if the Grisogono parameterization is less diffusive in stable conditions (Jeričević and Večenaj, 2009) this should lead to higher average concentrations in these cases. The temporal correlation coefficient, however, is a better measure for whether the new scheme provides a better physical description. Therefore, we focus on the changes in the correlation coefficient between the model results and observations.

The improvements are found in *r*(NO_2) up to 0.1 with the Grisogono scheme are found on 51% stations (mainly at stations in Central Europe) while on 14 % stations there was no change in *r* with the change of *K*(*z*) scheme, and on 35 % stations *r*(NO_2) is lower with the new scheme (Fig. 13a). Higher increase in *r* (SO_2) up to 20-50 % with the new *K*(*z*) scheme is found on 54% stations (Fig. 13b); *r* (SO_2) remained the same on 22% stations, while on 24 % stations a smaller decrease was found. For SO_2 (Fig. 13b), an improvement using the new scheme is found on more stations than for NO_2, except for the stations in Scotland and in the shipping area. There is a generally an increase in *r* (SO_4^{-2}) with the higher improvement in *r*, around 45 % and 20 %, on Slovakian stations SK02 and SK04 respectively (Fig. 13c). However, stations in the shipping and mountain area mainly did not exhibit improvements in *r*, except *r* SO_4^{-2}) increased in mountain area with implementation of the new *K*(*z*) scheme. Values of *RD* (*BIAS*) for NO_2, Fig. 14a, show that on 60% of analyzed stations *BIAS* (NO_2) is lowered ≈ 10 % with the new *K*(*z*) scheme. Stations with *RD* (*BIAS*) > 0, i.e. increased *BIAS* (NO_2) with the Grisogono scheme*,* are mainly those with an improvement in *r* except at SE02, SE08, CH01 and DE08.

Values of *RD* (*BIAS*) for SO_2 are shown in Fig. 14b, and mainly improvement is found with the new *K*(*z*) scheme; on 50 % stations *BIAS* (SO_2) is decreased, on 23% stations there is no change in *BIA S*(SO_2) values and on 26 % stations there is an increase in *BIAS* (SO_2). For SO_4^{-2} (see Fig. 14c) on nearly 64 % stations, lower *BIAS* with *D* (*BIAS*) ≈ -10 % is found with the new scheme.

Evidently SO_4^{2-} had the most harmonized changes, at most of analyzed stations, with the change of $K(z)$ scheme.

The spatially interpolated annual correlation coefficients a) $r(NO_2)$, b) $r(SO_2)$ and c) $r(SO4)$ for the operational EMEP model, and the spatially interpolated differences in annual r values, $D(r)$, acquired with the new $K(z)$ scheme d) $D(NO_2)$, e) $D(SO_2)$ and f) $D(SO_4)$ are shown in Fig. 15. The available measurements in the year 2001 from the EMEP network are used.

Upper panels represent the operational model performance while the lower panels shows improvements (blue colour) and deteriorations (red colour) in r values as a consequence of different $K(z)$ scheme employment in the EMEP model. There are still some areas where the OLD method has better performance. For NO_2 it is the Scandinavian and Central Europe area, for SO_2 it is mainly for the stations in northern part of Great Britain and for sulphate similar or lower results are obtained in the Scandinavia, Great Britain and Hungary. Spatial interpolation analysis should be carefully analyzed since results may be determined by a low number of stations (Central and Eastern Europe).

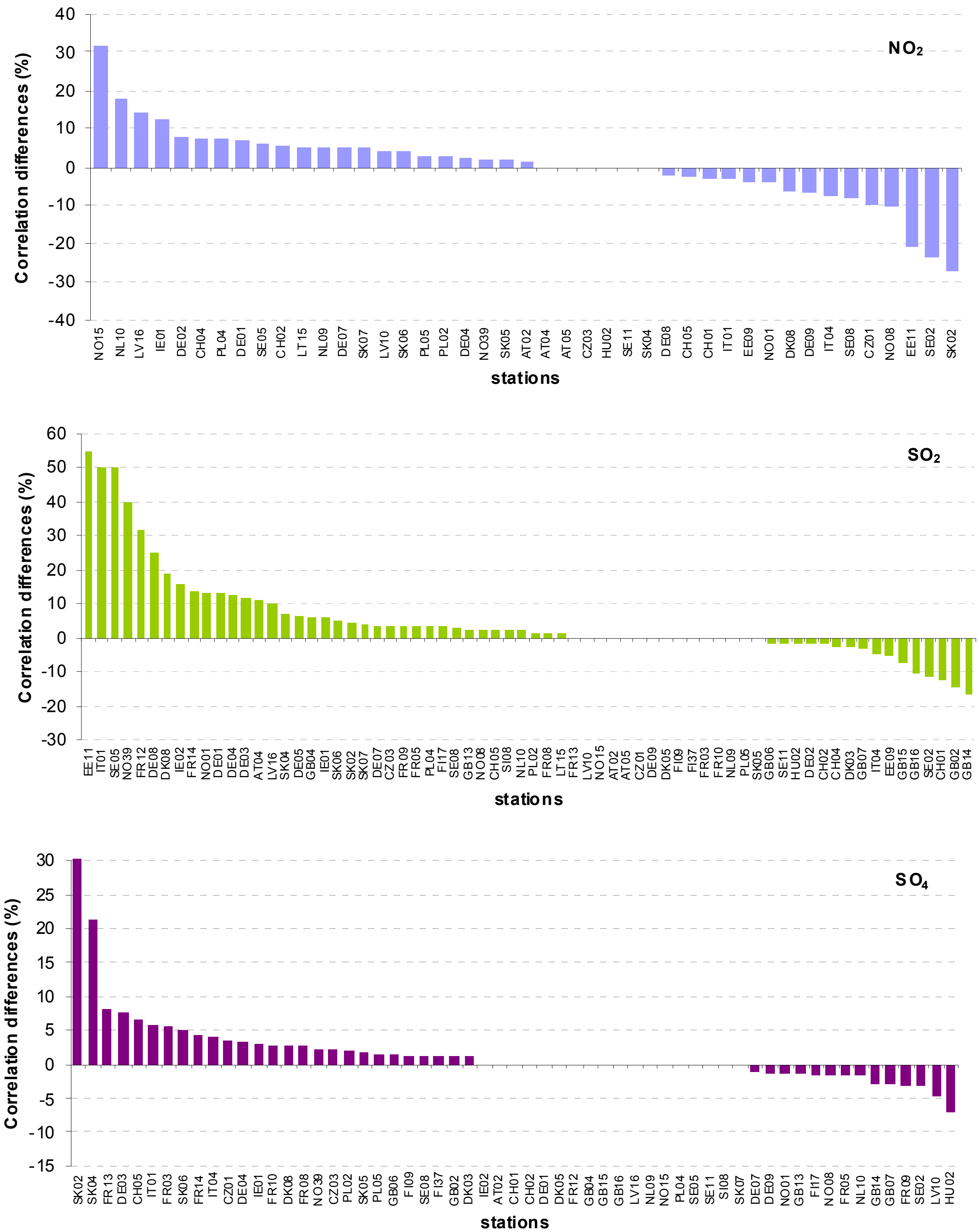

Fig. 13. Relative differences in correlation coefficients, $RD(r)$, calculated between the two EMEP modelled data sets and the observations from the EMEP stations in year 2001 for: a) NO_2, b) SO_2 and c) SO_4^{2-}. Values $RD(r)$ >0 denote a better performance of the Grisogono scheme.

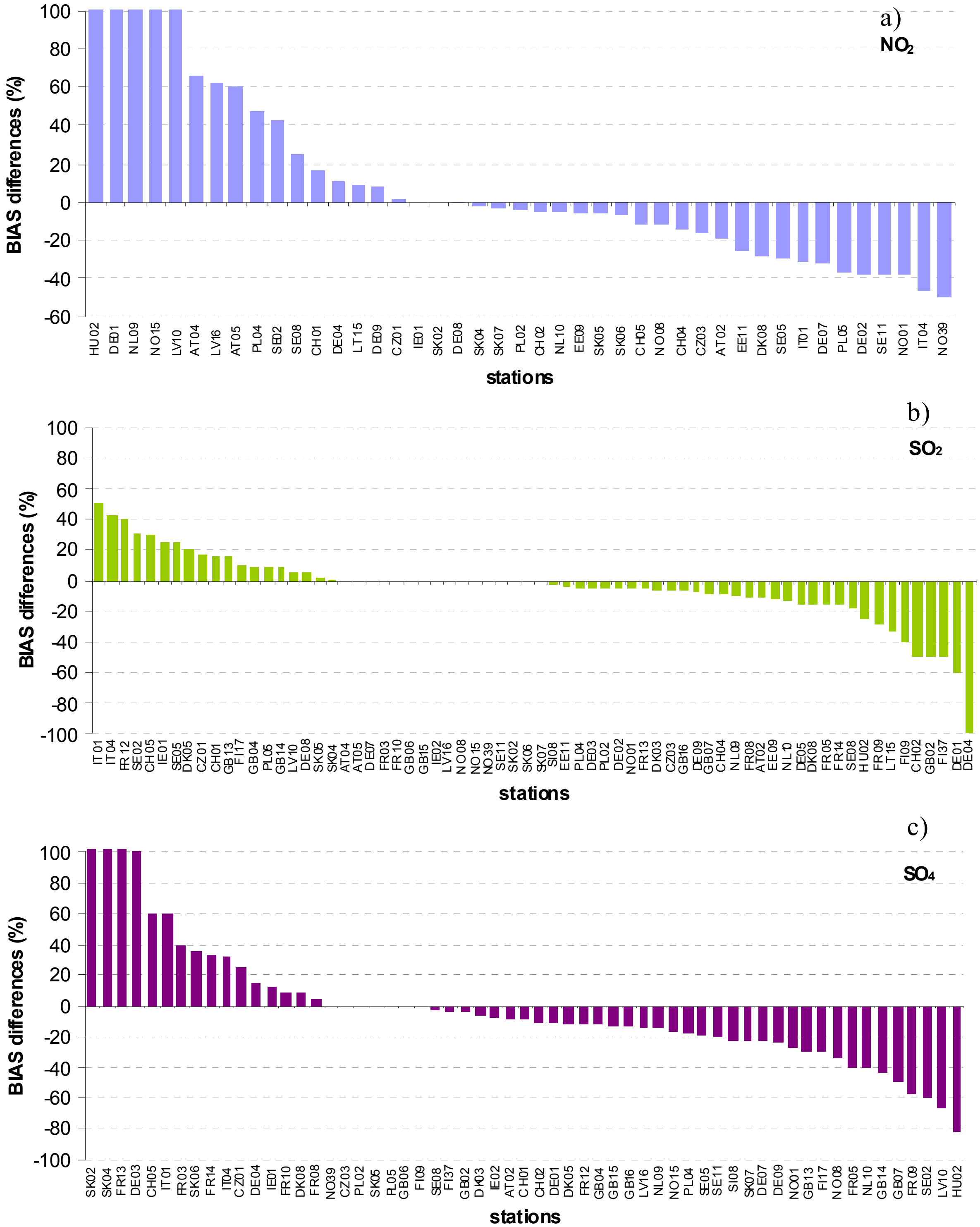

Fig 14. Same as in Fig 12 but for relative differences in *BIAS*, *RD* (*BIAS*). Now the values *RD* (*BIAS*) <0 denote a better performance of the Grisogono scheme.

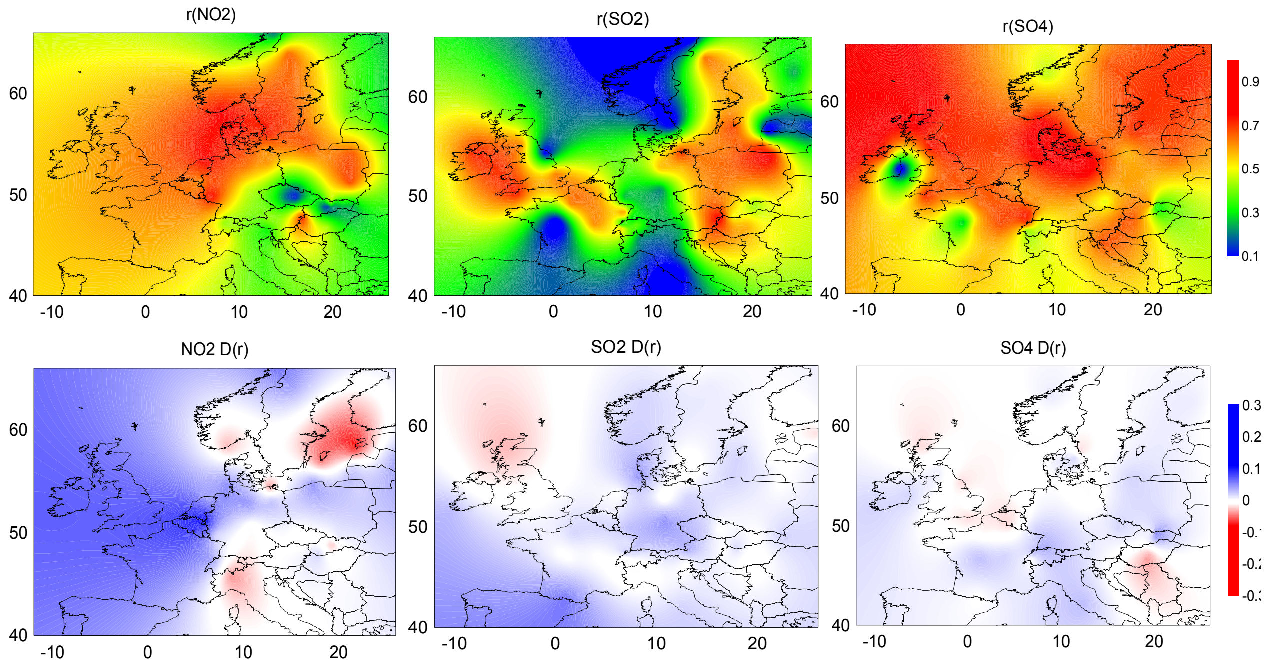

Fig 15. The spatially interpolated annual correlation coefficients a) $r(NO_2)$, b) $r(SO_2)$ and c) $r(SO_4^{2-})$ for the operational EMEP model, and the spatially interpolated differences in annual r values, $D(r)$, acquired with the new $K(z)$ scheme d) $D(NO_2)$, e) $D(SO_2)$ and f) $D(SO_4^{2-})$. The available measurements in the year 2001 from the EMEP network are used.

In order to investigate seasonal variability of $K(z)$, represented with the two different schemes, the NO_2 is further analyzed. Yearly course of a) r values, b) *BIAS* values, c) *RMSE* and d) average monthly concentrations of NO_2 calculated between the measurements and modelled $c(NO_2)$ values with two $K(z)$ schemes, the Grisogono (blue line) and the OLD (red line) are displayed in Fig. 16. All analyzed stations with $c(NO_2)$ measurements during year 2001 are taken into account. In Fig. 16a systematically higher r values with the new $K(z)$ scheme are shown in both: stable conditions, more characteristic during the colder part of the year, and unstable conditions, during the warmer part of the year. According to *BIAS* (Fig. 16b), in the warmer part of the year, the model underestimates $c(NO_2)$ with both $K(z)$ schemes. Furthermore, *RMSE* in Fig 16c is also the lowest during the summer time. The measured and modelled mean monthly NO_2 values in Fig 16d show decrease of $c(NO_2)$ during the warmer part of the year. This drop in $c(NO_2)$ is caused by increased photolysis of NO_2 and more vigorous vertical mixing during the warmer period. Note the higher $c(NO_2)$ values with the new $K(z)$ scheme during the warmer part of the year, which shows that the new $K(z)$ scheme is less diffusive in more convective conditions than the operational scheme. In Fig 16d note that average monthly values with both schemes are similar during the colder part of the year, while the second peak in November was not captured with the either model. Nevertheless, *r* is higher with the new scheme in winter stable conditions also.

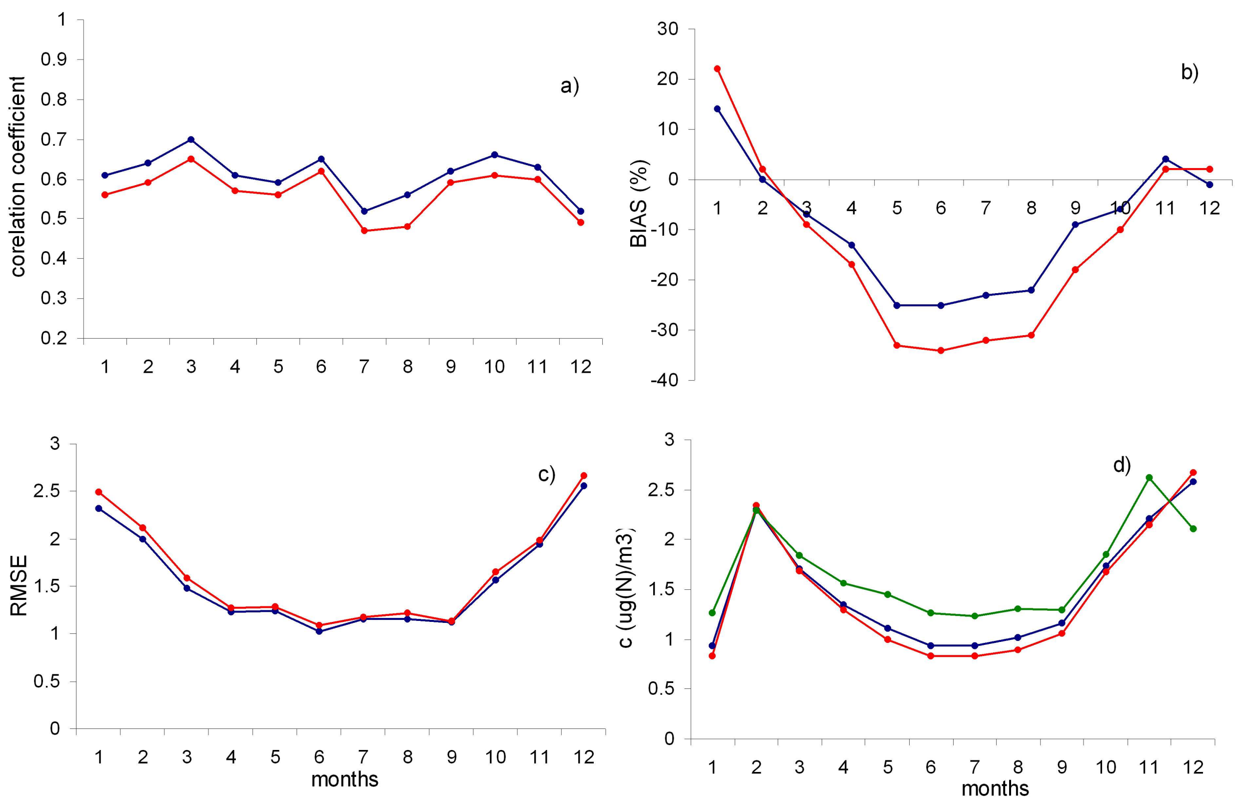

Fig. 16. Annual course of: a) *r*, b) *BIAS*, c) *RMSE* between the measured and modelled $c(NO_2)$ and d) average monthly $c(NO_2)$ values in year 2001. Two different *K*(*z*) schemes were used the OLD (red) and Grisogono (blue), monthly averages calculated from the observations are marked with green line (d).

Finally, r and $BIAS$ are also calculated for all stations for the year 2001 between the measured and the modelled $c(NO_2)$, $c(SO_2)$ and $c(SO_4^{-2})$ values. In Fig. 17 yearly scatter plots between the measured and modelled daily surface concentrations are shown. For NO_2, r = 0.65 with the Grisogono, while r = 0.63 is achieved with the OLD method. $BIAS$ is similar for NO_2, with the Grisogono method, $BIAS$ = -18 % and $BIAS$ = -17 % with the O'Brien method. The correlation coefficient r = 0.57 is found for SO_2 with the Grisogono while for the OLD method r = 0.55. According to the $BIAS$ values the model generally overestimates SO_2 around 27 % with the Grisogono and 30 % with the OLD method. It should be pointed out that the stations with large overestimations, i.e. mountain and stations under strong influence of shipping are excluded from this analysis because they are not representative for the model grid-cell. For SO_4^{2-}, the result is similar for both methods; $r \approx 0.64$ and $BIAS \approx$ -19 % with the original scheme and $BIAS \approx$ -13 % with the new $K(z)$ scheme.

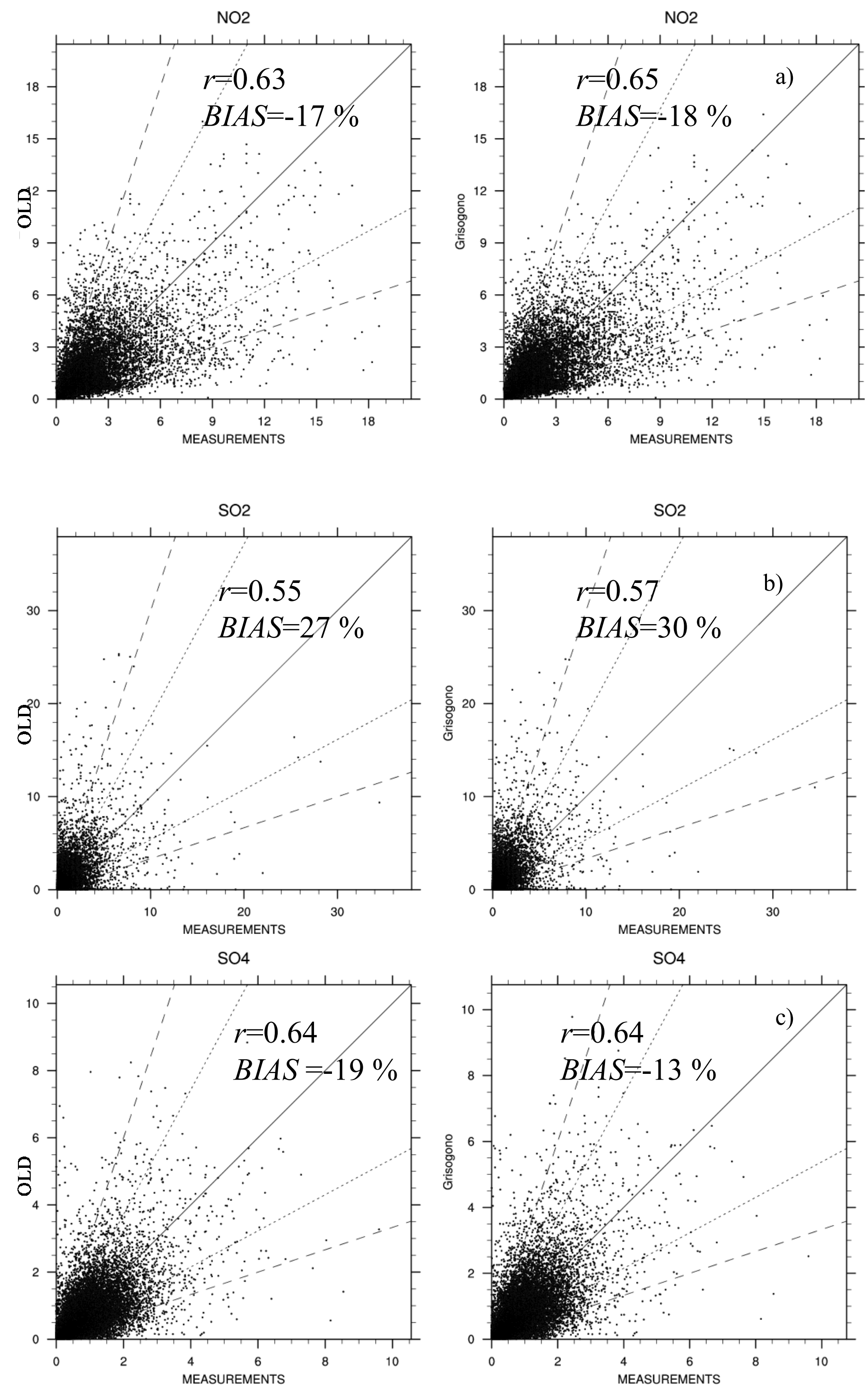

Fig 17. Annual scatter plots between the measured and modelled a) $c(NO_2)$, b) $c(SO_2)$ and c) $c(SO_4)$ values. Modelled concentrations are determined with two $K(z)$ schemes: OLD (left panel) and Grisogono (right panel) for all analyzed stations in the EMEP domain in 2001.

4.4 Boundary layer height verification

In the EMEP model schemes for calculation of H, the operational and the new ABL scheme based on Ri_B number are compared. Evaluation was performed on two data sets: (i) radiosoundings from 24 different measuring stations in Europe (Table 2) during January and July in year 2001 and (ii) on vertical temperature and wind measurements in year 2001 from the Cabauw tower.

4.4.1 Radiosounding data

For January and July in year 2001, *r* and *BIAS* values are calculated at available UTC times (Table 2) between H determined from the soundings (H_{sond}), and H calculated from the EMEP model (H_{EMEP}) with the operational scheme (H_{old}), and the Ri_B scheme (H_{new}). Values of H_{sond} are determined with the Ri_B scheme. Fig. 18a shows correlation coefficients in January, and for most of the analyzed stations $r \approx 0.5$. Lower values of $r \approx 0.3$ are found at Torshaven, Legionowo, Practica di Mare and Izmir station (Table 1), and higher values $r \approx 0.7$ are found at: Stavanger, Herstmonceux, Uccle and Trappes. While H_{new} shows a slight improvement in *r*, there is a considerable improvement in *BIAS* values, see Fig. 18b. The model underestimates H_{sond} with the operational scheme ($BIAS \approx$ - 50 %), while with the new ABL scheme the underestimation is significantly lower ($BIAS \approx$ - 20 %). Overestimations are found for Payerne and Meiningen, the two stations in the Alps area. Fig. 18c shows the average monthly H which is calculated from soundings ($\overline{H}_{sond}$), with values 200 m < $\overline{H}_{sond}$ < 600 m. The highest $\overline{H}_{sond}$ are found for the stations located in the Southern Europe e.g. Madrid, La Coruna and Izmir. The only exception among northern stations is Torshaven with a somewhat higher $\overline{H}_{sond}$. On the other hand, the lowest $\overline{H}_{sond}$ in January are found for the stations in the Central Europe e.g. Prague, Vienna, Wroclaw and Milan, which is expected, because of long stable conditions during the winter, which occur over the continent and the corresponding H are usually low. During January $\overline{H}_{sond}$ is generally higher than the average H calculated from the model with the old ($\overline{H}_{old}$), and the new ($\overline{H}_{new}$), scheme (see Fig. 17c). Average monthly H values for different stations are in range: 200 m < $\overline{H}_{old}$ < 400 m, while for the new method: 400 m < $\overline{H}_{new}$ < 600 m.

Fig. 19 shows time series of H in January for four selected locations; two with the higher r Herstmonceux and Stavanger, Figs 19a and 19b respectively, and two with the lower r Torshaven and Legionowo, Figs 19d and 19c respectively. For Herstmonceux and Stavanger the agreement between H_{sond} and H_{EMEP} is good, especially with the new ABL scheme. Note a period of low $H_{EMEP} \approx 50$ m (Figs 19b, 19c and 19d), simulated in the model which occurred from 13 to 20 January 2001. Simulated lower values of H_{EMEP} are connected with the high pressure system movement across the Northern Europe (not shown), starting from the Island at 13 January 2001 and moving across the Europe to its end position over Russia at 20 January 2001.

For that period at the stations Herstmonceux and Stavanger, $H_{sond} \approx H_{EMEP}$, and Torshaven and Legionowo are $H_{sond} - H_{EMEP} \approx 1000\,\mathrm{m}$ and $H_{sond} - H_{EMEP} \approx 500\,\mathrm{m}$ respectively. This disagreement between H_{sond} and H_{EMEP} at Torshaven and Legionowo during the stable conditions is the main cause for the corresponding lower r values.

July 2001 over the continent was characterized with convective, unstable conditions during the day time, and strong near surface inversions during the night. Generally, in July r is much higher for the both ABL methods, $r \approx 0.7$ (Fig. 20a) as compared with $r \approx 0.5$ (Fig. 18a) in January. During the summer time both ABL methods perform equally well, however slightly better results, according to r, are found with the operational ABL scheme than with the new ABL scheme employed in the EMEP model. According to *BIAS*, Figure 20(b), the model underestimates H_{sond} with the similar magnitude with both ABL methods. Note spatial variation of *BIAS* in July. The lowest *BIAS* values are found in the Central European area where *BIAS* ≈ -20%, see Figure 20b and the corresponding $\overline{H}_{sond} \approx 800$ m; $\overline{H}_{EMEP} = 700$ m, see Figure 20c. In the Northern Europe *BIAS* ≈ -40% and the corresponding $\overline{H}_{sond} = 1000$ m; $\overline{H}_{EMEP} = 600$ m. The underestimation is the highest in the Southern Europe with *BIAS* ranging from -60 % to -80 % where $\overline{H}_{sond}$ obtains the highest values, $\overline{H}_{sond} \approx 1200$ m. Time series in July (Fig. 21) show diurnal variation of H from the night-time low H in the statically stable conditions toward high daily H values in the convective unstable conditions. The model captures H_{sond} daily variations and good agreement between H_{sond} and H_{EMEP} is found e.g. for Meiningen $r = 0.91$ and Madrid $r = 0.84$ with the new ABL scheme. Note that, at Lisbon and Torshaven, H_{sond} are significantly higher than H_{EMEP}. The modelled H_{EMEP} were almost constant in time and consequently the corresponding lower r and higher *BIAS* values were found at those stations. Note that *BIAS* at Lisbon is the highest among all analyzed stations. Lisbon station is located near the boundary of the model domain where the modelled results are dominated by weakly varying lateral boundary conditions. Furthermore, the model was not able to reproduce variability shown in H_{sond} both in January and July at Torshaven station located on the Faroe Islands in the Atlantic Ocean. The Faroe Islands are situated entirely within one grid cell in the model and the model was incapable to realistically represent H in the complex coastal orography due to still relatively low model resolution.

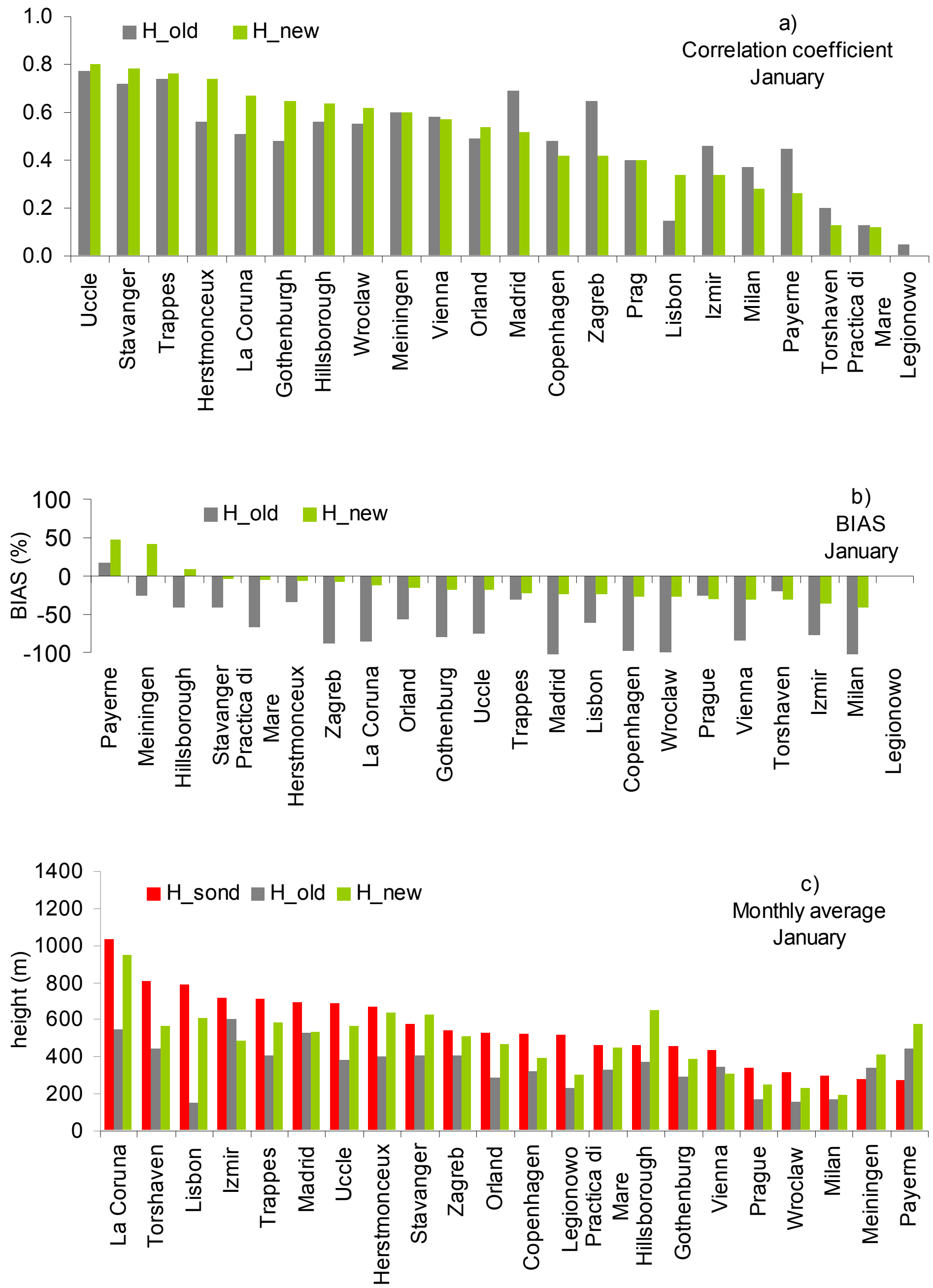

Figure 18. Monthly (a) *r*, (b) *BIAS* and (c) average calculated between the ABL height, H, determined from the soundings (H_{sond}), and H calculated from the EMEP model with the operational scheme (H_{old}) and with the Ri_B scheme (H_{new}) for different radiosounding stations in Europe (Table 1) in January 2001 at 12 and 00 UTC.

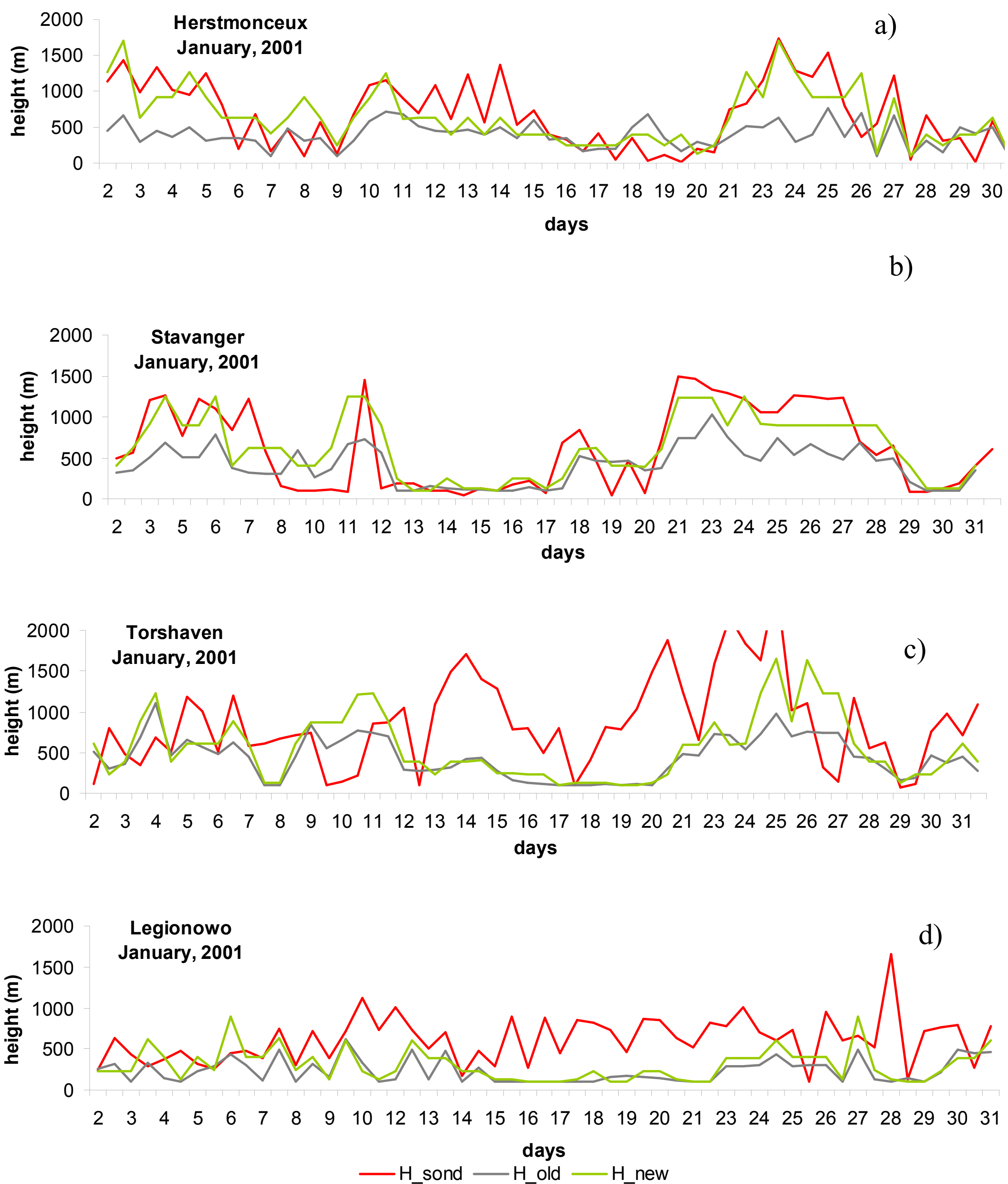

Fig 19. Time series of H_{sond}, H_{old} and H_{new} at (a) Herstmonceux, (b) Stavanger, (c) Torshavn and (d) Legionowo in January 2001.

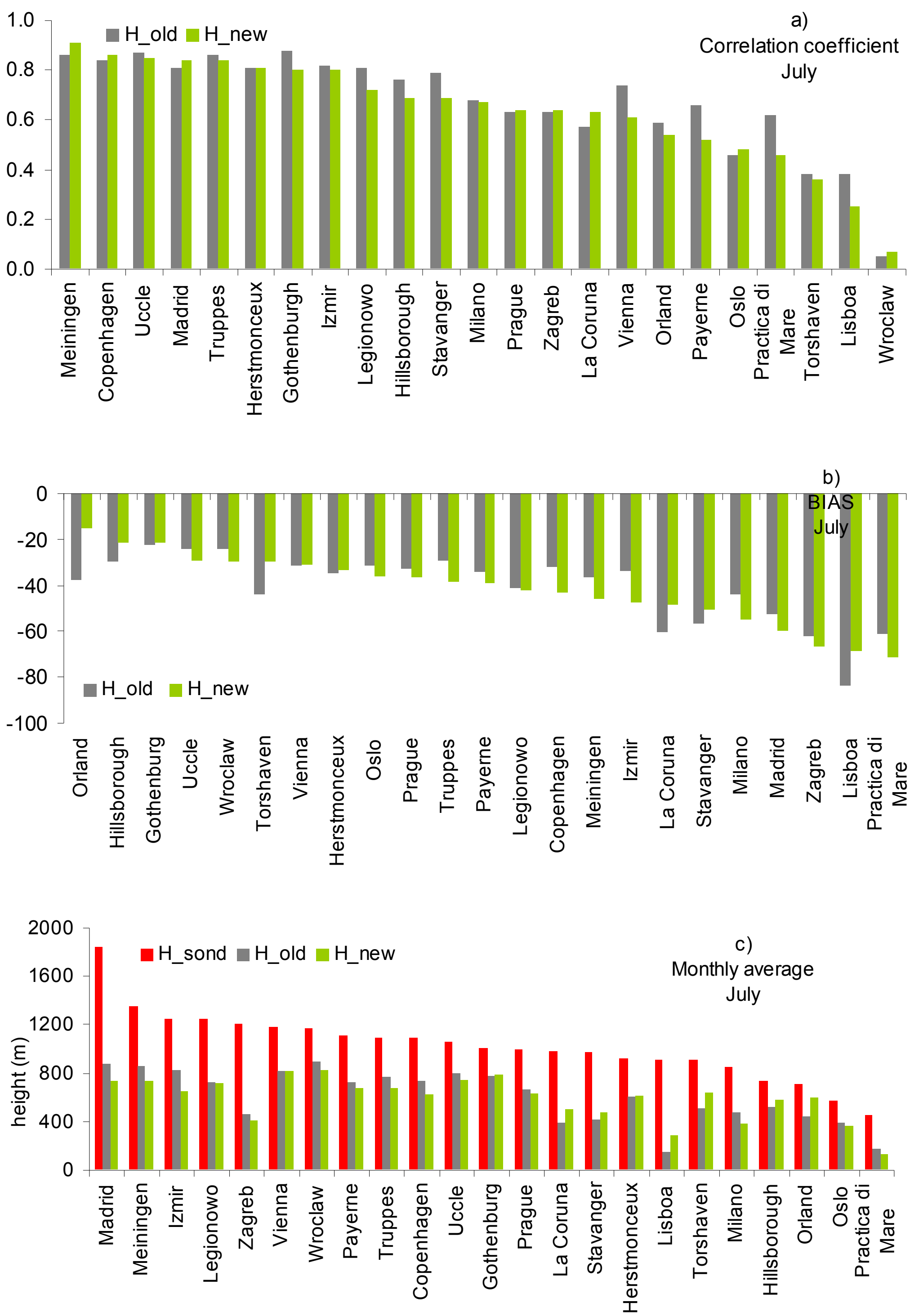

Figure 20. Same as Fig 18 but for July, 2001 at 12 and 00 UTC.

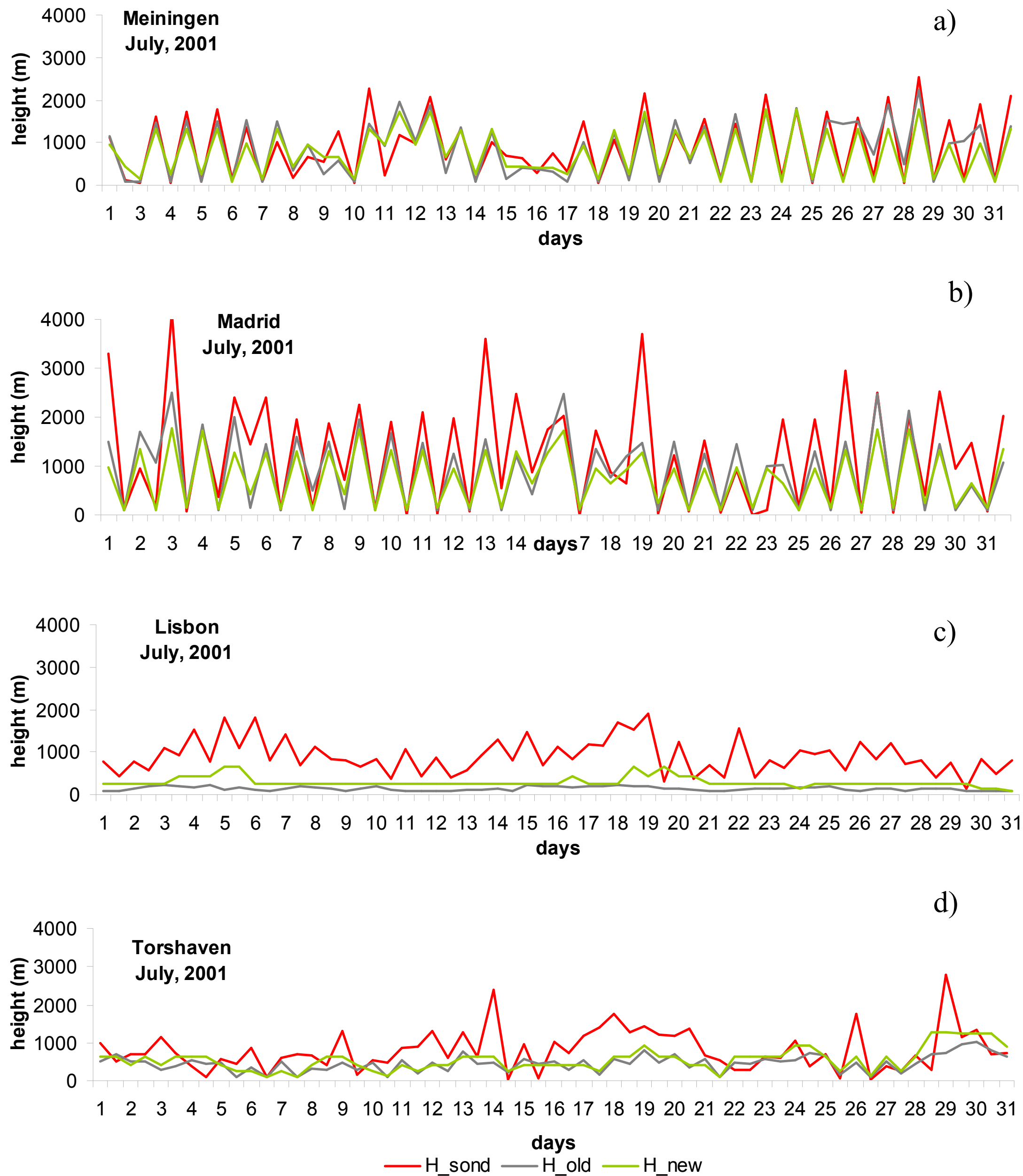

Figure 21. Same as Fig 19 but for (a) Meiningen, (b) Madrid, (c) Torshavn and (d) Lisbon in July 2001.

4.4.2 The Cabauw data

In this section a procedure for deriving H with the Ri_B number method from the Cabauw measurements is described first. Following average hourly vertical profiles of Ri_B number, ($\overline{Ri_B(z_j,t)}$), where j = 10, 20,…, 200 m are the measuring levels; and the corresponding H are analyzed and described for every month in year 2001 (Fig. 22).

As mentioned the boundary layer height from the Cabauw data (H_{tower}) is determined with the Ri_B method. Vertical profiles of the Ri_B number are calculated from the temperature and the wind measured at every tower level with the time interval Δt = 10 minutes during year 2001. In this way the sequence of $Ri_B(z,t)$ values for the year 2001 is produced and monthly averaged to obtain Ri_B daily courses, ($\overline{Ri_B(z_j,t)}$) for every month in year 2001 (Fig 22). It is relatively easy to follow daily and seasonal variations of H by looking at the Ri_{BC} = 0.25 (the top of blue area in Fig 22).

The analysis of $\overline{Ri_B(z_j,t)}$ provide good insight in processes of development and decay of the CBL and the SBL in different times of the year. The occurrence of the morning and the afternoon transition layer, characterized with a sudden and rapid decay/increase of the CBL, is also shown. In January, Fig. 22a, during the night-time H is often less than 100 m. Daily development of H starts after 10 AM reaching the maximum $H \approx$ 200 m at 1 PM and lasting approximately 1 hour after which H decreases. In Fig. 21b results for February are shown with SBL ranging between 100 m and 200 m, while CBL starts to develop around 8 AM reaching the maximum in the period between noon and 2 PM. In February the afternoon transition layer occurs around 3 PM. Note that the transition layer has similar characteristics for the most of the analyzed months in year 2001. In the following months of spring and summer, from March (Fig. 22c) to August (Fig. 21h), CBL is progressively intensifying, becoming more and more unstable. In the warmer part of the year CBL lasts longer, which is expected since CBL is strongly correlated with the incoming solar radiation. Note the appearance of the areas with $\overline{Ri_B(z_j,t)} < 0$ numbers (yellow area in Fig. 22) in April and becoming largest in June, Fig 22f. On the contrary, during SBL conditions, even in the warmer part of the year, strong near surface inversions and weak winds are measured in the surface layer. In the night-time SBL conditions, $Ri_B(z_j,t) >> Ri_{BC}$ (white areas in Fig. 22) is found and the corresponding H is extremely low. In September and October periods stable conditions prevail and the SBL is only 100 m - 150 m thick. In November and December, Fig. 22k and Fig. 22l respectively, dominantly stable conditions with mostly $\overline{Ri_B(z,t)} > 0$ prevail. In December unstable conditions occur from 10 AM to 14 PM and the average H is only 50 m.

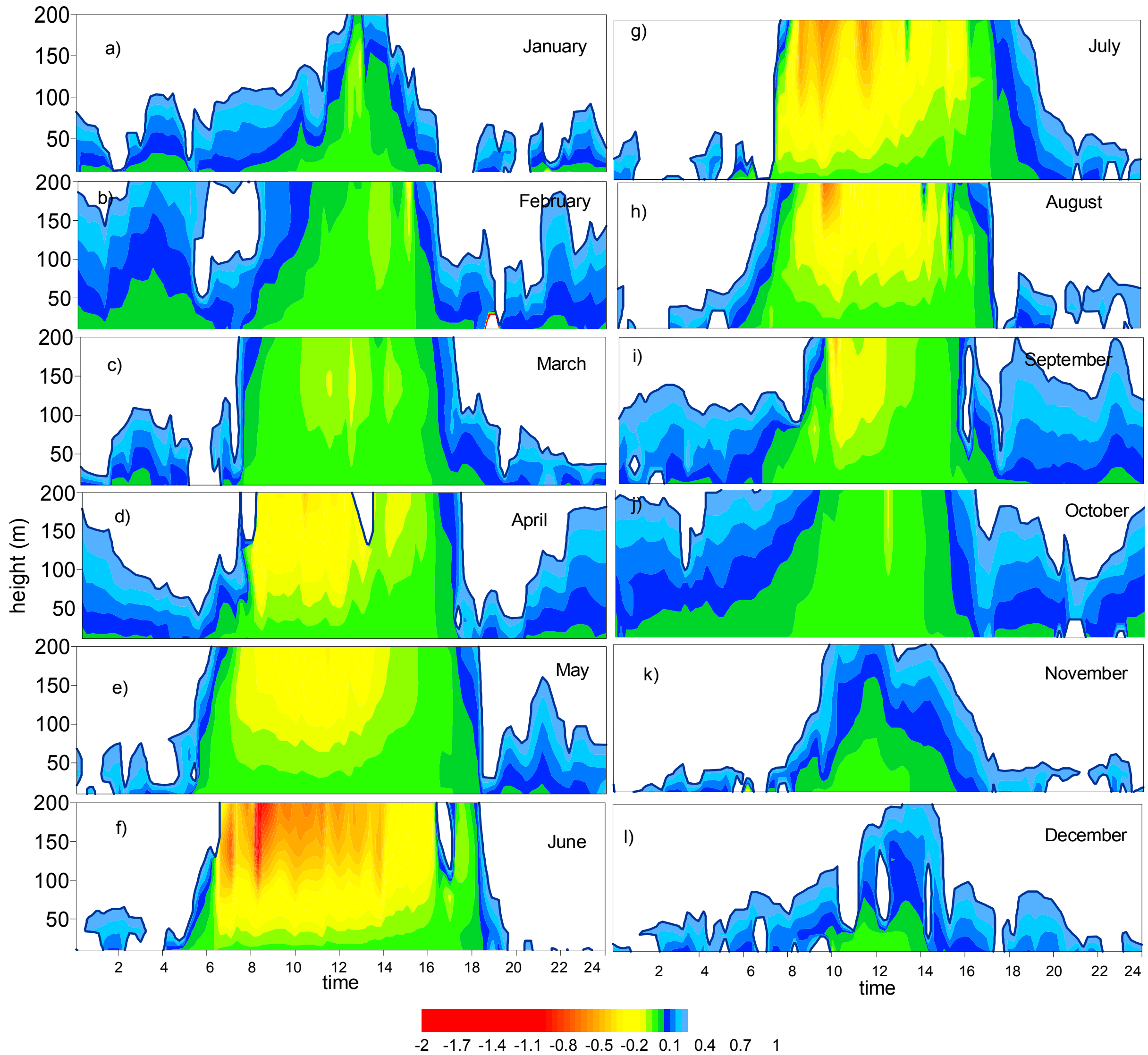

Figure 22. Monthly vertical profiles of average hourly Ri_B number calculated from the Cabauw data, the Netherlands, in from January (a) to December (l) in year 2001. The ABL height, H, is represented with $Ri_{BC} = 0.25$ (the top of the blue area).

Monthly correlation coefficients calculated between H determined from the measurements, H_{tower}, and the modelled values determined with the operational and Ri_B number method, H_{old} (red) and H_{new} (blue), respectively are displayed in Fig. 23. Obviously the new ABL scheme gives better results for all months except for June, July and August, i.e. the summer period, when both schemes performed equally well in the unstable surface layer. Since at the Cabauw tower there are no measurements above 200 m, during the strong CBL conditions it was only possible to investigate correlations regarding time evolution of the ABL and the strength of turbulence in the lowest part of the ABL. Higher vertical measurements would provide more information and help distinguishing between performances of the two ABL schemes. Nevertheless, higher or similar correlation coefficients for the two schemes during the warmer part of the year are in agreement with the radiosoundings results, which showed that the ABL scheme based on the Ri_B number method performs better in stable conditions than the operational one. According to correlation coefficients in February both schemes had similar performance. February was characterized with strong wind and higher instability with corresponding higher values of the Ri_B.

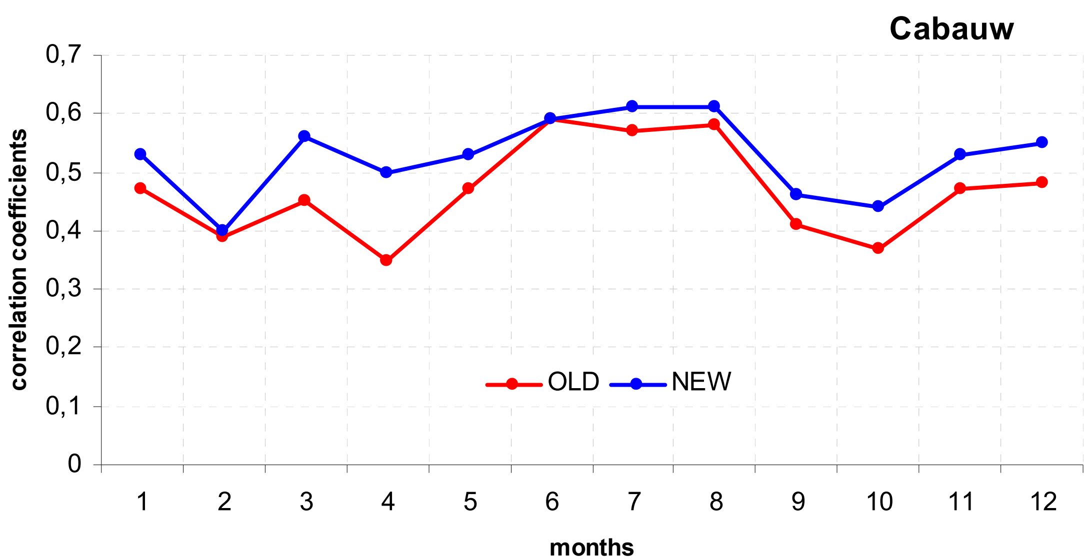

Figure 23. Monthly r between the H calculated from the Cabauw measurements, and the H calculated with the old (H_{old}) –red, and the new ABL scheme (H_{new}) – blue, in the EMEP model for year 2001.

Since estimated H exceeds 200 m for most of the year, especially during the warmer part, the model ABL evaluation is significantly limited (Fig. 23). Therefore the number of hourly H values higher than 200 m, N (%), determined from the observations (white bars) and from the EMEP model (blue bars) per month during the year 2001 at the Cabauw tower is presented in Fig. 17. It should be pointed out that in this work the Ri_B numbers are estimated differently from the observations and from the model. From the observations Ri_B numbers are estimated using values at 2 m as the lowest level, z_1= 2 m, while Ri_B estimated from the EMEP model use the first model level ($z_1 \approx 50$ m) as the lowest level. As a consequence considerably more cases, ~ 30 %, with $H > 200$ m are found in the observations than in the model (Fig. 24) which is in agreement with the findings of Vogelezang and Holtslag (1996). Annual course has 2 maxima during spring and autumn N ~ 80 % in the observations and N ~ 70 % in the model (Fig. 24). During the winter N is expectedly smaller with N ~ 60 – 70 % from the observations and N ~ 30 – 40 % from the model. During the summer N ~ 70 – 80 % of cases with H > 200 m is found in observations and N ~ 50 – 60 % from the model. Furthermore, in Fig. 25 relation between the r and N determined from the model is shown. Obviously N is related with r in the way that an increase in N is reflected in a decrease in r.

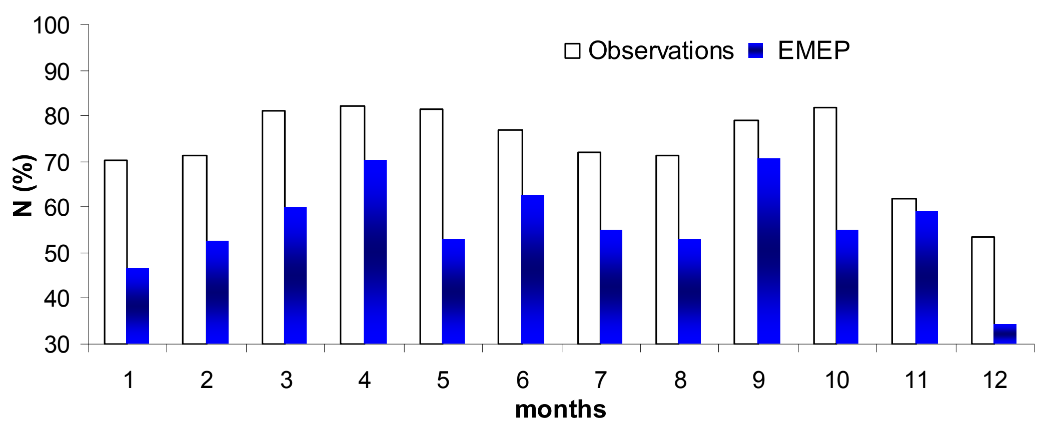

Figure 24. Number of hourly H values higher than 200 m, (%), determined from the observations (white bars) and from EMEP model (blue bars) per month during 2001 at the Cabauw tower.

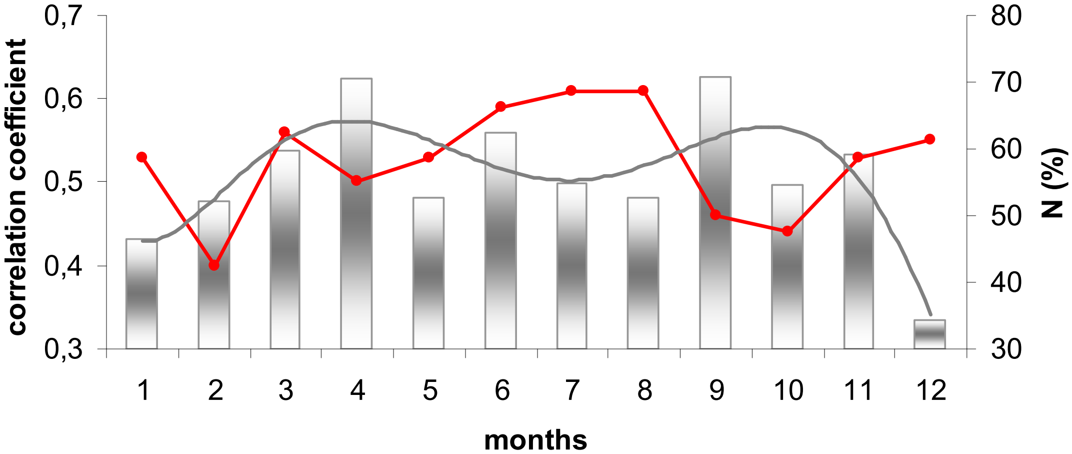

Figure 25. Number of hourly $H > 200$ m values, N (%) determined from the observations (bars, right axes) and the corresponding monthly correlation coefficient (red line, left axes) at the Cabauw tower during the year 2001. The grey line is a trend line of N.

According to the significance test it is found that there are certain differences among analyzed stations showing that the level of significance is higher for NO_2 at stations in Germany, Ireland, Netherlands, Norway and Sweden (not shown). Changes in the correlation coefficient are significant for Denmark and Spain, while for SO_4^{2-} there is no significant change in the r with the change of the vertical diffusion scheme in the model. The same procedure has been applied on the correlation coefficients calculated between the H determined from the radiosoundings and Cabauw data and the corresponding H values estimated with the EMEP model with the two different ABL schemes. Although the change in correlation coefficient is not significant according to this test, based on the evaluation provided from the radiosounding data, the level of significance is improved for Gothenburg, Herstmonceux, Zagreb, La Coruna and Madrid during January and for Stavanger, Copenhagen, Wroclaw, Meiningen, Vienna, Payerne and Practica di Mare in July (not shown). The change in correlation coefficient for Cabauw is significant during March and April; for other months the level of significance is satisfactory while for February and June the change in correlation coefficient is not significant.

New parameterization schemes for $K(z)$ and H gives slightly better results and improvement is evident although standard significance tests do not reflect it completely due to their own stated limitations in application at this particular data.

4.6 The ^{222}Rn data results

The observed hourly ^{222}Rn concentrations have been analyzed and compared to the corresponding modelled data with different $K(z)$ schemes employed in the model.

4.6.1 The Angus tower

In Fig. 26 average monthly ^{222}Rn concentrations at the Angus tower in the year 2006 are presented. Monthly average concentrations at the Angus tower ^{222}Rn concentrations range between 0.5 Bq m^{-3} and 1 Bq m^{-3}. The seasonal pattern is characterized by an autumn maximum and spring minimum. On average, the seasonal maximum in September is found to be higher by a factor of 3 than the April minimum.

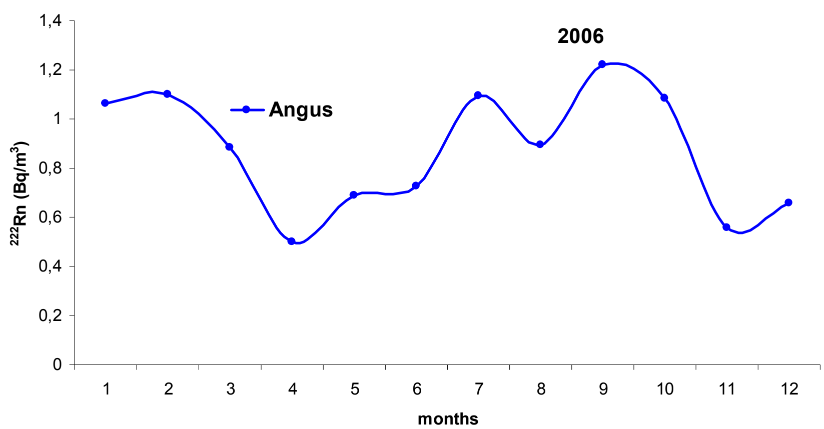

Figure 26. Average monthly ^{222}Rn concentrations determined from the measurements for the Angus tower in Scotland at 50 m during 2006.

A monthly time series of the observed and modelled hourly surface ^{222}Rn concentrations are shown in Fig 27. The model mainly overestimates the measurements and the overestimation with the TTE scheme is the highest. The measurements from the Angus tower are influenced by a lower emission rates from the sea and by the advection of a radon free air. Obviously meteorological conditions were in favour to the low ^{222}Rn concentrations, especially in November, December and April in the 2006.

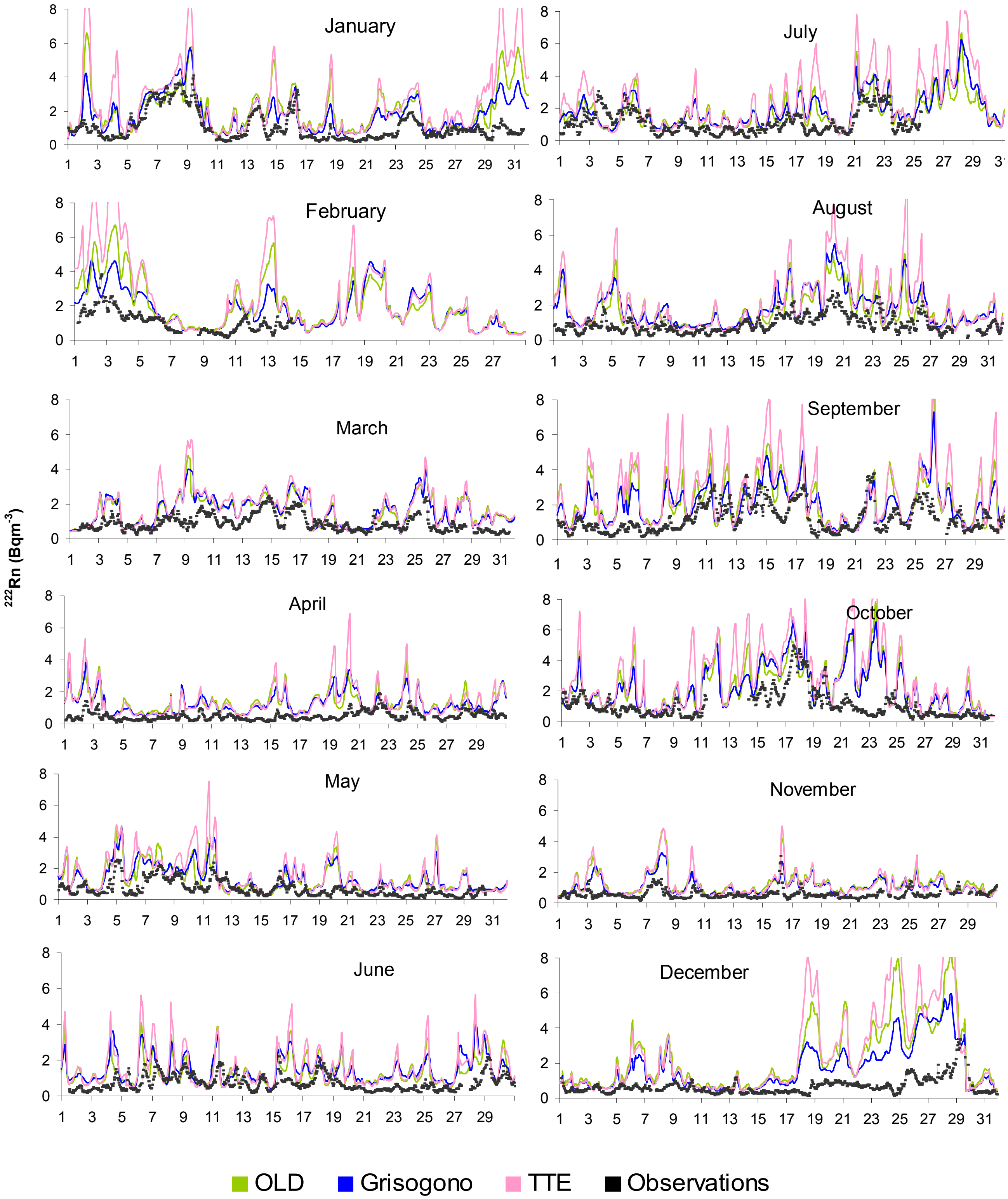

Figure 27. Monthly time series of the observed hourly ^{222}Rn concentrations against the corresponding modelled surface ^{222}Rn concentrations at Angus tower, Scotland during year 2006.

4.6.2 The Cabauw tower

In Fig. 28 observed average monthly ^{222}Rn concentrations values for the Cabauw at both measuring levels during the year 2006 are displayed. Monthly average concentrations at the Cabauw range between 1.5 and 4 Bq m^{-3} with higher concentrations measured at the higher tower level during March and April in the 2006.

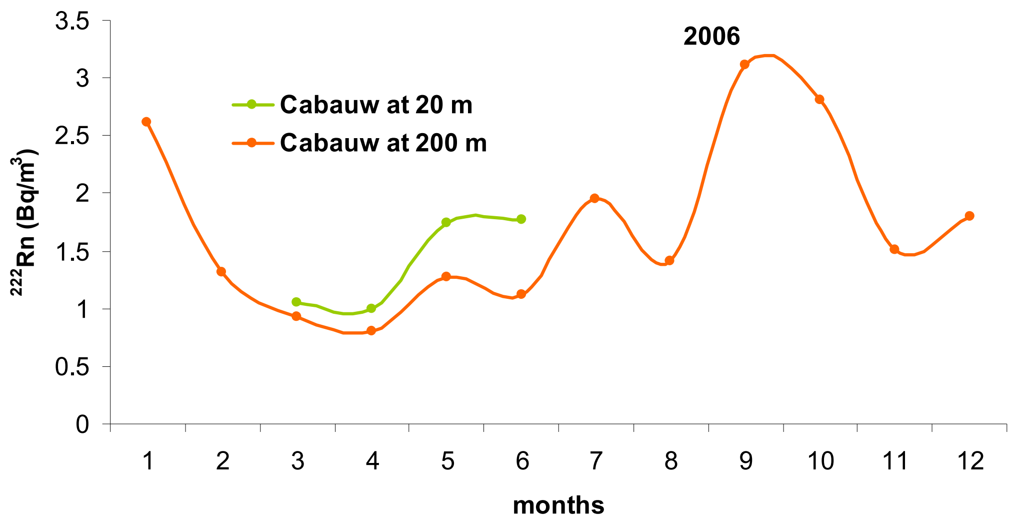

Figure 28. Average monthly ^{222}Rn concentrations determined from measurements for the Cabauw tower, the Netherlands at 20 m and 200 m during 2006.

The observed hourly ^{222}Rn concentrations averaged over one month are shown in Fig. 29 for April, May and June at the Cabauw, at the two measuring levels: 20 m (bars) and 200 m (lines), for the years 2006 (red) and 2007 (blue). Unfortunately, only three months of measurements at 20 m were available in year 2006. A diurnal variation of the ^{222}Rn concentration at the Cabauw tower at 20 m shows a maximum in the early morning and a minimum in the afternoon around 4 PM. On average, at 20 m the maximum is higher than the minimum by a factor of 2. A daily variation of the concentrations is more pronounced at the lower level, while at 200 m concentrations do not exhibit significant daily variations. Furthermore, concentrations at 20 m are systematically higher than the concentrations at the 200 m (i.e. blue bars are always above the blue line).

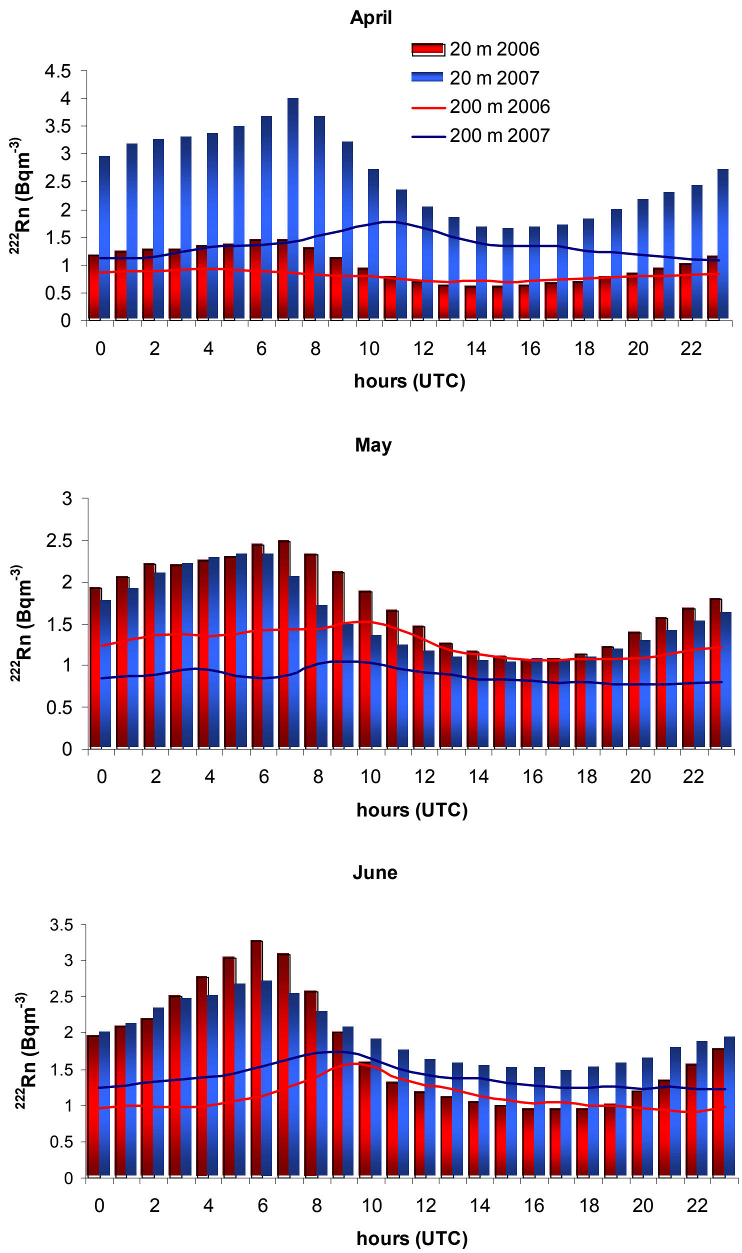

Figure 29. Observed hourly ^{222}Rn concentrations averaged over one month at the Cabauw, at two measuring levels: 20 m (bars) and 200 m (lines), in the 2006 (red) and the 2007 (blue).

The monthly time series of the observed hourly ^{222}Rn concentrations are shown in Fig. 30 and 31 against the corresponding model data for the Cabauw tower site at 20 m and 200 m height respectively. At 20 m agreement between the model and measurements is pretty good especially in June for the TTE scheme which produced hourly peaks of 8 Bq m^{-3}. At 200 m the agreement is also good except during September and October when higher daily variability, as well as higher values, are found in the measurements but not in the model.

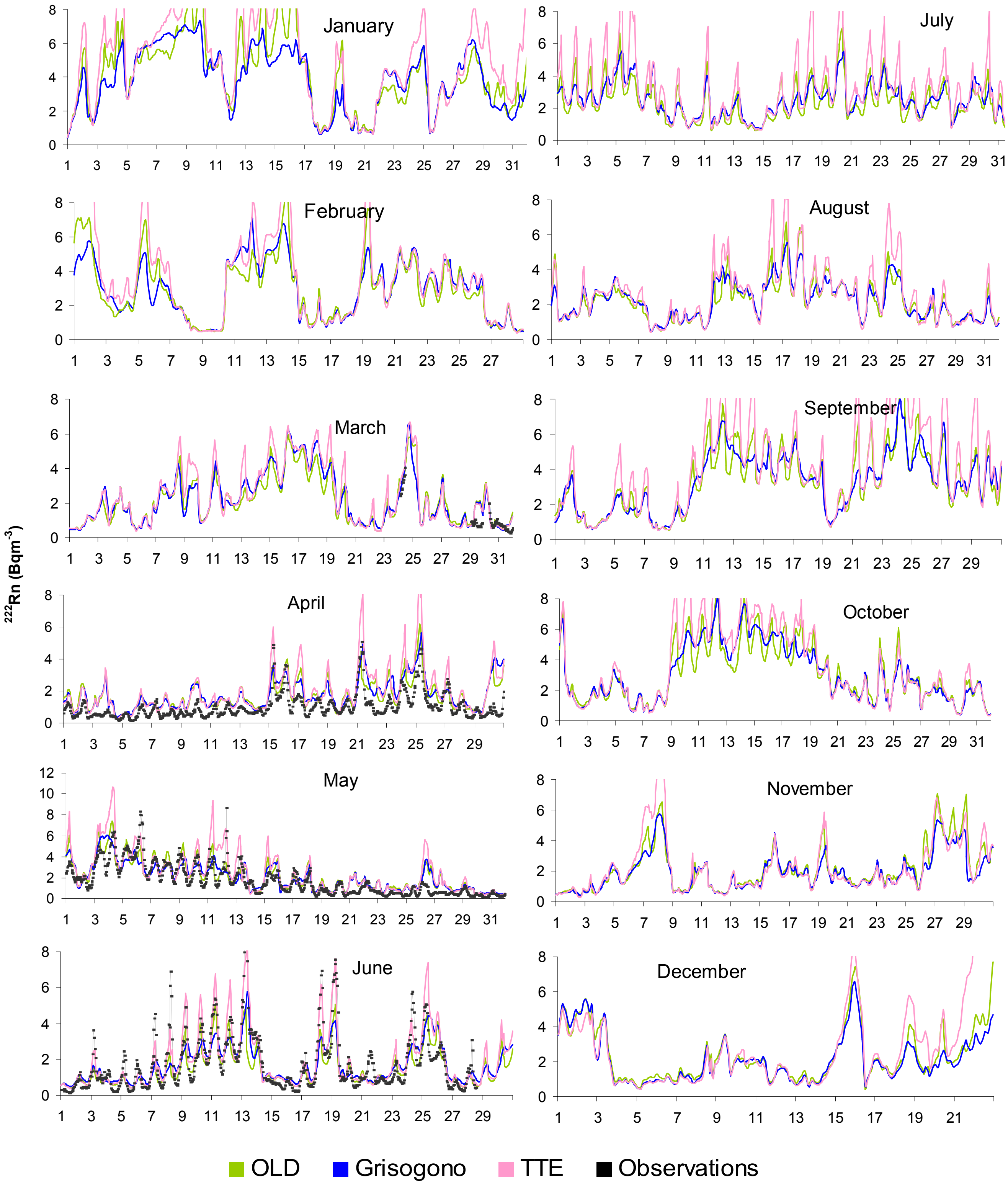

Figure 30. Same as Fig 27 but for the Cabauw at 20 m.

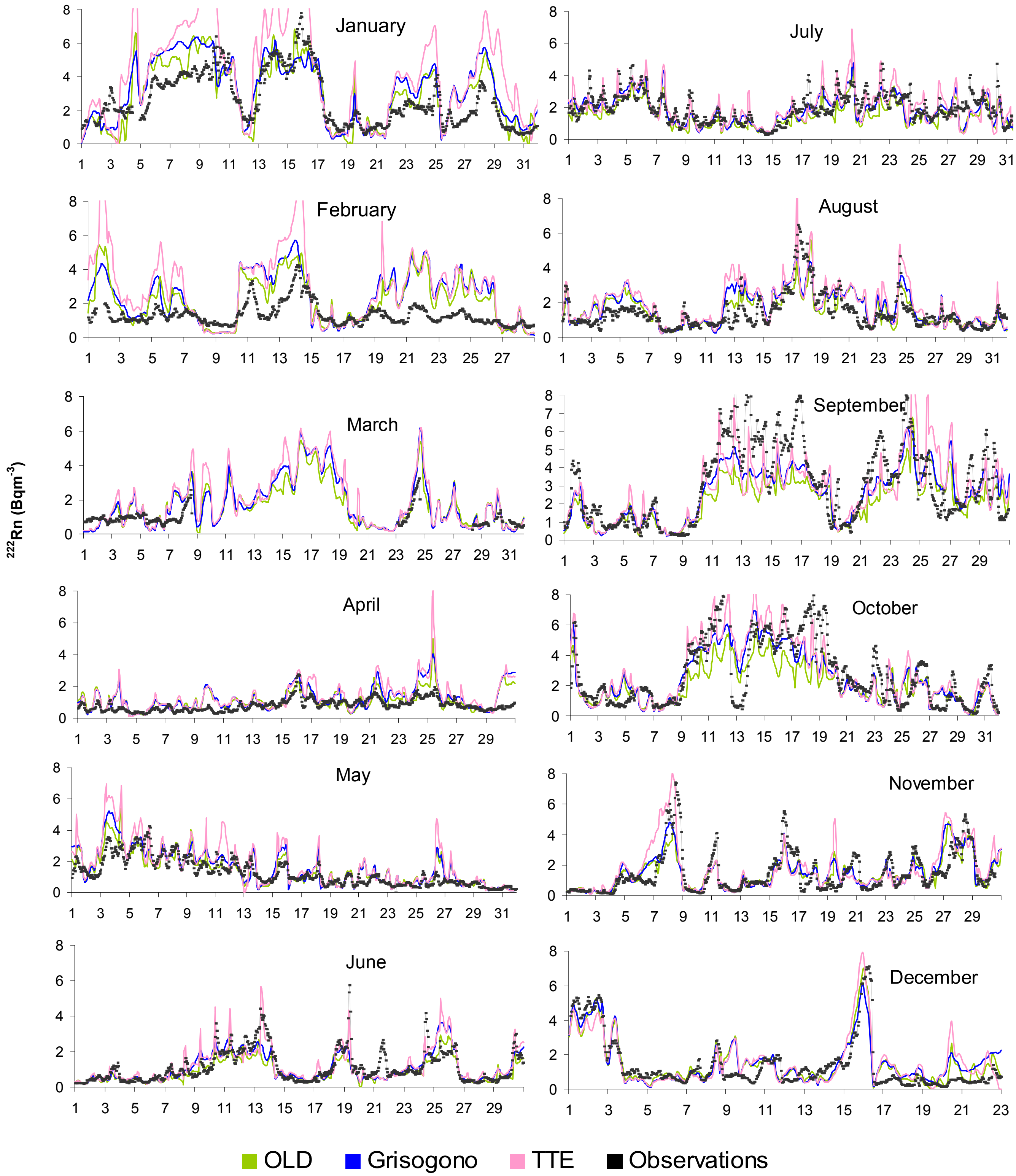

Figure 31. Same as Fig 27 but for the Cabauw at 200 m.

4.6.3 Schauinsland and Freiburg

Average monthly ^{222}Rn concentrations for the two German stations, Freiburg at the left axis and Schauinsland at the right axis during the 2005 are shown in Fig. 32. Generally the highest monthly concentrations were found at Freiburg, ranging between 4 and 10 Bq m^{-3}, while at Schauinsland located at the higher altitude ~ 1100 m, the corresponding concentrations are smaller as expected ranging between the 1.5 and 3.5 Bq m^{-3}. The seasonal pattern is characterized by an autumn maximum and an early summer minimum. On average, the seasonal maximum in September at Schauinsland and in October at Freiburg is found to be higher by a factor of 2 than the June minimum. Yearly courses are similar for Schauinsland and Freiburg with maximum values during September and October when more stable atmospheric conditions prevail.

The time series of the hourly ^{222}Rn concentrations at Freiburg and Schauinsland are shown in Figures 33 and 34 respectively in the 2005. The measured hourly concentrations at Freiburg, Fig. 33, are the highest in September reaching ≈ 20 Bq m^{-3}. The corresponding modelled values are lower and the highest hourly values ≈ 15 Bq m^{-3} are achieved with the TTE scheme. The measured hourly concentrations in Schauinsland (Fig. 34) are the highest in September and October ≈ 8 Bq m^{-3}.

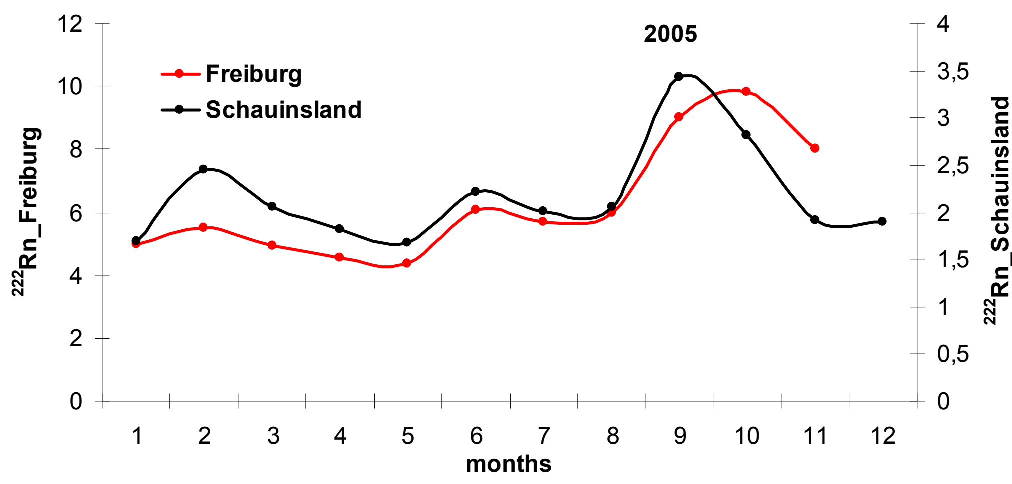

Fig 32. The average monthly measured ^{222}Rn concentrations at Freiburg and Schauinsland in Germany in year 2005.

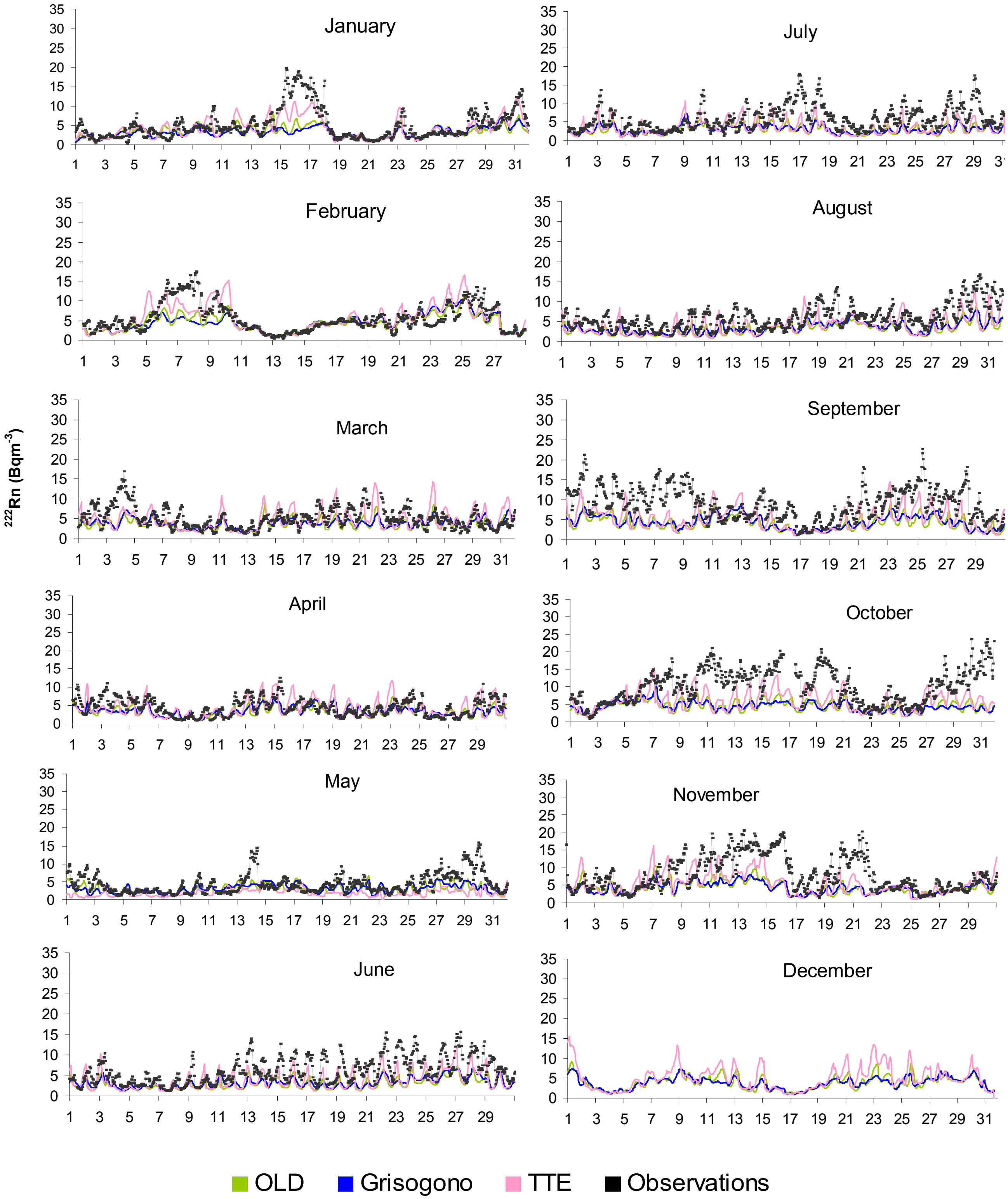

Figure 33. Same as Figure 27 but for Freiburg, Germany in year 2005.

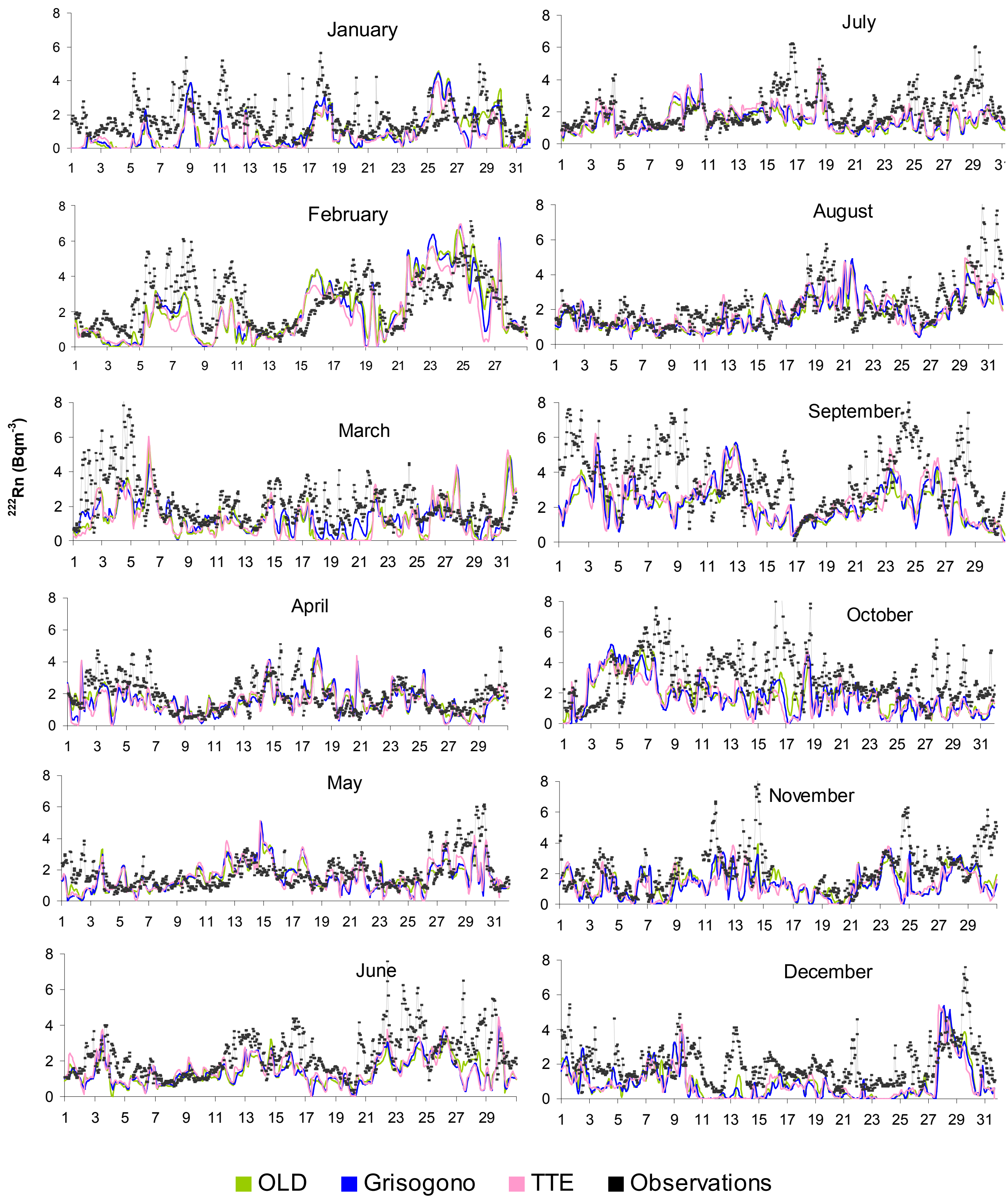

Figure 34. Same as Fig 27 but for Schauinsland, Germany in the year 2005.

4.6.4 Krakow

The average monthly ^{222}Rn concentrations calculated from the measurements at Krakow in Poland in year 2006 are shown in Figure 35. The highest average concentrations range between 8 and 12 Bq m^{-3} during January and October. The lowest average monthly concentrations are around 4 Bq m^{-3} during spring. Similar values and annual course is found at Freiburg, Germany.

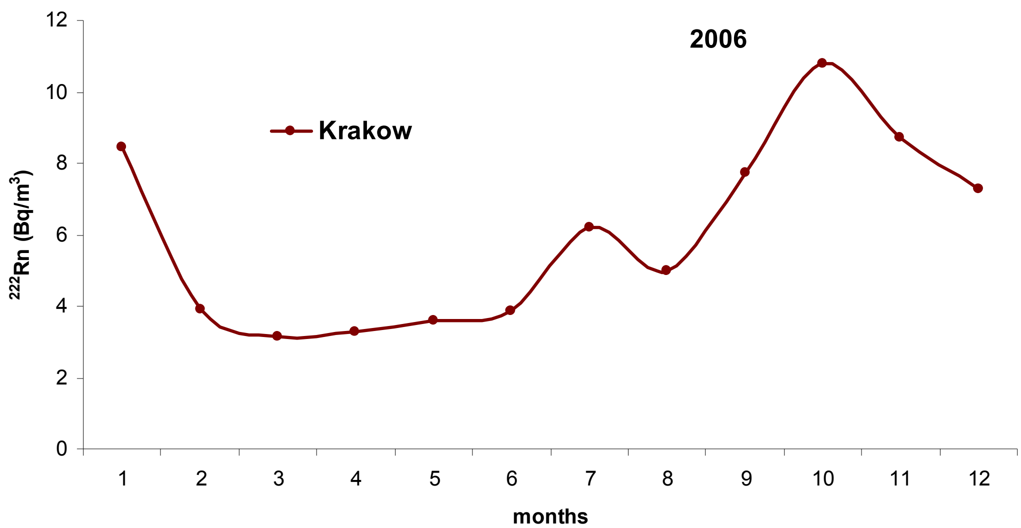

Fig 35. Average monthly ^{222}Rn concentrations determined from measurements Krakow in Poland in the 2006.

The time series of the hourly ^{222}Rn concentrations at Krakow are plotted in Figure 36 against the corresponding model data for all analyzed months in the 2006. The measured hourly concentrations reach up to ≈ 30 Bq m^{-3} in September, October and December, while the ^{222}Rn are the lowest in March. The TTE scheme is closest to the measurements with maximum values ~ 20 Bq m^{-3}. Some types of soils emit more of the natural ^{222}Rn which beside the meteorological conditions may also be a important factor contributing to the higher observed ^{222}Rn values in Krakow.

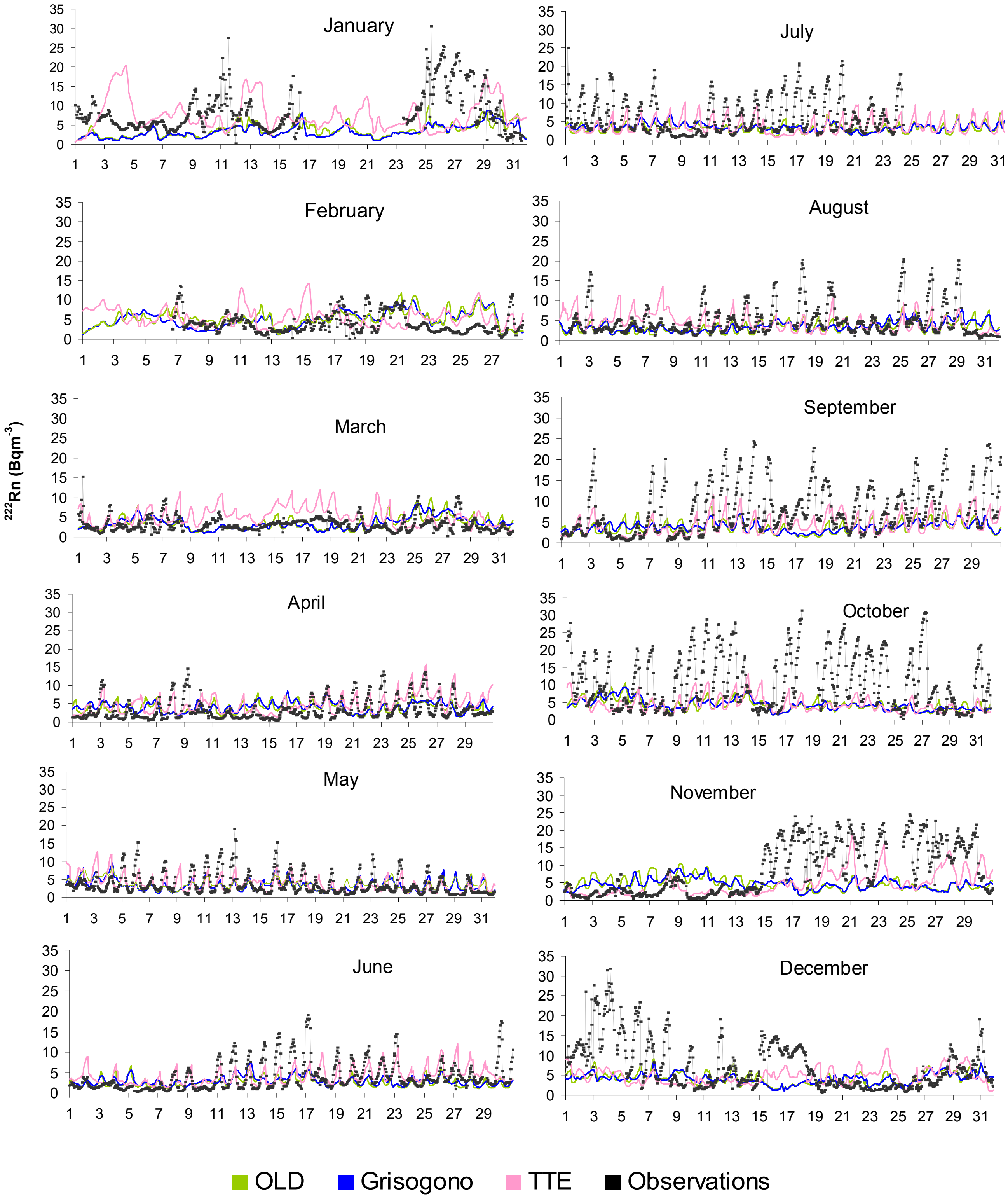

Figure 36. Same as Fig 27 but for Krakow, Poland in the year 2006.

4.6.5 Simulation of the ^{222}Rn vertical profiles in stable and unstable conditions

It is important to analyze the model performance with different $K(z)$ schemes separately in stable and unstable conditions. For that purpose the modelled vertical $K(z)$ profiles and corresponding vertical profiles of the ^{222}Rn concentrations are investigated during two different stability episodes for the Cabauw tower. The modelled hourly vertical $K(z)$ profiles during two days in warmer part of the year with pronounced daytime convective conditions are shown in Figure 37. The model runs are provided for 10th and 11th June 2006 for the Cabauw tower.

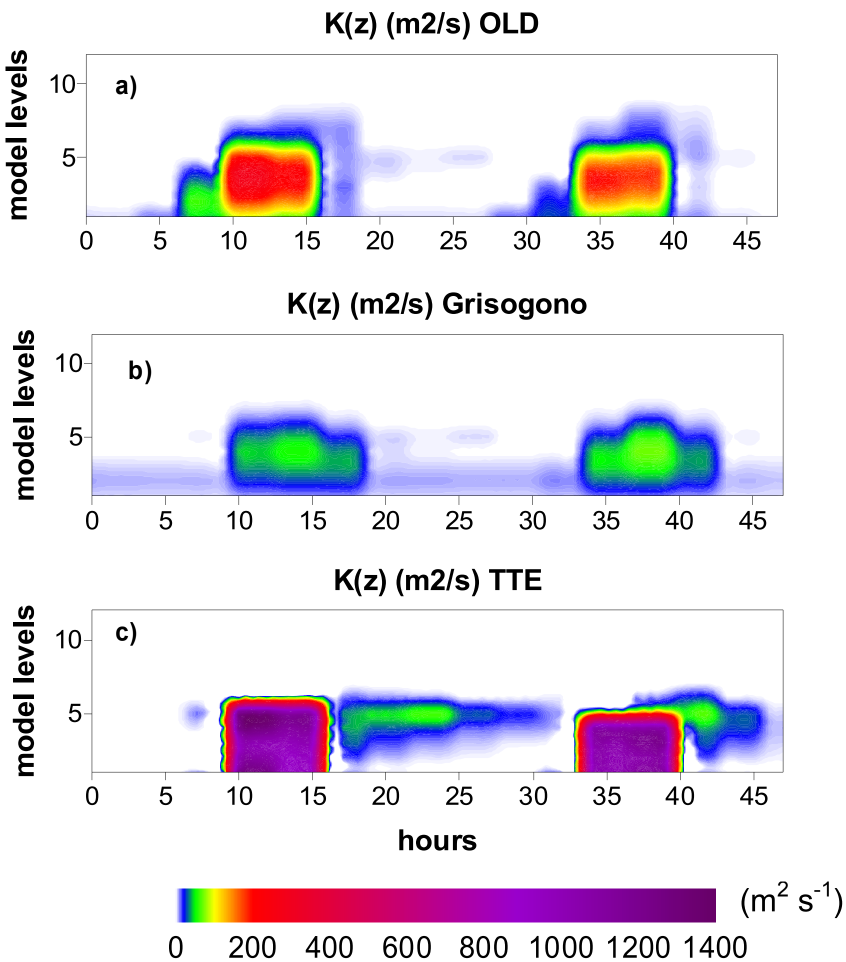

Figure 37. Modelled hourly vertical $K(z)$ (m^2 s^{-1}) profiles with the a) OLD, b) Grisogono and c) TTE schemes during 10th and 11th June 2006, for the Cabauw tower.

It can be easily noted that the Grisogono scheme gave lower $K(z)$ values during the daytime, in unstable conditions, compared to $K(z)$ profiles determined with the OLD and TTE schemes (in Fig. 37). A very intensified $K(z)$ in the CBL is produced with the TTE scheme reaching up to 1400 $m^2 s^{-1}$. In the SBL conditions the non-local Grisogono scheme produced higher values of $K(z)$ with $K_{max} \approx 6$ $m^2 s^{-1}$ at approximately 150 m height and decreased to ≈ 0 at 400 m (Fig 37b). However, K (z = 1) < 0.5 $m^2 s^{-1}$ and K (z > 1) ≈ 0 $m^2 s^{-1}$ with the OLD scheme i.e. Blackadar scheme, during the nighttime (Fig. 37a), while the TTE scheme produced low, intermittent vertical mixing. Note an occurrence of the intensified mixing with the TTE scheme (Fig 37c) at approximately 400 m which started to develop in the afternoon of 10th June reaching its maximum value around midnight and decreased gradually until approximately 6 in the morning of 11th June. The TTE scheme managed to reproduce a higher turbulence in the residual layer which was not visible with the other schemes. This area of intensified mixing may be a residual of the convective mixing or a low level jet resulted from the wave breaking. As turbulence and the mixed layer decay with sunset, the mixed layer air maintains many of the same values of the meteorological values. This layer becomes the residual layer (because its properties are residuals of the mixed layer) and forms above the stable boundary layer. While the nocturnal boundary layer has a very stable profile, the residual layer tends to have more of a neutral profile. The residual layer does not have contact with the earth's surface, and so is not influenced by turbulent stresses like the stable boundary layer below it. The residual layer is bounded above by a capping inversion, which approximates the height of the daytime height of the mixed layer.

A transition through different stability regimes affects concentration levels and a characteristic processes can be identified during an undisturbed summer day (Fig. 38). In SBL conditions, from 20 PM to 6 AM the accumulation of the surface Rn concentrations occurs. With the development of unstable conditions i.e. in CBL from 6 AM to 15 PM mixing is intensified, surface concentrations are diluted and higher concentrations are transported at higher levels. In the afternoon, neutral conditions take over, from 15 PM to 20 PM, the atmosphere is well mixed and the concentrations are uniformly vertically distributed. With the development of SBL nighttime conditions the accumulation starts again. In short we have accumulation → mixing → neutral → accumulation. Accumulation is the lowest with the Grisogono scheme while mixing is the highest with the TTE scheme. In the neutral period with the OLD and TTE scheme the atmosphere is more uniformly mixed while the Grisogono have higher concentrations near the surface.

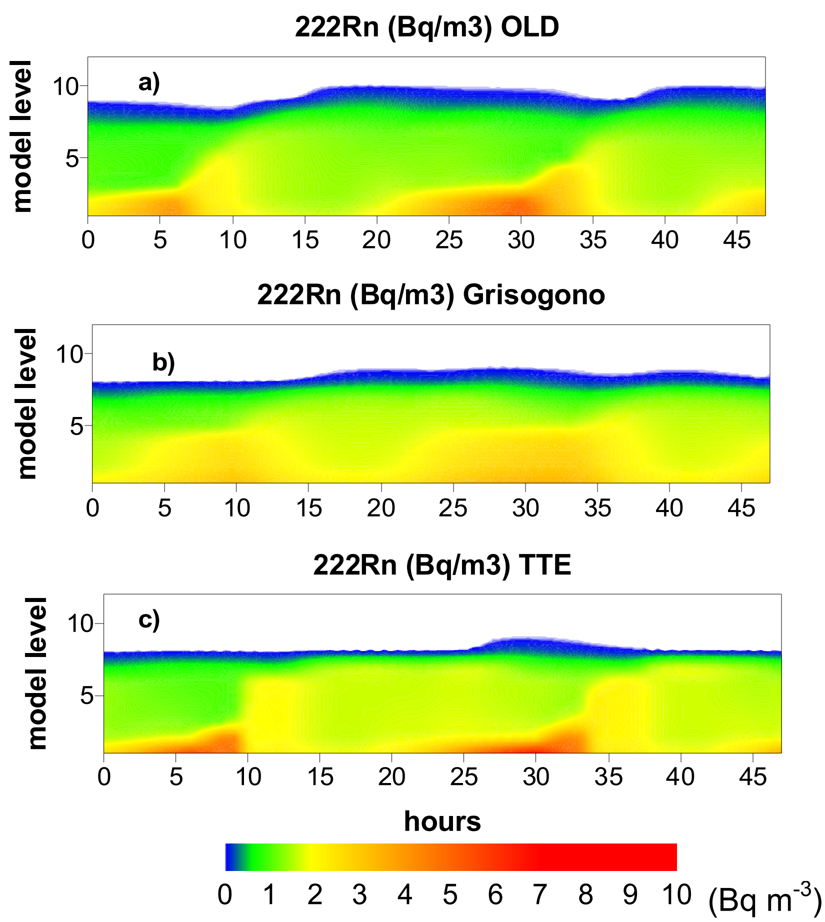

Figure 38. The simulated hourly vertical profiles of the ^{222}Rn concentrations (Bq m^{-3}) with the a) OLD, b) Grisogono and c) TTE schemes for 10 and 11 July 2006 at the Cabauw tower.

Two day model run i.e. for 7th and 8th November 2006 for the Cabauw tower is provided for a colder part of the year to analyze $K(z)$ profiles in stable conditions (Fig. 39). The SBL conditions were present during 7th November and during the first part of 8th November 2006. The atmosphere was synoptically unstable due to cold front passage over the analyzed area starting in the afternoon of 8th November until the end of the simulation. The vertical mixing is generally lower in November than in June, especially in the convective conditions. The OLD scheme has produced a higher mixing with $K(z) \approx 20$ m^2 s^{-1} while the Grisogono scheme has $K(z) \approx 10$ m^2 s^{-1} during the daytime convective conditions at 7th November (Fig. 39a). As previously pointed out, the vertical mixing is reaching higher levels with the Grisogono scheme and the species are lifted to a higher altitude in the atmosphere during stable conditions. The Grisogono scheme produced a very low vertical mixing in the layer of 200 m thickness during the stable conditions on 7th November (Fig 39b). The local schemes Blackadar and TTE produced a weak vertical mixing, mainly close to the ground, during the stable period (Fig 39a and 39c) from 16 hour of the model run on 7th November until 35 hour of the model run on 8th November. As a result higher surface ^{222}Rn concentrations are produced and mainly kept in the thin layer close to the ground (Fig 40a and 40c). There is no clear difference between the SBL and CBL regimes in this two day winter period. Mainly accumulation is present with a slight decrease in a concentration levels during mixing period. Unstable conditions occurred again at 36th hour of the model run on 8th November. During the period of increased instability $K(z)$ values are also increased with all schemes producing a decrease in the ^{222}Rn concentrations. Generally, the simulated surface ^{222}Rn concentrations are significantly higher in November than in June (Fig. 40). The highest surface ^{222}Rn concentrations are $\approx$ 4 Bq m^{-3} during the two simulated days in July, while the highest concentrations reached up to 8 Bq m^{-3} during the two days in November.

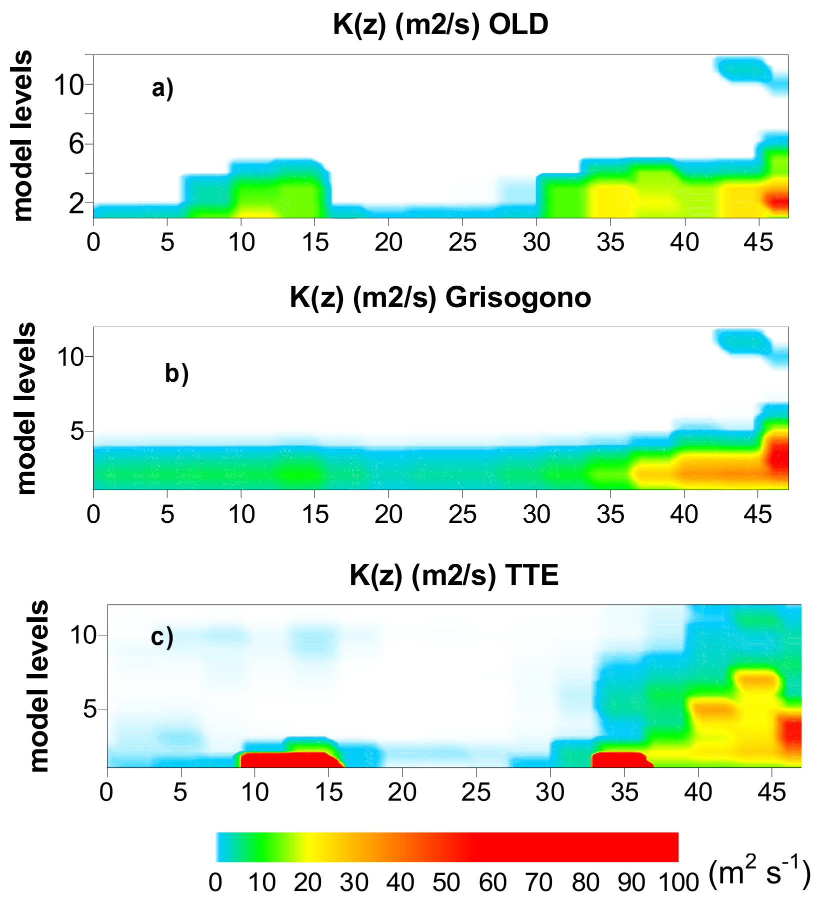

Figure 39. Same as Fig. 37 but for 7th and 8th November 2006 at Cabauw.

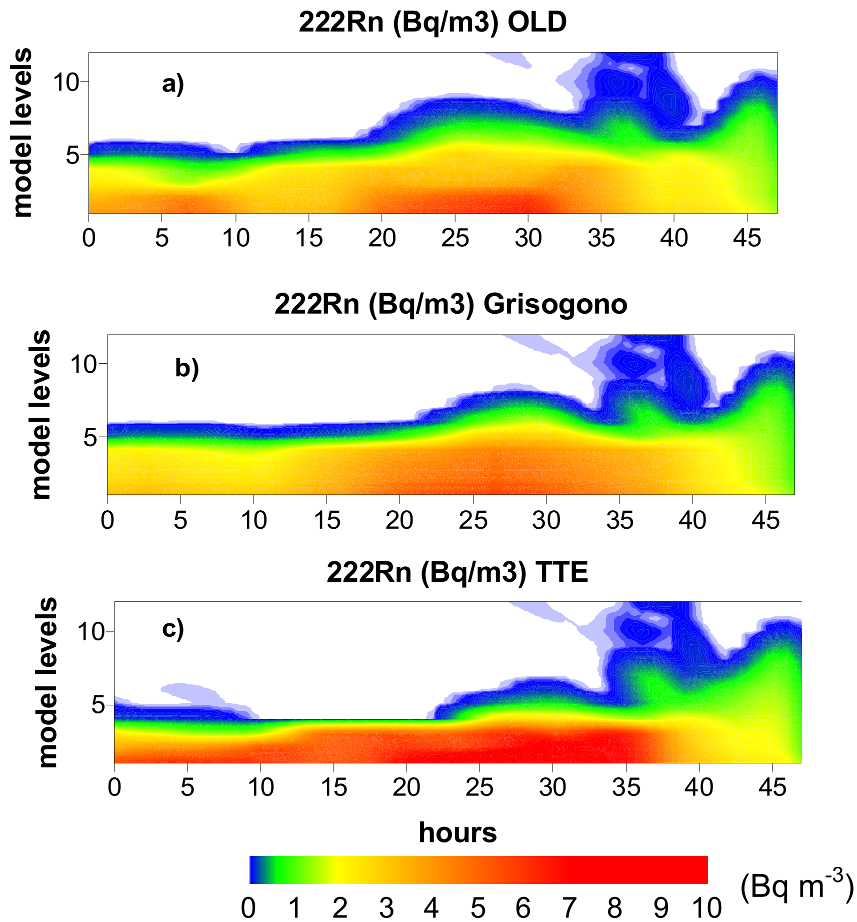

Figure 40. Same as Fig. 38 but for 7th and 8th November 2006 at Cabauw.

The hourly vertical gradients of the modelled and measured ^{222}Rn values, averaged over the available three months period, are shown in Fig. 41. The concentration gradients are divided in four groups according to different stability regimes: a) 00 UTC - 06 UTC, b) 07 UTC– 12 UTC, c) 13 UTC-18 UTC and d) 19 UTC – 23 UTC. In the period from 00 to 06 UTC (Fig 41a), when mostly stable conditions and accumulation of concentrations are present, the strongest negative gradients are produced with the TTE scheme ≈ 3 Bq m^{-4}, while with the Grisogono scheme the gradients are the weakest ≈ 0.5 Bq m^{-4}. The TTE scheme overestimates the measurements at 20 m, while at 200 m the measured ^{222}Rn are underestimated with the TTE scheme. This means that a vertical mixing with the TTE scheme is mainly generated and maintained near the ground. The OLD scheme overestimates the measurements at both levels, while the Grisogono scheme has the best agreement at the 20 m and an overestimation at 20 m. During the morning period (Fig 41b), characterized with intensifying unstable conditions, the concentrations at 20 m are decreasing with an increase of turbulent mixing in the atmosphere, while at 200 m the concentrations remain relatively unchanged (Fig 41b). The OLD and TTE scheme manage to reproduce the vertical exchange quite well, while the Grisogono scheme is less diffusive in the unstable conditions. Stability in the atmosphere is again increasing in the afternoon period (Fig. 41c) when buoyancy is decreasing, the atmosphere is well mixed and the stability is close to neutral conditions. In the neutral conditions the average measured concentrations are nearly constant with height, while an overestimation of the measurements is found for all schemes. The lowest overestimation in the neutral conditions is found for the TTE scheme. This implies the need for more intensive and more vertically pronounced vertical mixing. In the period from 19 to 23 UTC the concentrations at the lower level are increasing with time due to increased stability and weak vertical mixing. Therefore, the emitted pollutants are kept in the layer close to the ground, especially with the TTE scheme. The local schemes have stronger mixing close to the ground and a lower vertical extension in the vertical, while the Grisogono scheme has an enhanced vertical mixing and the resulting surface concentrations are lower.

Non-local schemes, the Grisogono and O'Brien, produce continuous vertical mixing whose extent depends on model's vertical resolution. Local schemes are able to produce a high local turbulence e.g. at one layer, while the non-local scheme Grisogono assume at least three levels. Therefore, model's vertical resolution has a significant influence on the vertical extent of the non-local $K(z)$ schemes. It may be concluded that for non-local schemes the model surface concentrations are more sensitive to the ABL height, and the height of the K_{max}, than on the K_{max} magnitude.

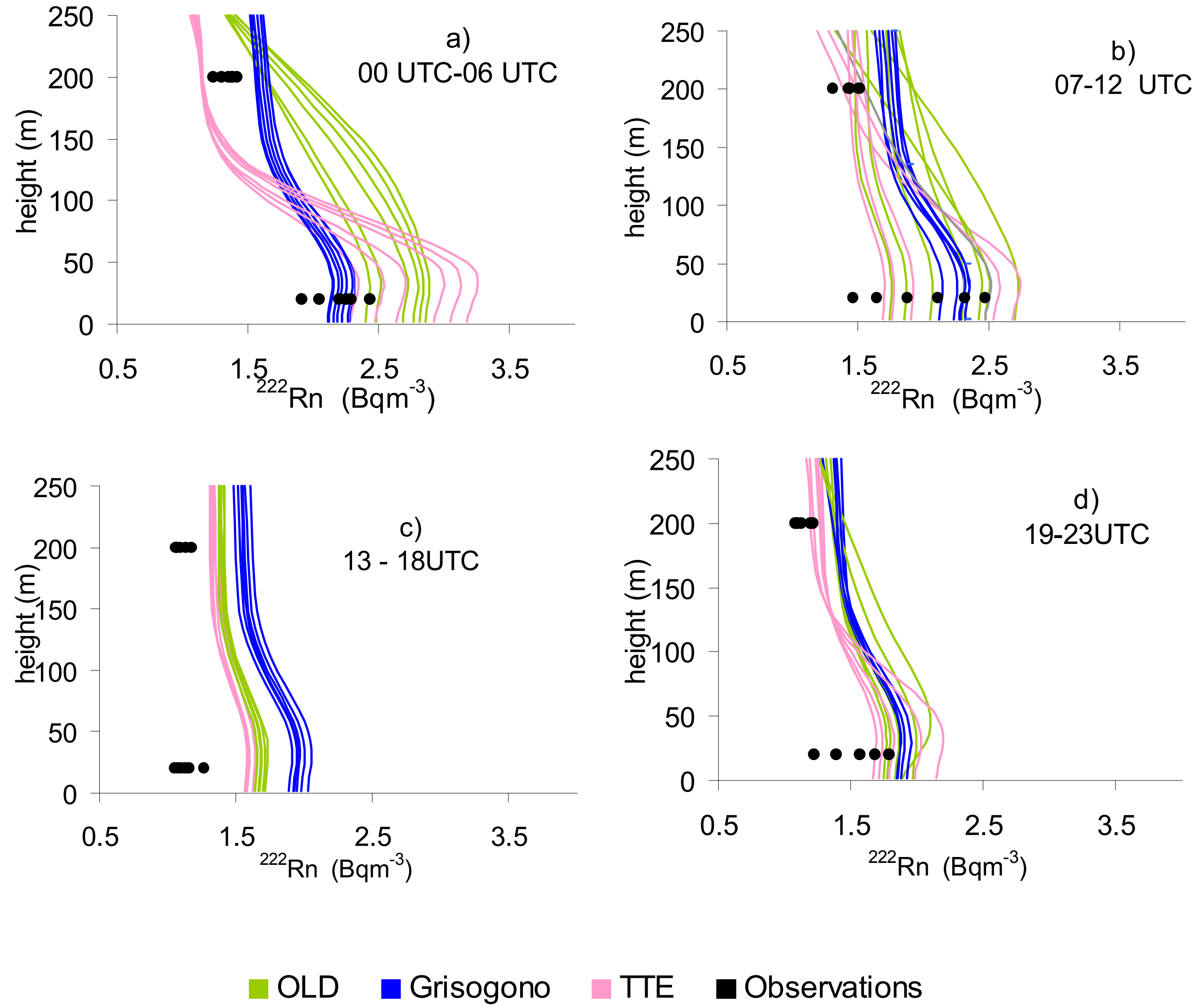

Figure 41. Comparison of the hourly average modelled and measured ^{222}Rn profiles computed over the measuring period or 3 months in year 2006 for a) 00-06 UTC, b) 07-12 UTC, c) 13-18 UTC and d) 19-23 UTC at the Cabauw, the Netherlands.

4.6.6 The model and K(z) evaluation based on the ^{222}Rn data

Annual scatter plots between the observed and modelled hourly ^{222}Rn concentrations are shown in Figure 42 for a) the Cabauw tower at 20 m, the Cabauw tower at 200 m, c) Angus tower at 50 m, d) Schauinsland, e) Krakow and f) Freiburg. Agreement is very good at the Cabauw and the best results are achieved with the Grisogono method (Fig 42a and 42b). The results for the Cabauw at 20 m are based at only three months of the measurements. At 200 m the scatter is the highest with the TTE scheme. Note that an overestimation with the OLD and TTE schemes occurs for the observed concentrations < 1 Bq m^{-3}. At the Angus tower (Fig 42c) there is also an overestimation of the corresponding low observed concentrations with the OLD and TTE schemes, while the Grisogono scheme has the best performance. For the Freiburg and Krakow there is an obvious model underprediction of the observed data. At Freiburg and Schauinsland the OLD scheme has the best results, while at Krakow the TTE scheme has the highest correlation coefficient.

The monthly r are calculated between the available hourly ^{222}Rn measurements and the corresponding modelled concentrations with three different $K(z)$ schemes applied in the EMEP model (Fig 43). At the Angus tower the Grisogono scheme has the highest r for all months except April, November and December when all schemes did not manage to simulate the extremely low observed concentrations $\leq$ 1 Bq m^{-3}. The monthly r at Angus is in the range $r = 0.4 - 0.72$. The monthly r at Cabauw is around 0.8 for both measuring levels. At Freiburg the TTE and OLD scheme have performed better in January and February while during other months the OLD and Grisogono scheme have better performance. At Schauinsland r is the highest in February ≈ 0.6.

Cumulative distribution function, CDF, shows the proportion of the population with values less than some prescribed concentration. To create these plots, all observed and modelled data are rank ordered, and each point on the plot represents a particular rank number. The goal of the CDF plot is to see whether the distributions of all the observed and predicted values as a whole are comparable, where it is not necessary to require that for e.g. the maximum of the observed and the maximum of the modelled concentrations take place under the same condition. In order to evaluate the model performance a cumulative distribution functions (CDF) are calculated at different stations, Fig 44. The evaluation is based on the observed and modelled concentrations with three different vertical diffusion schemes employed in the EMEP model. Obviously the model has the best results for the Cabauw tower at 200 m, Fig. 44. The observations are overestimated for Angus and Cabauw at 20 m and underestimated at Schauinsland, Freiburg and Krakow. At Angus 95th percentile is less than 2 Bq m^{-3} while at Cabauw and Schauinsland stations it is ≈ 4 Bq m^{-3}. The 95th percentile at Freiburg is ≈ 15 Bq m^{-3} and at Krakow it is ≈ 20 Bq m^{-3} and CDF of the TTE scheme is the closest to the observed CDF values. All schemes perform similarly at Schauinsland, while at Angus station the Grisogono is closest to the CDF calculated from the observations.

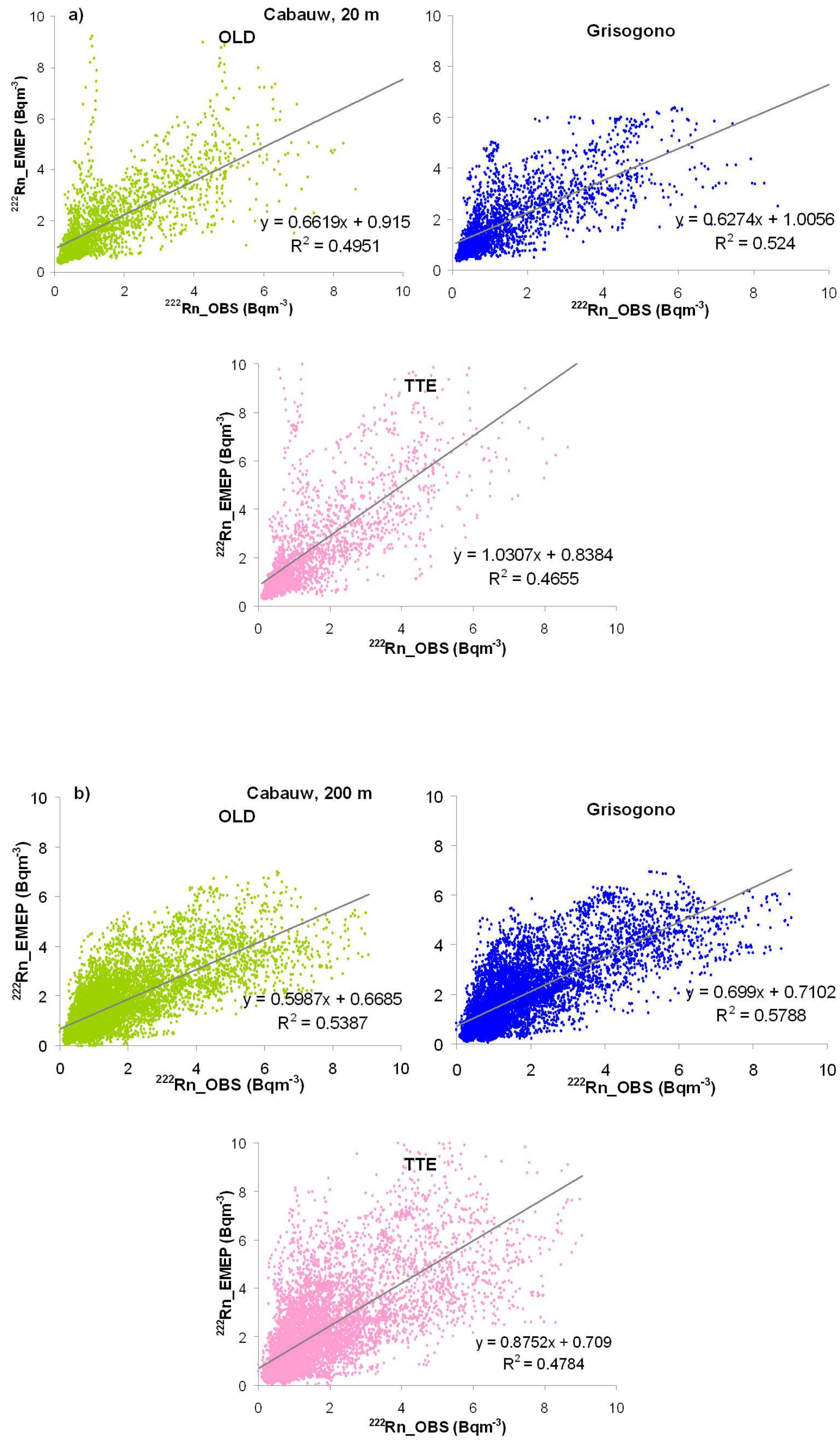

Figure 42. Yearly scatter plots between the observed and modelled hourly ^{222}Rn concentrations at a) the Cabauw at 20 m and b) the Cabauw at 200 m during the 2006. Different K(z) schemes are used in the EMEP model the OLD (green dots), Grisogono (blue dots) and TTE (pink dots) scheme.

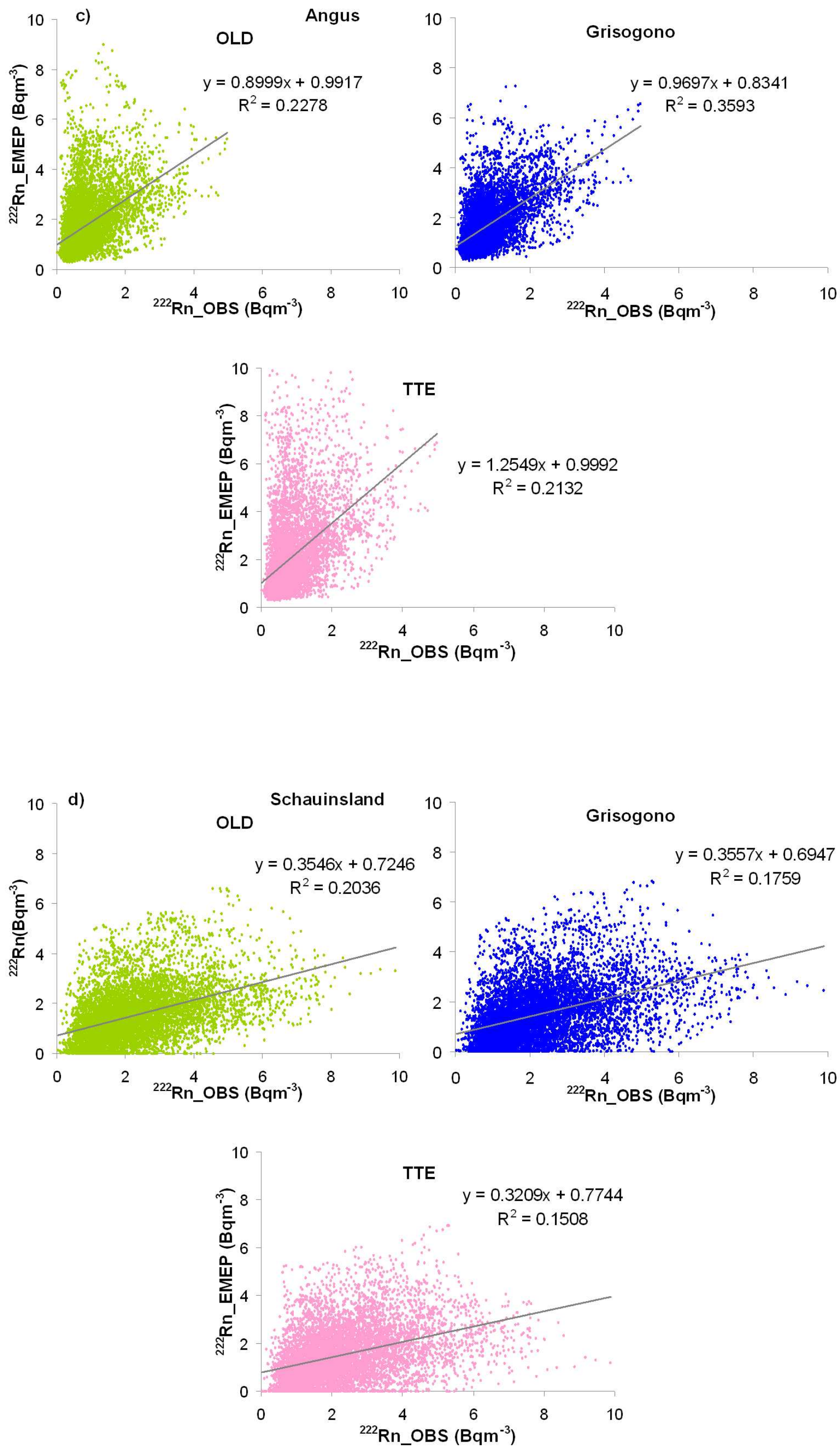

Figure 42-continued for c) Angus Scotland in 2006 and d) Schauinsland, Germany in 2005.

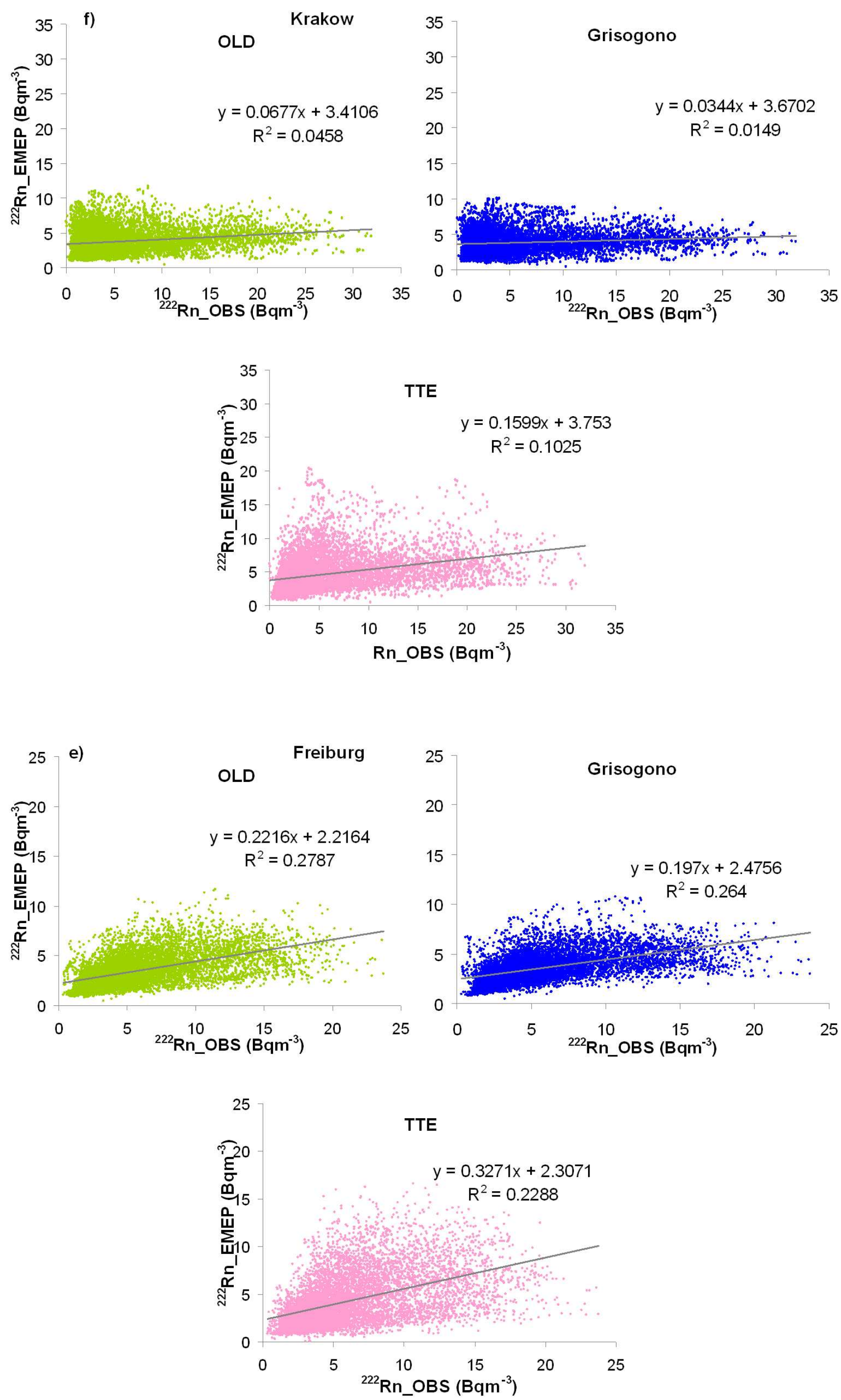

Figure 42-continued for d) Krakow, Poland in 2006 and e) Freiburg, Germany in 2005.

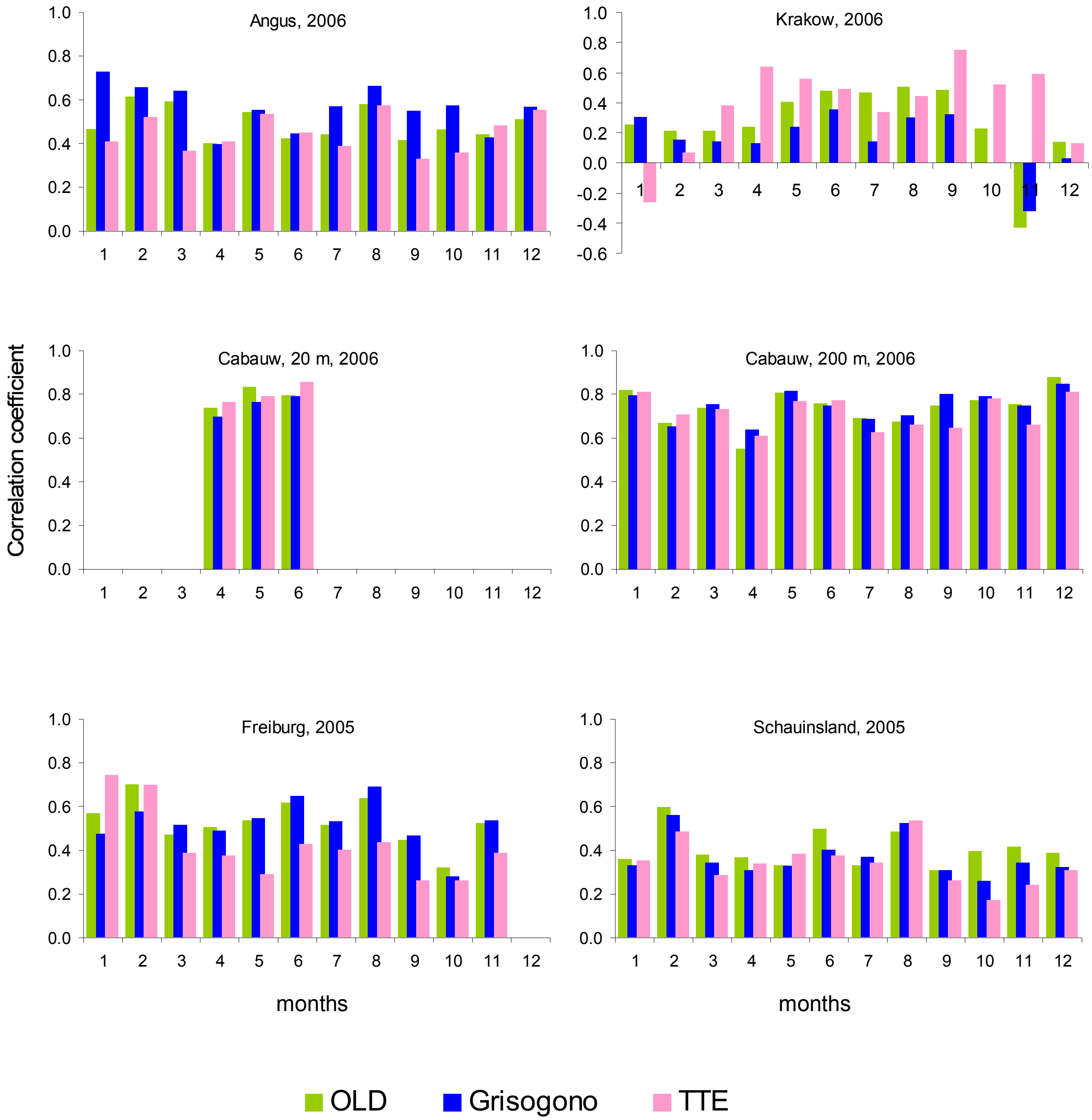

Figure 43. Monthly scatter plots between the observed and modelled hourly ^{222}Rn concentrations at a) the Cabauw at 20 m and b) the Cabauw at 200 m during the 2006. Different K(z) schemes are used in the EMEP model the OLD (green dots), Grisogono (blue dots) and TTE (pink dots) scheme.

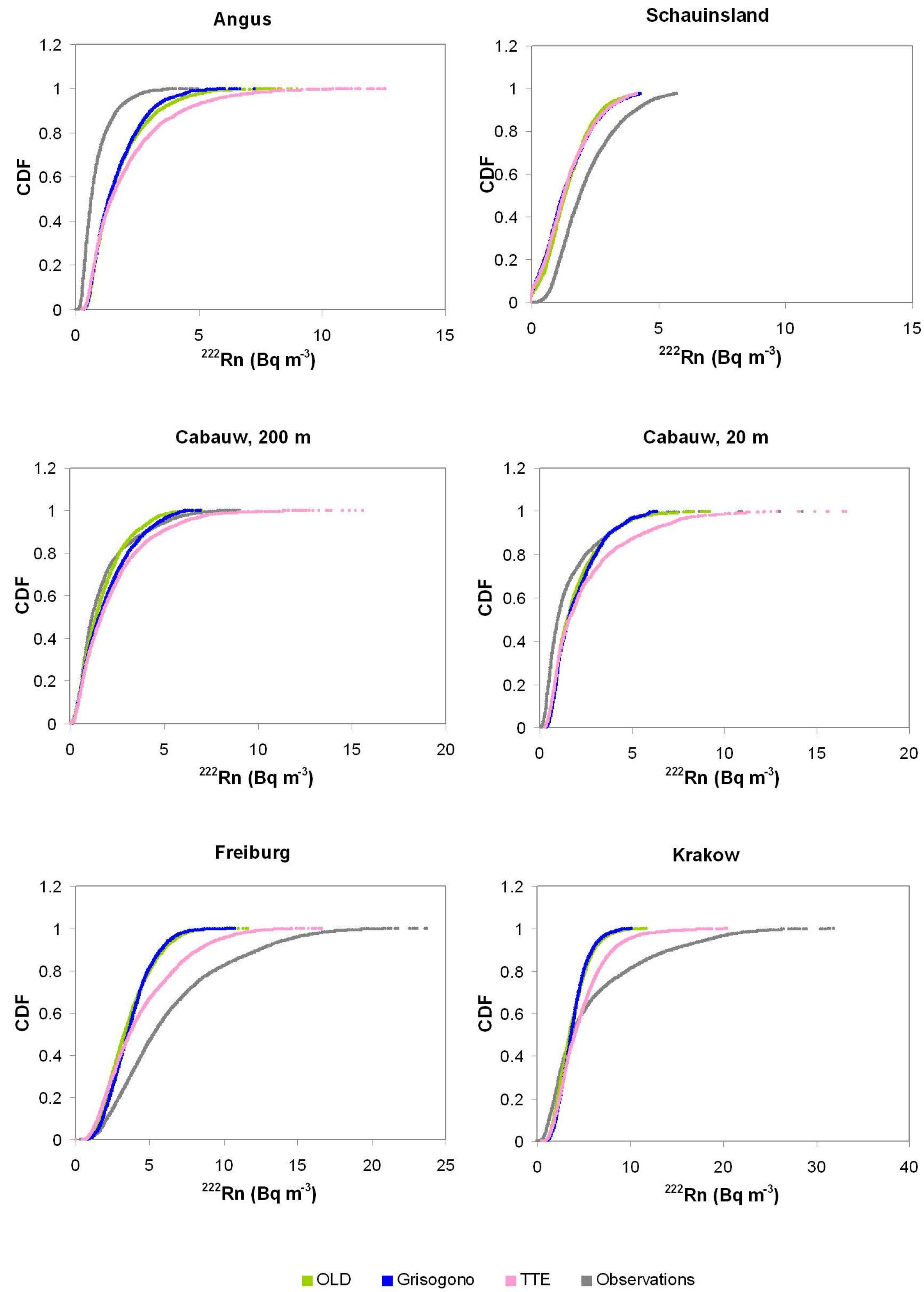

Figure 44. Cumulative density functions at different locations with three different $K(z)$ schemes employed in the EMEP model: the OLD, Grisogono and TTE scheme.

The annual *MAE* (Eq. 38), *MSE* (Eq. 39) and *RMSE* (Eq. 40) for all stations are shown in Figure 45. According to those values the model performs the best at the Cabauw, Angus and Schauinsland. At Freiburg and Krakow the *MAE*, *MSE* and *RMSE* are the highest. Intercomparison of different schemes based on *MAE*, *MSE* and *RMSE* is not conclusive.

The monthly *MAE*, *MSE* and *RMSE*, calculated for different $K(z)$ schemes applied in the model are shown in Figures from 46 to 50. Obviously highest discrepancies are found during colder part of the year at all stations. Note that the annual course is similar to the annual course of observed ^{222}Rn concentrations.

With the change of the parameterization schemes in the model systematic error i.e. $NMSE\_s$ should decrease as well as accuracy should increase. The results for *FB*, $NMSE\_s$, $NMSE\_u$ and total *NMSE* are shown in Table 5. At the Cabauw tower model performs almost perfect with *FB* nearly equal to zero and $NMSE\_s \approx 0$. The Grisogono scheme has the best performance at the Cabauw according to these measures. At Schauinsland the OLD scheme has slightly lower systematic error. However the total *NMSE* is reduced with the Grisogono scheme for all stations and with the TTE scheme, which managed to generate the highest concentrations, results are improved at Freiburg and Krakow.

Results of index of agreement, *d*, which is a descriptive, relative and bounded measure confirm that the best results are achieved with the Grisogono at the Cabauw tower, followed by Schauinsland where the OLD scheme still have the best results (Table 6). Improvements are found with the TTE scheme for Freiburg and Krakow.

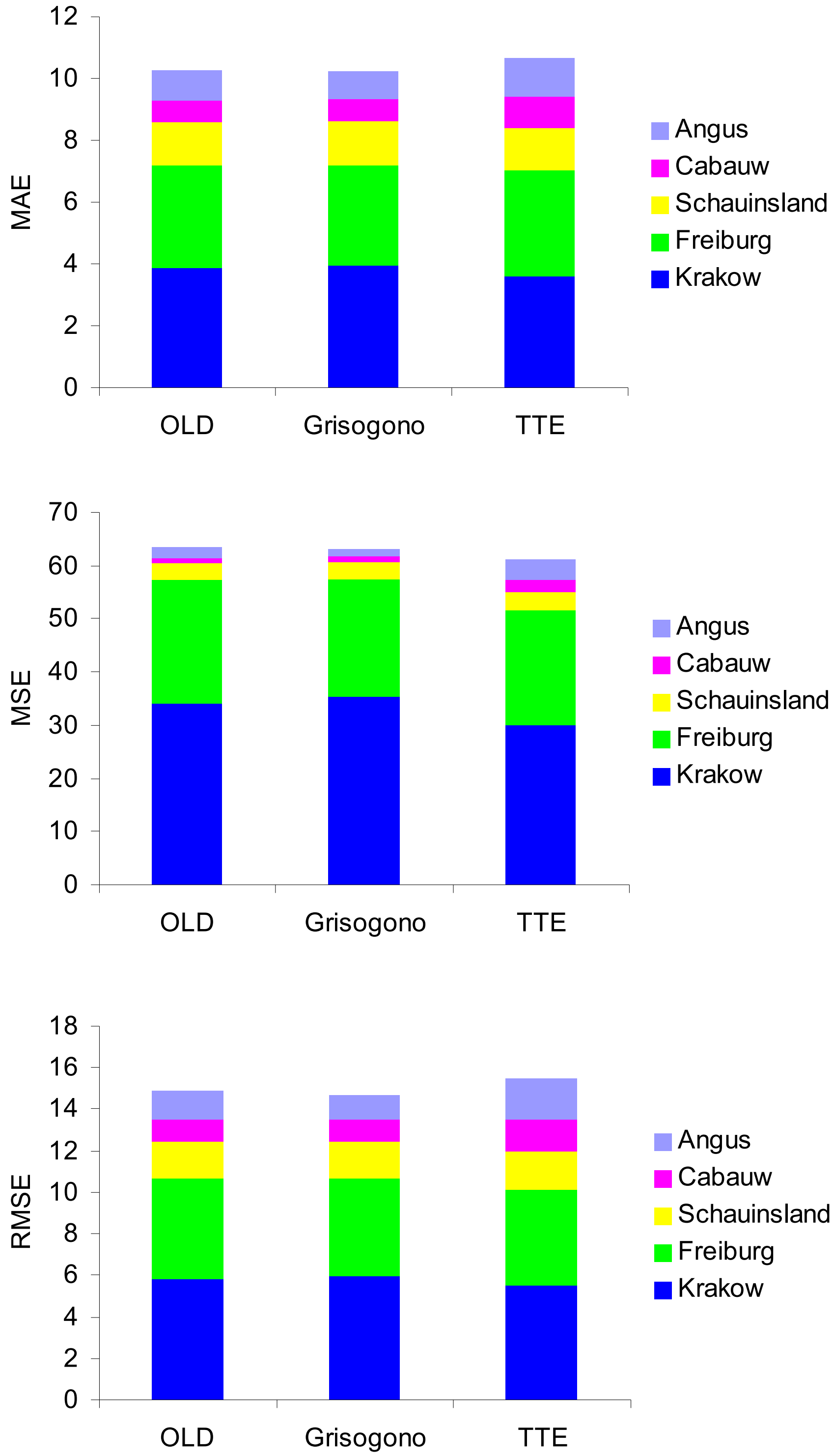

Figure 45. Annual *MAE*, *MSE* and *RMSE* for all stations with different $K(z)$ schemes applied in the model..

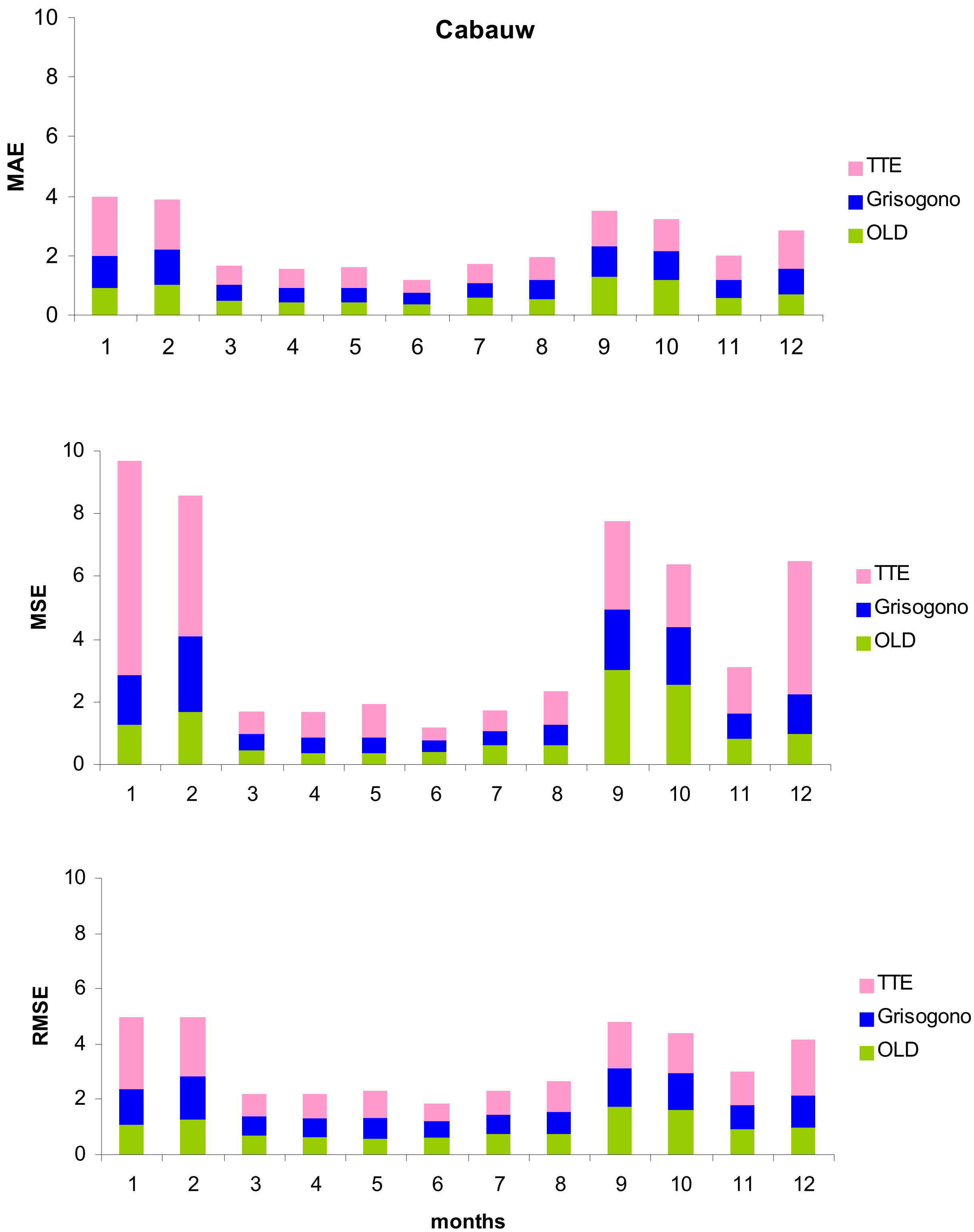

Figure 46. Monthly values of *MAE*, *MSE* and *RMS* for three different K(z) schemes applied in the EMEP model: the OLD, Grisogono and TTE, for Cabauw, the Netherlands.

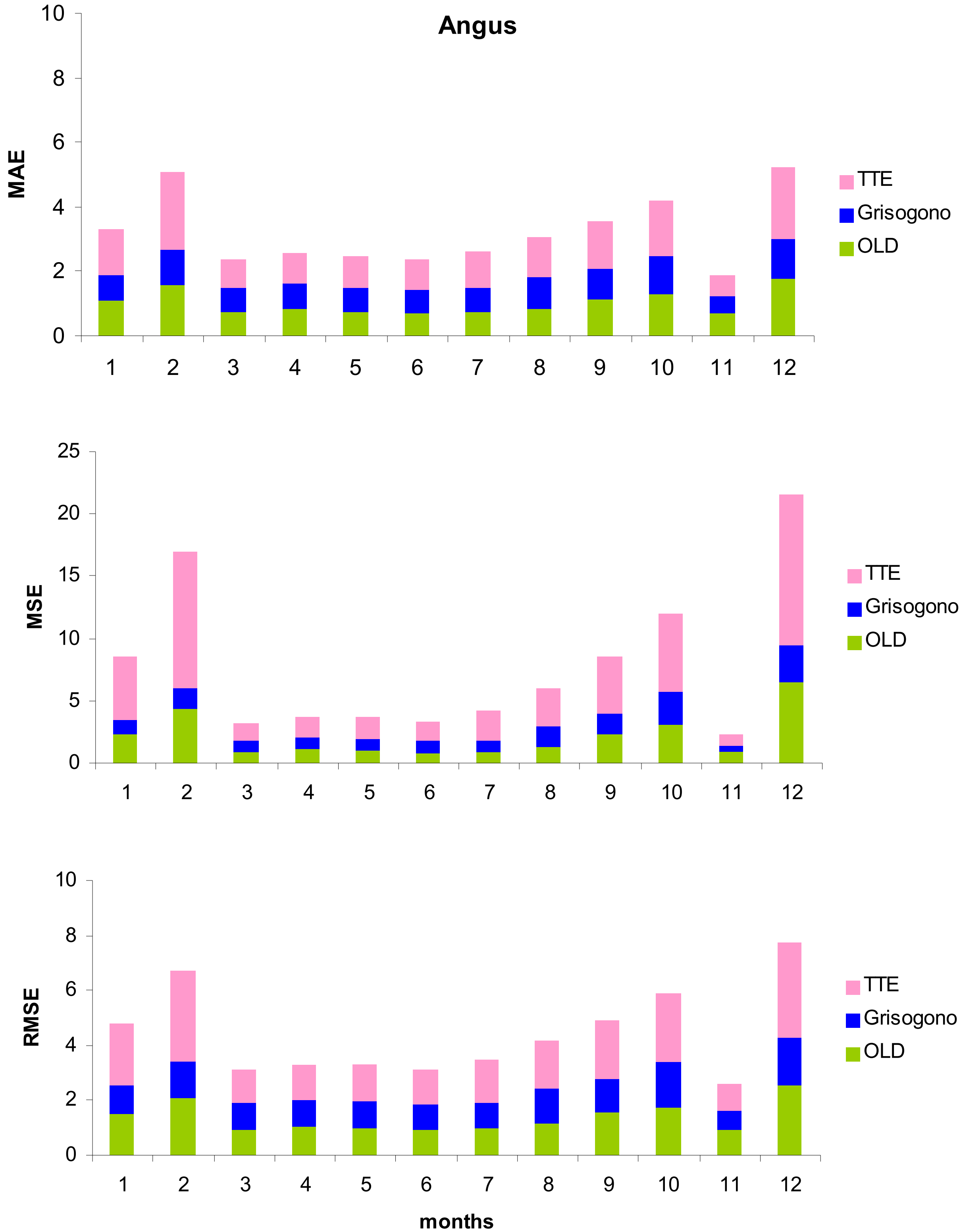

Figure 47. Same as Fig. 46 but for the Angus tower, Scotland.

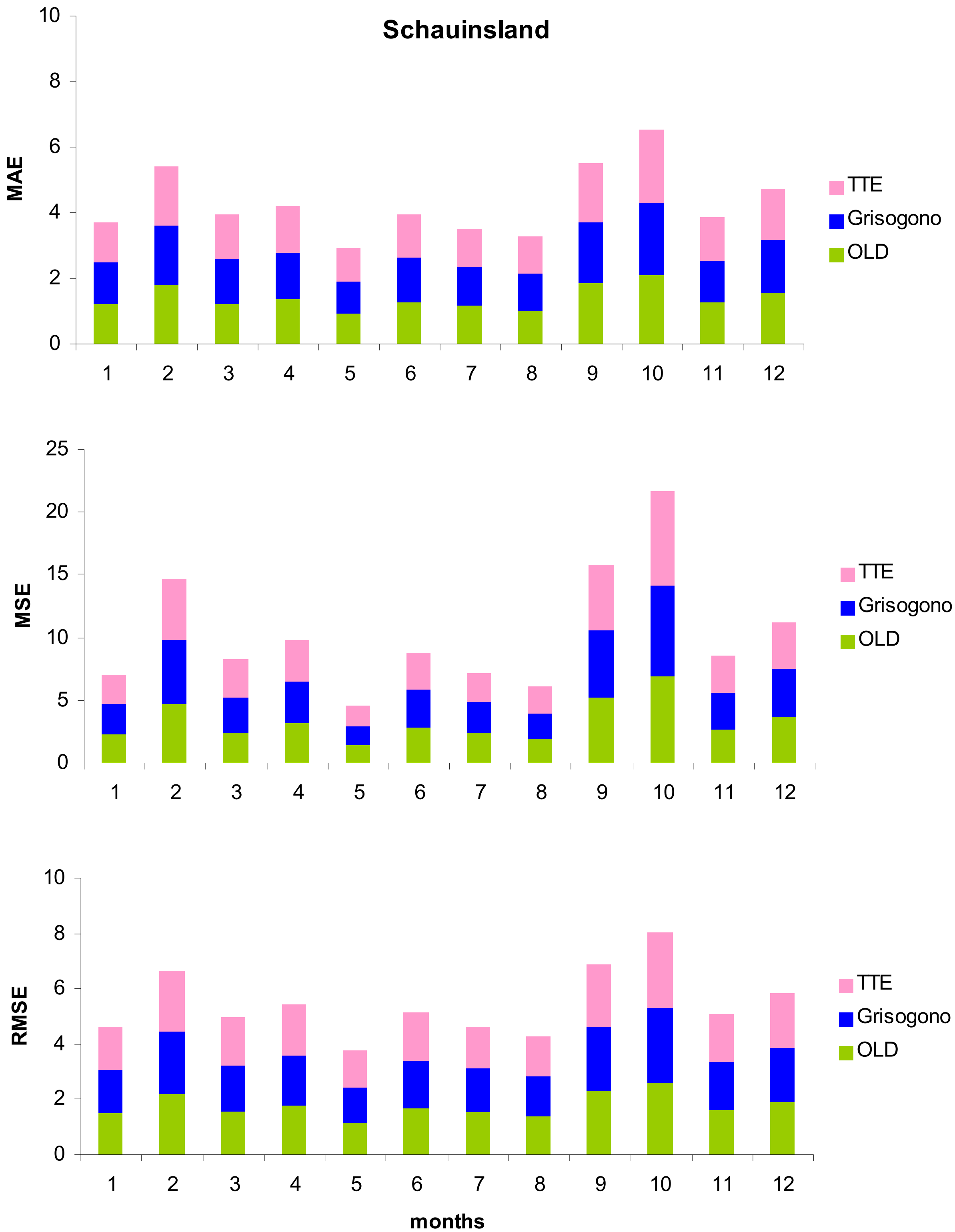

Figure 48. Same as Fig. 49 but for Schauinsland, Germany.

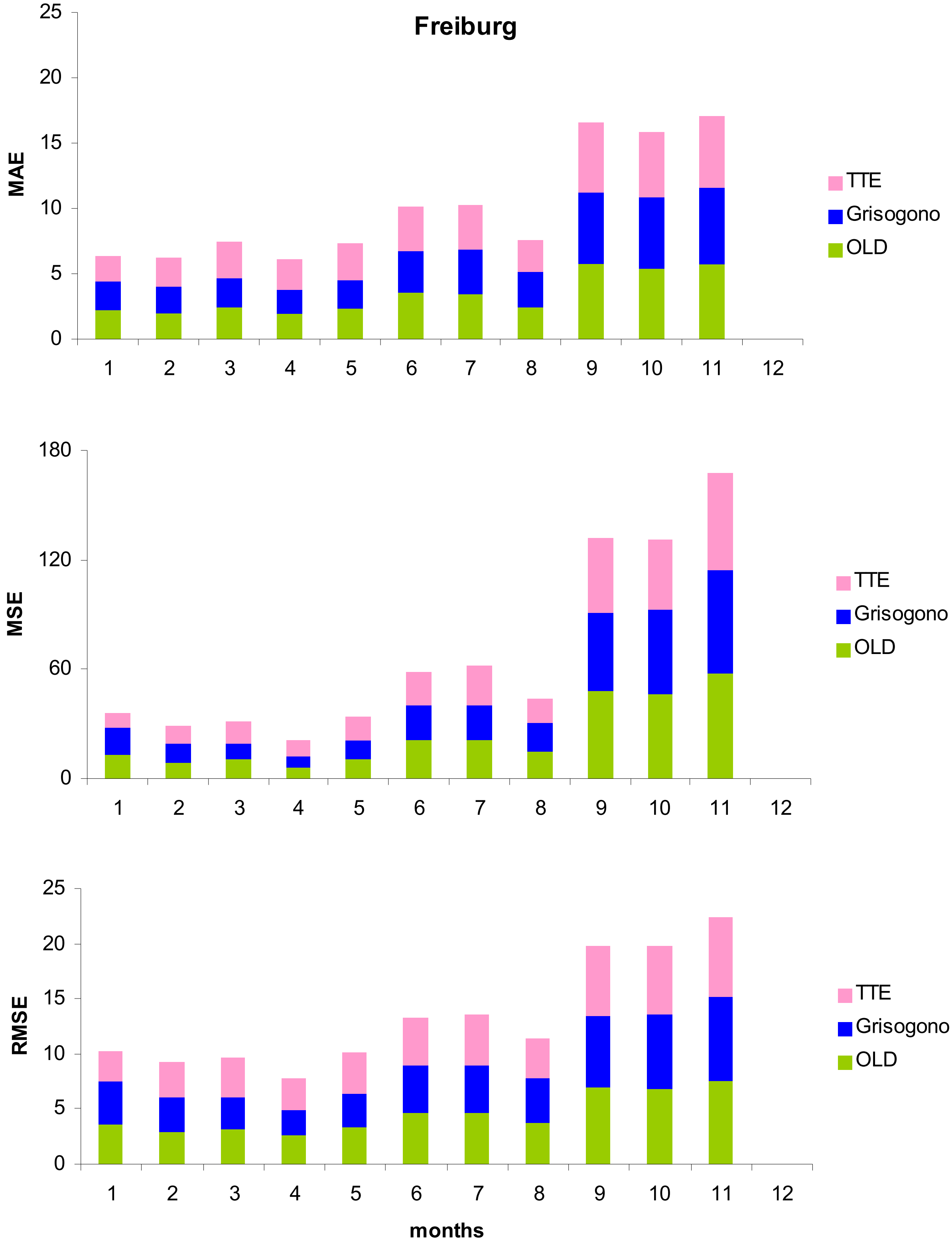

Figure 49. Same as Fig. 46 but for Freiburg, Germany.

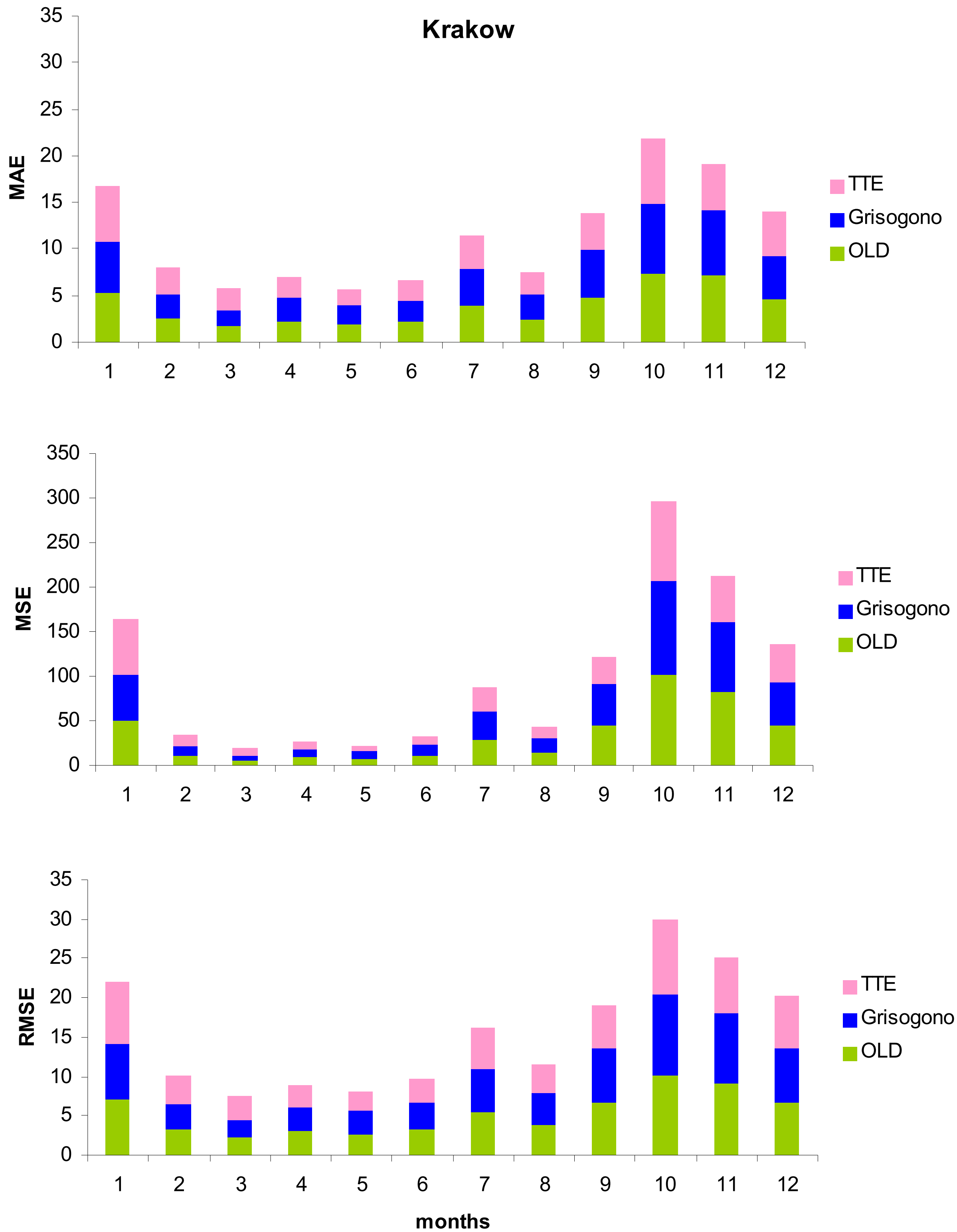

Figure 50. Same as Fig. 46 but for Krakow, Poland.

Table 5. Fractional bias (*FB*), systematic part of the normalised mean square error (*NMSE_s*), unsystematic part of the normalised mean square error (*NMSE_u*) and total normalised mean square error (*NMSE*) calculated between the modelled and measured hourly ^{222}Rn concentrations ($Bq\ m^{-3}$) for different stations: C-Cabauw tower at 200 m, the Netherlands; S-Schauinsland, Germany; K-Krakow, Poland; F-Freiburg, Germany and A-Angus tower, Scotland)

	FB			NMSE_s			NMSE_u			NMSE		
	OLD	G	TTE	OLD	G	TTE	OLD	G	TTE	OLD	G	TTE
C	0.03	-0.09	-0.22	0.00	0.01	0.05	0.40	0.33	0.49	0.40	0.34	0.54
S	0.37	0.39	0.38	0.14	0.16	0.15	0.45	0.51	0.54	0.60	0.67	0.69
K	0.43	0.42	0.25	0.20	0.18	0.06	1.31	1.34	1.01	1.50	1.52	1.07
F	0.55	0.52	0.37	0.32	0.29	0.14	0.51	0.51	0.47	0.83	0.80	0.61
A	-0.69	-0.64	-0.83	0.54	0.46	0.83	0.75	0.48	1.36	1.29	0.94	2.19

Table 6. Index of agreement, *d*, between the modelled and measured hourly ^{222}Rn concentrations ($Bq\ m^{-3}$) for different stations: the Cabauw tower at 200 m, the Netherlands; Schauinsland and Freiburg in Germany and Krakow, Poland during one year.

Index of agreement	OLD	Grisogono	TTE
Cabauw at 200 m	0.84	0.86	0.8
Schauinsland	0.62	0.61	0.59
Freiburg	0.57	0.55	0.63
Angus	0.50	0.62	0.45
Krakow	0.41	0.37	0.50

5. Conclusions

This work introduces two changes of the turbulence parameterization for the EMEP (European Monitoring and Evaluation Programme) Eulerian air pollution model: the replacement of the Blackadar in stable and O'Brien in unstable turbulence formulations with an analytical $K(z)$ profile called Grisogono, and a different mixing height determination, based on the bulk Richardson number formulation (Ri_B). The evaluation of the model performance on r and *BIAS* is conducted for the operational and the new model setup at all available measurements from EMEP stations in the year 2001. Representativeness of the observations is taken into account in order to determine the models ability to reproduce spatial variability in the simulation of different chemical species. Stations that are more affected by the local emission sources, as well as mountain stations do not show significant improvement with the change of the $K(z)$ scheme. On those stations the magnitude of the error is much higher than the magnitude of the variability resulting from the change of the $K(z)$ scheme. Therefore, a higher horizontal resolution, as well as better defined emissions, is needed in order to be able to simulate air pollution transport in a complex coastal terrain under the influences of local sources. It should be pointed out that the model *BIAS* is an overall measure for an improvement evaluation since it is very sensitive to changes in parameterization and the modelled absolute values can easily be right for the wrong reasons. Therefore, with the respect to the model performance for NO_2, SO_2 and SO_4^{2-} the conclusions are based on the changes in r between the observations and model results. Standard significance Fishers z-test (e.g. Pavlić, 1988) was conducted on the r determined between the measurements and the modelled data in order to find whether the change in r, due to changes in the parameterization schemes, reflects the change of stochastic relation between the two data sets. However, the appropriateness of this procedure was questioned because initial assumptions for its application were not completely satisfied (Fox, 1980; Willmott, 1982). Further evaluation of the model and the $K(z)$ parameterization schemes was based on ^{222}Rn data which was found to be a good element to study dynamical processes in the atmosphere. Simulations of ^{222}Rn with the EMEP model are performed during the years 2005 and 2006 and compared to the available ^{222}Rn measurements in Europe: the Cabauw, Angus, Freiburg, Schauinsland and Krakow. In addition to non-local schemes, the O'Brien and Grisogono, a new scheme which is local and based on total turbulent energy (TTE) closure (Mauritsen et al., 2007) is implemented in the EMEP model and analyzed (Jeričević et al., in preparation). In order to evaluate the predictions of a model with observations according to e.g. Wilmot (1982) and Chang and Hanna (2004) following statistical performance measures are used: the correlation coefficient (r), bias ($BIAS$), mean absolute error (MAE), mean square error (MSE), root mean square error ($RMSE$), fractional bias (FB), the normalized mean square error ($NMSE$) and the index of agreement (d).

The main conclusions are：

- The EMEP model shows a moderate improvement in r with the Grisogono scheme for NO_2 and SO_2 and a slight improvement for SO_4^{2-} for the most of the analyzed stations. The $r(NO_2)$ is improved around 0.1 on 51 % of the analyzed stations, while $r(SO_2)$ with the Grisogono scheme have an increase from 0.02 up to 0.12 on 54 % of the stations. For sulphate there is an increase in $r(SO_4^{2-})$ from 0.02 to 0.1. The annual r between the measured and modelled daily surface concentrations at all analyzed stations except those with higher uncertainties in the measurements show improvement in from 0.63 to 0.65 for NO_2, and from 0.55 to 0.57 for SO_2 with the new scheme. For the SO_4^{2-} correlation coefficient is around 0.61 with both schemes.
- The empirical coefficients based on LES data (DATABASE64; Esau and Zilitinkevich, 2006) in stable and neutral conditions are used in the Grisogono approach (Jeričević and Večenaj, 2009). However, the empirical constants contain a certain, although small, variability which may affect the intensity of the $K(z)$ scheme in different stability conditions. It is worth mentioning that the accuracy of the empirical constants depends on the reliability of the LES data. On the other hand the O'Brien scheme represents $K(z)$ as a polynomial function that depends on parameters: K_H, K_{H_S}, H, H_S which may be difficult to resolve (e.g. Zilitinkevich and Calanca, 2000; Jeričević and Grisogono, 2006; Mahrt, 2007). The local schemes are less dependent on the ABL depth than the non-local schemes. However, the Blackadar method, applied in the model for stable conditions, is based on the M-O theory (Monin and Obukhov, 1954). There are many studies which show that the surface-layer formulations based on the M - O theory are often not applicable in statically stable conditions (e.g. Mahrt, 1999; Pahlow et al., 2001; Poulos and Burns, 2003; Mauritsen et al., 2007; Grisogono et al., 2007). The Grisogono method is more technically convenient since only two input variables are demanded instead of

four. Therefore, the Grisogono scheme for $K(z)$ determination is recommended for practical applications, yielding an improvement in overall model results.

- In air quality modelling, $K(z)$ schemes depend on capabilities of used meteorological drivers as well as on model's horizontal and vertical grid resolution. Improvements in the NWP model performance would yield to appreciable differences in terms of both magnitude and spatial distribution of pollutants which would in the end improve the air quality model performance.
- The ABL height, H, calculated with the EMEP model is in a good agreement with the radiosounding measurements from different stations in Europe. The EMEP model is able to reproduce spatial and temporal variability of H, with r from 0.7 to 0.9 during convective conditions, and r from 0.4 to 0.6 in stable conditions with both ABL height schemes. However, the new ABL height scheme based on the Ri_B number performs better in stable conditions compared to the method based on the Blackadar $K(z)$ profiles which is also confirmed with significantly lower *BIAS* values. A considerable number of cases with $H > 200$ m, i.e. N, during the CBL conditions at the Cabauw tower is found, and also a negative effect of N on r values is established. The sensitivity of the Ri_B scheme on the choice of the lowest layer is confirmed in this paper, showing that in the case of strong surface influenced lowest layer, a considerably more cases ~ 30 %, with $H > 200$ m are found (Fig. 24) which is in the agreement with the results of Vogelezang and Holtslag (1996). In this paper the model's ability to simulate time evolution of the ABL and the strength of turbulence in the lowest part of the ABL is investigated and validated. Vertical measurements on the higher levels would help to identify the differences between the two ABL height schemes performances. Nevertheless, generally higher r and similar performance of the both ABL height schemes during the warmer part of the year is in agreement with the radiosoundings results, which showed that the ABL height scheme based on the Ri_B number method performs better in stable conditions than the operational one.
- Intercomparison of different local and non-local schemes on the ^{222}Rn data showed that the non-local scheme Grisogono is less diffusive in CBL conditions than the O'Brien and TTE scheme. Both non-local methods, the O'Brien and Grisogono, mainly depend on the position and intensity of $K_{\max}$. The local schemes produce higher surface concentrations

in SBL conditions, while the Grisogono scheme produces enhanced vertical and concentrations are transported to the higher levels. According to the Cabauw data in April, May and July; mixing should be even more intensive in the CBL conditions.

- Results of the model evaluation on radon data showed that the model has the best results for the Cabauw tower. The Cabauw tower is representative for model evaluation due to its position in a flat terrain. Furthermore the model has a good performance in Schauinsland. Since Schauinsland is only 8 km horizontal distance from Freiburg, and horizontal resolution in the model is 50 km x 50 km, the level closest to the height of the station is chosen as a representative for that mountain station. Results show that accuracy and systematic error in Schauinsland are low and that the chosen level is representative for the analyzed station. The model overestimates the measurements and the *NMSE* levels are quite high at the Angus tower. On the other hand the model underestimated the measurements at Freiburg and Krakow. It is likely that the observed ^{222}Rn concentrations at Freiburg and Kakow are influenced by higher local natural emissions that are not included in the model. However with the TTE scheme the systematic error is decreased and accuracy in increased in the model for Freiburg and Krakow. The Grisogono scheme performed the best at the Cabauw and Angus towers, while the OLD scheme has the best performance in Schauinsland.

This comprehensive evaluation research of different $K(z)$ and ABL schemes applied in the EMEP model provides a basis for further model evaluation and development of Croatian air quality modelling tools.

6. References

Allen, D.J., Rood, R.B., Thompson, A.M., and Hudson, R.D.: Three-dimensional radon 222 calculations using assimilated meteorological data and a convective mixing algorithm, J. Geophys. Res., 101, 6871-6881, 1996.

Andren, A., Brown, A., Graf, J., Moeng, C.H., Mason, P.J., Nieuwstadt, F.T.M., and Schumann, U.: Large-eddy simulation of neutrally-stratified boundary layer: a comparison of four computer codes. Q. J. Roy. Meteorol. Soc., 120, 1457-1484, 1994.

Athanassiadis, G., Trivikrama, R., Jia-Yeong, K., and Clarc, R.: Boundary layer evolution and its influence on ground level ozone concentrations, Environ. Fluid Mech., 2 (4), 339-357, doi:10.1023/A:102456018087, 2002.

Belušić, D., Koračin, D., Kos, I., Jeričević, A., and Horvath, K.: Simulations of the turbulence and dispersion processes in a coastal region. 11th Conference on Mountain Meteorology and the Annual Mesoscale Alpine Program (MAP), Bartlett, NH, USA, 21-25 Jun, 2004.

Beljaars, A. C. M., and Bosveld, F. C.: Cabauw data for the validation of land surface parameterization schemes, J. Climate, 10 (6), 1172-1193, doi:10.1175/1520-0442(1997)010<1172;CDFTVO>2.0.CO;2, 1997.

Berge, E., and Jakobsen, H. A.: A regional scale multi-layer model for the calculation of long-term transport and deposition of air pollution in Europe, Tellus, 50, 205–223, doi:10.1034/j.1600-0889.1998.t01-2-00001.x, 1998.

Bešlić, I., Šega, K., Čačković, M., Bencetić Klaić, Z., Bajić, A.: Relationship between 4-day air mass back trajectories and metallic components in PM_{10} and $PM_{2.5}$ particle fractions in Zagreb air, Croatia, Bull. Environ. Contam. Toxicol., 80, 270-273, 2008, DOI: 10.1007/s00128-008-9360-6.

Biswas, J., and Rao, T.: Uncertainties in episodic ozone modeling stemming from uncertainties in the meteorological fields, J. Appl. Meteorol., 40, 117-136, doi:10.1175/1520-0450(2001)040<0117:UIEOMS>2.0.CO;2, 2000.

Blackadar, A. K.: Modeling pollutant transfer during daytime convection. In: Fourth Symposium on Atmospheric Turbulence Diffusion and Air Quality, AMS, Reno, NV, pp. 443-447, 1979.

Chang, J.C., and Hanna, S.R.: Air quality model performance evaluation, Meteorol. Atmos. Phys., 87, 167-196, 2004.

Chen, T. H., Henderson-Sellers, A., Milly, P. C. D., Pitman, A., Beljaars, A. C. M., Abramopoulos, F., Boone, A., Chang, S., Chen, F., Dai, Y., Desborough, C., Dickinson, R., Duemenil, L., Ek, M., Garratt, J., Gedney, N., Gusev, Y., Kim, J., Koster, R., Kowalczyk, E., Laval, K., Lean, J., Lettenmaier, D., Liang, X., Mengelkamp, T.-H., Mahfouf, J.-F., Mitchell, K., Nasonova, O., Noilhan, J., Polcher, J., Robock, A., Rosenzweig, C., Schaake, J., Schlosser, C.A., Schulz, J.P., Shao, Y., Shmakin, A., Verseghy, D., Wetzel, P., Wood, E., Xue, Y., Yang, Z.-L., and Zeng, Q.-C.: Cabauw experimental results from the Project for Intercomparison of Land-surface Parameterization Schemes (PILPS), J. Climate, 10, 1194–1215, doi:10.1175/1520-0442(1997)010<1194;CERFTP>2.0.CO;2, 1997.

Conen, F., and Robertson, L.B.: Latitudinal distribution of radon-222 flux from continents, Tellus, 54B, 127-133, 2002.

Deardorff, J.W.: Convective velocity and temperature scales for the unstable planetary boundary layer and for Raleigh convection, J. Atmos. Sci., 29, 91-115, 1970.

Deardorff, J. W.: Parameterization of the planetary boundary layer for use in general circulation model, Mon. Weather Rev., 100, 93–106, doi:10.1175/1520-0469(19729029<0091:NIONAU>2.0.CO;2, 1972.

Dentener, F., Feichter, J., and Jeuken, A.: Simulation of the transport of 222Rn using on-line and off-line global models at different horizontal resolutions: a detailed comparison with measurements, Tellus B, 51, 573-602, 1999.

Ding, F., Arya, S. P., Lin, Y.L.: Large-eddy simulations of the atmospheric boundary layer using a new subgrid-scale model. Part II: Weakly and moderately stable cases, Environ. Fluid Mech., 1, 49-69, 2001.

Ek, M. B., and Holtslag, A. A. M.: Evaluation of a land-surface scheme at Cabauw, Theor. Appl. Climatol., 80, 213–227, DOI:10.1007/S00704-004-0101-4, 2005.

ENVIRON: User's Guide to the Comprehensive Air Quality Model with Extensions (CAMx) Version 2.00. ENVIRON International Corporation, 101 Rowland Way, Suite 220, Novato, California, 94945-5010, http://www.camx.com/, 1998.

Esau, I., and Zilitinkevich, S. S.: Universal dependences between turbulent and mean flow parameters in stably and neutrally stratified planetary boundary layers, Nonlinear Proc. Geoph. 13, 122-144, 2006.

Fagerli, H., and Eliassen, A.: Modified parameterization of vertical diffusion. In: Transboundary Acidification, Eutrophication and Ground Level ozone in Europe, EMEP Summary Status Report 2002, Joint CCC & MSC-W Research Report No. 1&2/01, Norwegian Meteorological Institute, Oslo, Norway, p.p. 74, available from http://emep.int/publ/common_publications.html#2003, 2002.

Fagerli, H., Simpson, D., and Aas, W.: Model performance for sulphur and nitrogen compounds for the period 1980 to 2000, In L. Tarrasón, Editor, Transboundary Acidification, Eutrophication and Ground Level Ozone in Europe. EMEP Status Report 1/2003, Part II Unified EMEP Model Performance, pp. 66, The Norwegian Meteorological Institute, Oslo, Norway, 2003.

Fagerli, H., Simpson, D., and Tsyro, S.: Unified EMEP model: Updates. In EMEP Report 1/2004, Transboundary acidification, eutrophication and ground level ozone in Europe, Status Report 1/2004, pp. 11–18, The Norwegian Meteorological Institute, Oslo, Norway, 2004.

Fagerli, H., Legrand, M., Preunkert, S., Simpson, D., Vestreng, V., and Cerqueira, M.: Modeling historical long-term trends of sulphate, ammonium and elemental carbon over Europe: A comparison with ice core records in the Alps, J. Geophys. Res., 112, D23S13, doi:10.1029/2006JD008044, 2007.

Fagerli, H., and Aas, W.: Trends of nitrogen in air and precipitation: Model results and observations at EMEP sites in Europe, 1980-2003. Environ. Pollut., 154, 448–461, doi: 10.1016/j.envpol.2008.01.024, 2008.

Fay, B., Schrodin, R., Jacobsen, I., and Engelbart, D.: Validation of mixing heights derived from the operational NWP models at the German Weather Service. In: The determination of the mixing height – current progress and problems, EURASAP Workshop Proceedings 1-3 Oct 1997, (ed. S.-E. Gryning), Report Risø-R-997 (EN), ISBN 87-550-2325-8, Risø National Laboratory, Roskilde, Denmark, pp 55-58, 1997.

Fox, D.G.: Judging air quality model performance: A summary of the AMS Workshop on Dispersion Model Performance, Bull. Am. Meteorol. Soc., 62, 599-609. doi: 10.1175/1520-0477(1981)062<0599:JAQMP>2.0.CO;2, 1981.

Galmarini, S.: One year of 222-Rn concentration in the atmospheric surface layer, Atmos. Chem. Phys. 6, 2865–2887, 2006.

Garratt, J. R: The atmospheric boundary layer, Cambridge University Press, pp. 316, 1992.

Geleyn, J. F., Banciu, D., Bubnova, R., Ihasz, I., Ivanovici, V., LeMoigne, P., and Radnoti, G: The international project ALADIN: Summary of events October 1992–October 1993., LAM Newsletter, 23, 1992.

Grisogono, B.: A generalized Ekman layer profile within gradually-varying eddy diffusivities, Q. J. Roy. Meteorol. Soc., 121, 445-453, 1995.

Grisogono, B., and Oerlemans, J.: A theory for the estimation of surface fluxes in simple katabatic flows, Q. J. Roy. Meteorol. Soc., 127, 2725-2739, 2001.

Grisogono, B., and Oerlemans, J.: Justifying the WKB approximation in pure katabatic flows, Tellus A, 54, 453-462, doi:10.1034/j.1600-0870.2002.201399.x, 2002.

Grisogono, B., Kraljević, L., and Jeričević, A.: The low-level katabatic jet height versus Monin-Obukhov height, Q. J. Roy. Meteorol. Soc., 133, 2133-2136, 2007.

Grisogono, B., and Belušić, D.: Improving mixing length-scale for stable boundary layers, Q. J. Roy. Meteorol. Soc., 134, 2185-2192, 2008.

Gryning, S.-E., and Batchvarova, E.: Marine boundary layer and turbulent fluxes over the Baltic sea: measurements and modelling, Bound.-Lay. Meteorol., 103, 29-47, 2002.

Holtslag, A. A. M., and Moeng, C. H.: Eddy diffusivity and countergradient transport in the convective atmospheric boundary layer, J. Atmos. Sci., 48, 1690–1698, doi:10.1175/1520-0469(1991)048<1690:EDACTI>2.0.CO;2, 1991.

Holtslag, A. A. M., and Boville, B. A.: Local versus nonlocal boundary-layer diffusion in a global climate model, J. Climate, 6, 1825–1842, doi:10.1175/1520-0442(1993)006<1825:LVNBLD>2.0.CO;2, 1993.

Ivatek-Šahdan, S., and Tudor, M.: Use of high-resolution dynamical adaptation in operational suite and research impact studies, Meteorol. Z., 13 (2), 99-108, 2004.

Jakobsen, H. A., Berge, E., Iversen, T., and Skalin, R.: Status of the development of the multilayer Eulerian model, EMEP/MSC-W Note 3/95, available from http://www.emep.int/mscw/ mscw_publications.html#1995, 1995.

Jeričević, A.: Atmospheric boundary layer height in urban conditions, Master Thesis, Department of Geophysics, Faculty of Science, University of Zagreb, 63 pp, 2005.

Jeričević, A. and Grisogono, B.: The critical bulk richardson number in urban areas: verification and application in a numerical weather prediction model, Tellus A, 58, 19-27, doi:10.1111/j.1600-0870.2006.00153.x, 2006.

Jeričević, A., Kraljević, L., Vidič, S., and Tarrasón, L.: Project description: High resolution environmental modelling and evaluation programme for Croatia (EMEP4HR), Geofizika, 24 (2), 137-143, available form http://geofizika-journal.gfz.hr/vol24.htm, 2007.

Jeričević, A., and Večenaj, Ž.: Improvement of vertical diffusion analytic schemes under stable atmospheric conditions, Bound.-Lay. Meteorol., 131, 293-307, doi: 0.1007/s10546-009-9367-5, 2009.

Jeričević, A., Fagerli, H., and Grisogono, B.: Local and non-local vertical diffusion schemes evaluation with simulation of ^{222}Rn regional transport, in preparation for Atmos. Chem. Phys., 2009.

Jeričević, A., Kraljević, L. Grisogono, B., Fagerli, H., and Večenaj, Ž.: Parameterization of vertical diffusion and the atmospheric boundary layer height determination in the EMEP model, Atmos. Chem. Phys. Discuss, 9, 9597-9645, 2009.

Jonson, J. E., Bartnicki, J., Olendrzynski, K., Jakobsen, H. A., and Berge, E.: EMEP Eulerian model for atmospheric transport and deposition of nitrogen species over Europe, Environ. Pollut., 102, 289–298, 1998.

Jonson, J. E., Simpson, D., Fagerli, H., and Solberg, S.: Can we explain the trends in European ozone levels?, Atmos. Chem. Phys., 6(1):51–66, available from http://www.atmos-chem-phys.net/6/51/2006/acp-5-51-2006.pdf, 2006.

Josse, B., Simon, P., and Peuch, V.-H.: Radon global simulations with the multiscale chemistry and transport model MOCAGE, Tellus B, 56, 339-356, 2004.

Klaić, Z.: A lagrangian one-layer model of long-range transport of SO_2, Atmos. Environ., 24 A, 1861-1867, 1990.

Klaić, Z., and Cvitan, L.: The applicability of the several methods of estimation of the wind profile to the 925 hPa pressure level winds, Rivista di meteorologia aeronautica, 53, 7-19, 1993.

Klaić, Z: A lagrangian model of long-range transport of sulphur with the diurnal variations of some model parameters, J. Appl. Meteorol., 35, 574-586, 1996.

Klaić, Z., and Beširević, S.: Modelled sulphur depositions over Croatia, Meteorol. Atmos. Phys., 65, 133-138, 1998.

Klaić Z.B.: Assessment of wintertime atmospheric input of European sulfur to the Eastern Adriatic, Il Nuovo Cimento C, 26 C, 1-6, 2003.

Kos, I., Belušić, D., Jeričević, A., Horvath, K., Koračin, D., and Telišman Prtenjak, M.: A Description of Atmospheric Lagrangian Particle Stochastic (ALPS) Dispersion Model, Geofizika, 21, 37-52, 2004.

Kosovic, B., and Curry, J.A.: A quasi steady state of a stable stratified atmospheric boundary layer: a large-eddy simulation study, J. Atmos. Sci., 57,1052-1068, 2000.

Koračin, D., Isakov, V., and Frye, J.: A Lagrangian particle dispersion model (LAP) applied to transport and dispersion of chemical tracers in complex terrain. Preprints 10th Joint 50 I. KOS ET AL.: EDUCATION AND RESEARCH – DISPERSION MODEL Conf. of the Appl. of Air Pollution Meteor. with the Air and Waste Manag. Assoc. (AWMA), AMS, Phoenix, AZ, 227–230, 1998.

Koračin, D., Isakov, V., Podnar, D., and Frye, J.: Application of a Lagrangian random particle dispersion model to the short-term impact of mobile emissions. Proceedings of the Transport and Air Pollution Conference, Graz, Austria, 31 May – 2 June 1999.

Kraljević, L., Belušić, D., Bencetić Klaić, Z., Bennedictow, A., Fagerli, H., Grisogono, B., Jeričević, A., Mihajlović, D., Špoler Čanić, K., Tarrasón, L., Valiyaveetil, S., Vešligaj, D., and Vidič, S.: Application of EMEP Unified model on regional scale – EMEP4HR, Croat. Meteorol. J., 43, Proceedings from a 12 HARMO conference Part 1: Oral Presentations, /Đuričić, Vesna (Ed.), Zagreb, 151-151, available from http://www.harmo.org/Conferences/Proceedings/_Cavtat/topicIndex.asp?topicID=0, 2008.

Lee, H. N., and Larsen, R. J.: Vertical diffusion in the lower atmosphere using aircraft measurements of 222Rn, J. Appl. Meteorol., 36, 1262-1270, doi:10.1175/1520-0450(1997)036<1262:VDITLA>2.0.CO;2, 1997.

Liu, S. C., McAfee, J. R., and Cicerone, R. J.: Radon 222 and tropospheric vertical transport, J. Geophys. Res., D5, 7291–7297,1984

Louis, J. F.: A parametric model of vertical eddy fluxes in the atmosphere, Bound.-Lay. Meteorol., 17, 187–202, 1979.

Mahrt, L.: Modelling the depth of the stable boundary layer, Bound.-Lay. Meteorol., 21, 3-19, 1981.

Mahrt, L.: Stratified Atmospheric Boundary Layers, Bound.-Lay. Meteorol., 90, 375-396, doi:10.1023/ A:1001765727956, 1999.

Mahrt, L.: The influence of nonstationarity on the turbulent flux-gradient relationship for stable stratification, Bound.-Lay. Meteorol., 125, 245-264, doi:10.1007/s10546-007-9154-0, 2007.

Mahrt, L., and Vickers, D.: Extremely weak mixing in stable conditions. Boundary-Layer Meteorol., 119:19-36, 2006.

Mauritsen, T., Svensson, G., Zilitinkevich, S., Esau, I., Enger, L., and Grisogono, B.: A total turbulent energy closure model for neutrally and stably stratified atmospheric boundary layers, J. Atmos. Sci., 64, 4113-4126, doi:10.1175/2007JAS2294.1, 2007.

McNider, R.T., and Pielke, R.A.: Diurnal boundary layer development over sloping terrain, J. Atmos. Sci., 38, 198-2212, doi:10.1175/1520-0469(1981)038<2198:DBLDOS>2.0.CO;2, 1981.

Monin, A. S., and Obukhov, A. M.: Basic laws of turbulent mixing in the surface layer of the atmosphere, Tr. Geofiz. inst. Akad. Nauk SSSR, 151, 163-187, 1954.

Nowacki, P., Samson, P. J., and Sillman, S.: Sensitivity of Urban Airshed Model (UAM-IV) Calculated Air Pollutant Concentrations to the Vertical Diffusion Parametrisation During Convective Meteorological Situations, J. Appl. Meteorol., 35, 1790-1803, doi:10.1175/1520-0450(1996)035<1790:SOUAMI>2.0.CO;2, 1996.

O’Brien, J. J.: A Note on the vertical structure of the eddy exchange coefficient in the planetary boundary layer, J. Atmos. Sci., 27, 1213-1215, doi:10.1175/1520-0469(1970)027<1213:ANOTVS>2.0.CO;2, 1970.

Oliviè, D. J. L., Van Velthoven, P. F. J., and Beljaars, A. C. M.: Evaluation of archived and off-line diagnosed vertical diffusion coefficients from ERA-40 with 222Rn simulations, Atmos. Chem. Phys., 4, 2313-2336, available from http://www.atmos-chem-hys.net/4/issue9_10.html, 2004.

Pavlić, I.: Statistička teorija i primjena, pp 343, Tehnička knjiga, Zagreb, 1988 (ponovljeno izdanje).

Pahlow, M., Parlange, M. B., and Porté-Agel, F.: On Monin-Obukhov similarity in the stable atmospheric boundary layer, Bound.-Lay. Meteorol., 99, 225-248, doi:10.1023/A:1018909000098, 2001.

Peljto (Jeričević) A., and Klaić B. Z: Accidental release of hydrogen sulphide in Nagilengel, Hungary on November 14, 1998- A trajectory study, Geofizika, 16-17, 43-51, 1999-2000.

Petersen, A. J., Spee, E. J., van Dop, H., and Hundsdorfer, W.: Sensitivity of atmospheric transport model performance to numerical advection schemes and resolution, J. Geophys. Res., 103, 19253-19259, 1998.

Pielke, R.A.: Mesoscale Meteorological Modeling, 2nd ed., Academic Press, London, pp 672, 2002.

Poulos, G. S., and Burns, S. P.: An evaluation of bulk Ri-based surface layer flux formulas for stable and very stable conditions with intermittent turbulence, J. Atmos. Sci., 60, 2523-2537, doi:10.1175/1520-0469(2003)060<2523:AEOBRS>2.0.CO;2, 2003.

Prtenjak, M. T., Jeričević, A., Kraljević, L., Bulić I.H., Nitis, T., and Klaić, Z. B. : Exploring atmospheric boundary layer characteristics in a severe SO_2 episode in the north-eastern Adriatic, Atmos. Chem. Phys. Discuss., 9, 6283-6324, 2009.

Schäfer, K., Emeis, S., Hoffmann, J., and Jahn C.: Influence of mixing height upon air pollution in urban and suburban areas, Meteorol. Z., 15, 647-658, 2006.

Seibert, P., Beyrich, F., Gryning, S.-E., Joffre, S., Rasmussen, A., and Tercier, Ph.: Review and intercomparison of operational methods for the determination of the mixing height, Atmos. Environ., 34, 1001-1027, doi:10.1016/S1352-2310(99)00349-0, 2000.

Seinfeld, J.H., and Pandis, S.N.: Atmospheric chemistry and physic: from air pollution to climate change, John Wiley and Sons, Inc., New York, pp. 1326, 1998.

Simpson, D., Fagerli, H., Jonson, J.E., Tsyro, S., Wind, P., and Tuovinen, J.-P.: The EMEP Unified Eulerian Model. Model Description. Technical Report EMEP MSC-W Report 1/2003, The Norwegian Meteorological Institute, Oslo, Norway, 2003.

Simpson, D., Butterbach-Bahl, K., Fagerli, H., Kesik, M., and Skiba, U.: Deposition and emissions of reactive nitrogen over European forests: A modelling study, Atmospheric Environment, 40(29), 5712–5726, 2006a.

Simpson, D., Fagerli, H., Hellsten, S., Knulst, K., and Westling, O.: Comparison of modelled and monitored deposition fluxes of sulphur and nitrogen to ICPforest sites in Europe, Biogeosciences, 337–355, 2006b.

Simpson, D., Yttri, K.E., Klimont, Z., Kupiainen, K., Caseiro, A., Gelencs´er, A., Pio, C., and Legrand, M.: Modeling carbonaceous aerosol over Europe. Analysis of the CARBOSOL and EMEP EC/OC campaigns, J. Geophys. Res., 112, D23S14, doi: 10.1029/2006JD008158, 2007.

Skamarock, W. C., J. B. Klemp, J. Dudhia, D. O. Gill,D. M. Barker, W. Wang, and J. G. Powers, 2005: A description of the advanced research WRF version 2. NCAR/TN-468+STR, 88 pp.

Sørensen, J.H., Rasmussen, A., and Svensmark, H.: Forecast of atmospheric boundary-layer height for ETEX real-time dispersion modelling, Phys. Chem. Earth, 21, 435-439, doi:10.1016/SOO79-1946(97)81138-x, 1996.

Stull, R.B.: An Introduction to Boundary Layer Meteorology', Kluwer Academic Publishers, Dordrecht, the Netherlands, pp. 666, 1988.

Šinik, N.: A model for calculation of ground level concentrations, Rasprave, 16, 47–54, 1981.

Šinik, N., Lončar, E., Vidič, S., and Bajsić, M.: Primjena Gausovskog modela na Plomin 1 i 2, Konferencija o zaštiti Jadrana, Budva, 16. i 17. studeni 1984.

Špoler Čanić, K., and Jeričević, A.: Modelled concentrations of air pollutant depending on input data, Proceedings of the 10th International Conference on "Harmonization within Atmospheric Dispersion Modeling for Regulatory Purposes" / A. N. Skouloudis, P. Kassomenos, J. Bartzis (ed.), Heraklion, September, 255-259, 2005.

Tsyro, S., Simpson, D., Tarrasón, L., Klimont, Z., Kupiainen, K., Pio, C., and Yttri, K. E.: Modeling of elemental carbon over Europe, J. Geophys. Res., 112, D23S19, doi: 10.1029/2006JD008164.2, 2007.

Troen, I. B., and Mahrt, L.: A simple model of the atmospheric boundary layer; sensitivity to surface evaporation, Bound.-Layer. Meteorol., 37, 129-148, doi:10.1007/BF00122760, 1986.

van Ulden, A.P. and Wieringa, J.: Atmospheric boundary layer research at Cabauw, Bound.-Lay. Meteorol., 78, 39-69, doi:10.1007/BF00122486, 1995.

Vidič, S.: Local distribution of meteorological parameters incorporated in an investigation of the gaussian diffusion model sensitivity, Rasprave, 16, 55–63, 1981.

Vidič, S.: Ovisnost proračuna maksimalnih prizemnih koncentracija zagađujućih materija o ulaznim parametrima modela. Zbornik radova s I Jugoslavenskog kongresa o očuvanju čistoće vazduha, Zenica, 455–463, 1989.

Vieno, M., Dore, A. J., Wind, P., Di Marco, C., Nemitz, E., Phillips, G., Tarrasón, L., and Sutton, M. A.: Application of the EMEP Unified Model to the UK with a horizontal resolution of 5 × 5 km^2 in: Atmospheric ammonia: Detecting emission changes and environmental impacts. (Ed. Sutton, M. A , Baker, S., and Reis, S.), Springer, pp. 367-372, 2009.

Vieno, M., Dore, A. J., Stevenson, D. S., Doherty, R., Heal, M., Reis, S., Hallsworth, S., Tarrasón, L., Wind, P., Fowler, D. Simpson, D., and Sutton, M. A.: Modelling surface ozone during the 2003 heat wave in the UK, (in preparation to be submitted to the Atmos. Chem. Phys.), 2009.

Willmott, C.J.: Some comments on the evaluation of model performance, Bull. Am. Meteorol. Soc., 63, 1309-1313, doi: 10.1175/1520-0477(1982)063<1309:SCOTEO>2.0.CO;2, 1982.

Vinuesa, J.-F., and Galmarini, S.: Characterization of the 222Rn family turbulent transport in the convective atmospheric boundary layer, Atmos. Chem. Phys., 7, 697–712, 2007, http://www.atmos-chem-phys.net/7/697/2007/.

Wyngaard, J.C., Brost, R.A.: Top-down and bottom-up diffusion of a scalar in the convective boundary layer, J. Atmos. Sci., 41, 102-112, 1984.

Zhang, Y., Pun B., Wu, S.-Y., Vijayaraghavan, K., and Seigneur, C.: Application and evaluation of two air quality models for particulate matter for a southeastern U. S. episode, J. Air Waste Manage., 54, 1478-1493, 2004.

Zilitinkevich, S., and Calanca, P.: An extended theory for the stably stratified atmospheric boundary layer, Q. J. Roy. Meteorol. Soc., 126, 1913-1923, doi:10.1256/smsqj.56617, 2000.

Zilitinkevich, S., and Baklanov, A.: Calculation of the height of the stable boundary layer in practical applications, Bound.-Layer. Meteorol., 105, 389-409, doi:10.102376832738, 2002.

Zilitinkevich, S., Esau, I.N.: The effect of baroclinicity on the equilibrium depth of neutral and stable planetary boundary layers, Q. J. Roy. Meteorol. Soc. 129:3339-3356, 2003.

Zilitinkevich, S.S., Elperin, T., Kleorin, N., Rogachevskii, I.: Energy and flux-budget (EFB) turbulence closure model for stably stratified flows, Atmospheric Boundary Layers. A. Baklanov & B. Grisogono (eds.), 2008, doi: 10.1007/978-0-387-74321-9_3

Zilitinkevich, S., Elperin, T., Kleorin, N., Rogachevskii, I., Esau, I., Mauritsen, T., and Miles, M.: Turbulence energetics in stably stratified geophysical flows: strong and weak mixing regimes, Q. J. Roy. Meteorol. Soc., 134, 793-799, doi:101002/qj.264, 2008.

Žagar, M., and Rakovec, J.: Small scale surface wind prediction using dynamical adaptation, Tellus A**,** 51, 489-504, doi:10.1034/j.1600-0870.1999.t01-4-00003.x, 1999.

7. Abstract

Based on gradient transport theory or K-theory, turbulent transport in the atmosphere has been parameterized using the eddy diffusivity. Due to its simplicity, this approach has often been applied in many numerical and air quality models but it is rarely verified on observations. Here, the widely used O'Brien cubic polynomial approach has been validated together with an exponential approach against eddy diffusivity profiles determined from measurements and from LES data in stable conditions. It is shown based on Large Eddy Simulation (LES) that the Grisogono method performs better than the O'Brien's polynomial, especially in the stable conditions. Verification is completed by analyzing the variability effects on pollutant concentrations of two different vertical diffusion, $K(z)$, schemes incorporated in an atmospheric chemical model, i.e. Unified EMEP (European Monitoring and Evaluation Programme) model. The operational and proposed new parameterization for eddy diffusivity $K(z)$ have been validated against observed daily surface nitrogen dioxide (NO_2), sulphur dioxide (SO_2) and sulphate (SO_4^{2-}) concentrations at different EMEP stations during year 2001. Moderate improvement in the correlation coefficient and bias for NO_2 and SO_2 and slight improvement for sulphate is found for most of the analyzed stations with the Grisogono $K(z)$ scheme, which is recommended henceforth for further application due to its scientific and technical advantages. Special emphasis is given to the representation of the atmospheric boundary layer (ABL) in order to capture vertical transport and dispersion of atmospheric air pollution. Furthermore, two different ABL schemes are evaluated against radiosounding data in January and July 2001, and against data from the Cabauw tower, the Netherlands, in the same year. Based on validation of the ABL parameterizations, it is found that the EMEP model is able to reproduce spatial and temporal mixing height variability. Improvements are identified especially in stable conditions with the new ABL scheme based on the bulk Richardson number (Ri_B). Simulations of ^{222}Rn are performed during year 2005 and 2006 and compared to available ^{222}Rn measurements in Europe in order to validate vertical mixing. In addition to the non-local schemes, the O'Brien and Grisogono, a new scheme which is a local and based on total turbulent energy (TTE) closure (e.g., Mauritsen, 2007) has been implemented in the EMEP model and evaluated. This work has been conducted within the EMEP4HR project which main purpose is to develop and test an

operative framework for environmental control of air pollution problems in a broader region of Croatia.

8. Prošireni sažetak

Sažetak

Na temelju teorije gradijentnog transporta ili *K*-teorije, turbulentni je transport u atmosferi parametriziran pomoću vrtožne difuzivnosti. Upravo zbog svoje jednostavnosti ovaj se pristup često koristi u mnogim numeričkim modelima, jednako kao i u modelima kakvoće zraka, ali je vrlo rijetko testiran na mjerenjima. U ovom radu validirane su tzv. Grisogonova i široko primjenjena O'Brienova shema bazirana na polinomu trećeg reda. Najprije su primjenjene u stabilnim uvjetima za proračun profila vrtložne difuzivnosti određenima iz mjerenja i iz LES (*Large Eddy Simulation*; Model simulacija velikih vrtloga) podataka. Pokazano je da Grisogonova metoda daje bolje rezultate nego O'Brienova metoda, naročito u stabilnim uvjetima. Evaluacija je upotpunjena analizom varijacijskih efekata u koncentracijama polutanata primjenom dviju shema vertikalne difuzije, $K(z)$, u atmosferskom kemijskom modelu, ovdje je korišten *Unified* EMEP model (*European Monitoring and Evaluation Programme*; Ujedinjeni model europskog programa praćenja i procjene). Operativna i predložena shema za parametrizaciju $K(z)$ validirane su na mjerenim dnevnim površinskim koncentracijama dušičnog dioksida (NO_2), sumpornog dioksida (SO_2) i sulfata (SO_4^{-2}) dobivenih sa raspoloživih postaja iz EMEP domene tijekom 2001. godine. Prema proračunatim koeficijentima korelacije i vrijednostima sustavne pogreške (*BIAS*) ustanovljeno je poboljšanje na većini postaja za NO_2 i SO_2, kao i poboljšanje relativno manjeg razmjera za sulfat, sa Grisogonovom $K(z)$ shemom koja se preporuča za daljnju praktičnu upotrebu zbog svojih znanstvenih (ne temelji se na M.-O. teoriji) i tehničkih prednosti (treba samo 2 ulazne varijable) nad operativnom metodom. Posebno je analizirana shema proračuna visine graničnog sloja (H) u modelu kako bi se ustanovila njena efikasnost u simulaciji vertikalnog transporta i disperzije atmosferskog onečišćenja. Dvije različite sheme za proračun H uspoređene su sa odgovarajućim visinama procijenjenim iz radiosondažnih mjerenja na različitim postajama u Europi u siječnju i srpnju 2001., kao i sa H određenima iz mjerenih vertikalnih profila temperature i vjetra sa Cabauw tornja u Nizozemskoj tijekom iste godine. Na temelju validacije H parametrizacija, ustanovljeno je da EMEP model dobro reprezentira prostorno vremensku varijabilnost od H sa značajno poboljšanim rezultatima s novom H shemom koja se temelji na integralnom Richardsonovom broju (Ri_B). Ovaj rad izveden

je u okviru EMEP4HR projekta čiji je glavni cilj razvoj i verifikacija sustava za modeliranje kakvoće zraka na području Hrvatske u svrhu njegove operativne primjene u području praćenja i planiranja zaštite okoliša od atmosferskog onečišćenja.

Uvod

U današnje vrijeme modeli kakvoće zraka prepoznati su kao važno oruđe za procjenu kakvoće zraka. Iako su mjerenja i dalje osnova za procjenu kakvoće zraka, postoji nekoliko pogodnosti omogućenih modelima za kakvoću zraka a to su: visoka prostorna i vremenska rezolucija simuliranih podataka, prognoza kakvoće zraka na temelju promjena u emisijama onečišćujućih tvari kao i na temelju promjena meteoroloških uvjeta. Nadalje, modeli kakvoće zraka omogućuju bolje razumijevanje fizikalnih procesa koji utječu na transport onečišćujućih tvari u atmosferi.

Već 30 godina Europski program za praćenje i procjenu (*European Monitoring and Evaluation Programme*; EMEP) osnovan pod Konvencijom za prekogranični daljinski transport (*Long-Range Transboundary Air Pollution*; LRTAP) odgovoran je za razvoj sustava modeliranja kakvoće zraka koji podržavaju donošenje upravljačkih strategija okoliša na području Europe. Tzv. Ujedinjeni EMEP model razvijen je i korišten u svrhu simulacije prekograničnog transporta onečišćenja zraka na europskoj skali. Odnedavno posebne verzije EMEP modela su razvijene na većoj prostornoj rezoluciji i združene sa različitim meteorološkim modelima: EMEP4UK (npr. Vieno i sur., 2009) i EMEP4HR (Jeričević i sur., 2007; Kraljević i sur., 2008). Razvoj EMEP modela uključuje složene meteorološke efekte čija važnost progresivno raste sa horizontalnom skalom modela. Jedan od tih složenih meteoroloških efekata je i turbulencija, a u ovom radu implementirana je i testirana shema za parametrizaciju vertikalne turbulentne difuzije, $K(z)$, kao i visine graničnog sloja u EMEP modelu.

U dosadašnjim istraživanjima pokazano je kolika je važnost i utjecaj parametrizacija $K(z)$ na simulaciju raznih kemijskih elemenata (npr. Nowacki i sur., 1996; Biswas i Rao, 2000; Olivie i sur., 2004). Razni autori daju različite parametrizacije za $K(z)$ koje ovise o stabilnosti u atmosferskom graničnom sloju (AGS) (npr. O'Brien, 1970; Deardorff, 1972; Louis, 1979; Holtslag i Moeng, 1991; Holtslag i Boville, 1993; Grisogono, 1995). O'Brien predlaže jednostavnu parametrizaciju za $K(z)$ koja se koristi u mnogim modelima kakvoće zraka od jednostavnih jednodimenzionalnih modela (npr. Lee and Larsen, 1997) do primjena u kompleksnim kemijskim modelima npr. *Comprehensive Air Quality Model with Extensions*

(CAMx, http://www.camx.com/; ENVIRON, 1998; Zhang i sur., 2004) gdje je O'Brienova shema jedna od nekoliko opcija za proračun $K(z)$. U EMEP modelu također se koristi O'Brienova shema (npr. Fagerli i Eliassen, 2002) u konvektivnom graničnom sloju (KGS) dok je u stabilnom graničnom sloju (SGS) $K(z)$ parametrizacija bazirana na Monin - Obukhov (M-O; Monin i Obukhov, 1954) teoriji sličnosti (MOST).

U mnogim znanstvenim radovima pokazano je da formulacije prizemnog graničnog sloja (PGS) utemeljene na MOST često nisu primjenjive u statički stabilnim uvjetima (npr. Mahrt, 1999; Pahlow i sur., 2001; Poulos i Burns, 2003; Mauritsen i sur., 2007; Grisogono i sur., 2007). U ovom radu predložena je i implementirana nova, tzv. Grisogonova shema $K(z)$ koja nije utemeljena na M-O teoriji sličnosti. Grisogonova shema koristi eksponencijalnu funkciju koja opada s visinom, a koja generalizira O'Brienov polinom 3. reda (npr. Grisogono i Oerlemans, 2001 i 2002). Na temelju rezultata modela simulacija velikih vrtloga (tzv. *Large Eddy Simulation*; LES) kao i evaluacije na eksperimantalnim nizovima podataka, pokazano je da Grisogonova metoda daje bolje rezultate od O'Brienovog polinoma (Jeričević i Večenaj, 2009).

U ovom radu posebna je pažnja dana procjeni učinkovitosti AGS shema EMEP modela da simuliraju vertikalni transport i disperziju polutanata u atmosferi. Naime Schäfer i sur. (2006) pokazuju značajan utjecaj visine PGS-a na površinske koncentracije dušičnih oksida (NO_x) i čestica (PM) u urbanim i sub-urbanim područjima, dok Athanassiadis i sur., (2002) pokazuju da je točnost određivanja H potrebna kako bi se pravilno simulirale razine onečišćenja u fotokemijskim modelima. Štoviše, H je eksplicitno uključena u obje $K(z)$ parametrizacije u EMEP modelu, te je stoga izrazito važno procijeniti mogućnosti EMEP modela da pravilno simulira prostornu i vremensku varijabilnost od H. Operativna (npr. Jakobsen i sur., 1995; Seibert i sur., 2000) i nova shema za proračun H temeljena na integralnom Richardsonovom broju (Ri_B) su evaluirane. Korištena metoda integralnog Richardsonovog broja je standardni i često primjenjivan pristup za proračun H iz numeričkih prognostičkih modela kao i iz radiosondažnih mjerenja (npr. Mahrt, 1981; Troen i Mahrt, 1986, Sørensen i sur., 1996; Fay i sur., 1997; Seibert i sur. 2000; Zilitinkevich i Calanca, 2000; Zilitinkevich i Baklanov, 2002; Gryning i Batchvarova, 2002; Jeričević, 2005; Jeričević i Grisogono, 2006).

S obzirom da je kemijski atmosferski model vrlo složen i obuhvaća nelinearne kemijske reakcije, izrazito je teško procijeniti efekte promjena parametrizacijskih shema dinamičkog transporta polutanata na temelju usporedbe sa mjerenjima u jednoj točki. Stoga su prije implementacije i evaluacije $K(z)$ schema u EMEP modelu, metode uspoređene na rezultatima modela simulacija velikih vrtloga (*Large Eddy Simulation*) i eksperimantalnim podacima. Nakon toga su modelirane prizemne koncentracije onečišćenja, dobivene nezavisnim simulacijana operativne i nove verzije EMEP modela, uspoređene sa odgovarajućim srednjim dnevnim prizemnim koncentracijama kemijskih elemenata izmjerenih na postajama u EMEP mreži tijekom 2001. godine. Na temelju te evaluacije ustanovljena je i analizirana nepouzdanost i u mjerenim i u modeliranim podacima. Analizom ustanovljenih razlika u izvedbi dviju verzija EMEP modela procijenjeni su efekti fizikalnih parametrizacija na simulaciju onečišćenja u složenom atmosferskom kemijskom modelu i predložena je praktična primjena Grisogonove metode. Rezultati ovog istraživanja doprinose znanju o atmosferskom kemijskom modeliranju u području parametrizacija vertikalne difuzije i razvoja AGS-a. Rad je izveden u okviru EMEP4HR projekta čiji je osnovni zadatak razvoj i verifikacije sustava za modeliranje kakvoće zraka na području Hrvatske u svrhu njegove operativne primjene u području praćenja i planiranja zaštite okoliša od atmosferskog onečišćenja. Projekt omogućava stabilni, dugoročni razvoj hrvatskih stručnih i znanstvenih kapaciteta koji će podupirati sustav i strategiju zaštite okoliša.

Cilj ove radnje je unaprijediti saznanja o turbulentnim procesima i njihovim efektima u atmosferskim kemijskim modelima validacijom različitih shema za parametrizaciju vertikalne difuzije, kao i shema za proračun atmosferskog graničnog sloja na temelju različitih nizova mjerenih podataka.

2. Opis modela i podataka

2.1.FLOSSII i CASES-99

U ovom radu korišteni su vertikalni profili dvaju skupova podataka: *Fluxes over Snow-covered Surfaces* II (FLOSSII) i *Cooperative Atmosphere-surface Exchange study*-1999 (CASES-99) analizirane u radu Mahrt i Vickers (2006). Ovi eksperimentalni skupovi podataka sadrže mjerenja u stabilnim atmosferskim situacijama. FLOSSII sadrži podatke mjerenja noćnih turbulentnih flukseva sa tornja visokog 30 m, na 7 nivoa i obuhvaća razdoblje od 1. prosinca 2002. do 31. ožujka 2003. na području sjeverozapadnog Kolorada u SAD. CASES-99 ima mjerenja za vrijeme jednog mjeseca dobivenih na 7 različitih nivoa na tornju visokom 60 m na južnom dijelu centralnog Kanzasa, SAD.

2.2 Model simulacija velikih vrtloga (LES)

Budući da mjerenja sadrže podatke samo u najnižih 30 m u AGS-u u FLOSSII-ju i 60 m u CASES-99 bilo je potrebno koristiti modelirane vrijednosti stabilnih atmosferskih situacija kako bi se omogućila iscrpna studija. LES modeli se smatraju vrlo korisnim u brojnim studijama AGS-a (npr. Deardorff 1970; Wyngaard i Brost, 1984; Andrèn i sur., 1994; Kosovic i Curry; 2000; Ding i sur., 2001; Zilitinkevich i Esau, 2003; Mauritsen i sur., 2007). U svrhu verifikacije dviju različitih metoda za proračun vertikalne difuzije korišteni su LES podaci iz DATABASE64 (npr. Esau and Zilitinkevich, 2006) uključujući široki spektar neutralnih i stabilno stratificiranih slučajeva klasificiranih prema uzgonskoj (Brunt-Väisälä) frekvenciji $N = \left(\frac{g}{\theta_0} \frac{\partial \theta}{\partial z} \right)^{1/2}$ i površinskim toplinskim fluksevima (Tablica 1). Analizirani su konvencionalno neutralni, noćni i dugoživući stabilni slučajevi. Modelirani normalizirani profili srednjeg vjetra, potencijalne temperature i turbulentnih flukseva za svaku klasu prikazani su na Slici 1.

U svim slučajevima definirani su inicijalni profili temperature (neutralani ili sa konstantnom stratifikacijom), konstantna vrijednost geostrofičkog vjetra, duljina površinske hrapavosti i površinski toplinski tok. Konvencionalno neutralni slučaj se javlja u vjetrovitim situacijama kada je površinski toplinski tok zanemariv. Tzv. noćni granični sloj se razvija u atmosferi čija je stabilnost blizu neutralne uz gubitak topline na površini tla, a javlja se noću iznad kopna uz prisustvo rezidualnog sloja. U dugoživućim stabilnim slučajevima površinsko ohlađivanje dominira nad stabilnom stratifikacijom i može se naći zimi na visokim atmosferskim širinama. Svaka LES simulacija trajala je 15 sati kako bi dostigla kvazi-stacionarno stanje.

2.3 EMEP model

Ujedinjeni EMEP model (http://www.emep.int/) razvijen je u Norveškom meteorološkom institutu pod EMEP programom. Ujedinjeni EMEP model je razvoj ranijih verzija EMEP modela (Berge i Jakobsen, 1998; Jonson i sur. 1998), i potpuno je dokumentiran u radu Simpson i sur. (2003), te Fagerli i sur. (2004). Model simulira atmosferski transport i depoziciju zakiseljavajućih i eutrofikacijskih elemenata, fotooksidanata i čestica nad Europom. Domena modela pokriva

Europu i Atlantski ocean sa 50 km x 50 km horizontalnom rezolucijom dok po vertikali ima 20 sigma nivoa do visine od 100 hPa. Ujedinjeni EMEP model koristi ulazna meteorološka polja dobivena svaka 3 sata iz modela *PARallel Limited Area Model with Polar Stereographic map projection* (PARLAM-PS), koji je posebna verzija *HIgh Resolution Limited Area Model* (HIRLAM) modela namjenjena EMEP-u. U ovom radu korištena je verzija rv2_6_1 EMEP modela.

2.4. Opis mjerenja korištenih u svrhu verifikacije rada EMEP modela

Sa ciljem evaluacije EMEP modela korištena su mjerenja: (i) dnevne površinske NO_2, SO_2 i SO_4^{2-} koncentracije na različitim postajama u EMEP mreži za vrijeme 2001. godine Slika 2, (ii) radiosondažna mjerenja iz raznih europskih gradova tijekom siječnja i srpnja 2001 Tablica 2 i (iii) 10-minutni profili vjetra i temperature sa Cabauw tornja, Nizozemska za vrijeme 2001. godine.

2.4.1 Mjerenja sa EMEP postaja

Sa ciljem evaluacije modela korištena su mjerenja sa EMEP postaja (http://www.emep.int/) budući da su dobro dokumentirana, kvaliteta im je kontrolirana i uglavnom predstavljaju pozadinske uvjete nad širim područjem. Analizirane postaje prikazane su na slici 2. Nadmorska visina većine postaja je ispod 300 m, no neke stanice su planinske, na visinama većim od 1000 m (npr. Alpe). Treba naglasiti da planinske postaje nisu dobro reprezentirane u modelu, te su obično prenisko pozicionirane u modelima grube horizontalne rezolucije što je dobro poznat i istraživan problem (npr. Žagar i Rakovec, 1999; Ivatek Šahdan i Tudor, 2004).

2.4.2 Radiosondažna mjerenja

Radiosondaže se često koriste pri određivanjui verifikaciji*H* (npr. Seibert i sur., 2000). Budući da se radiosondažna mjerenja obavljaju uglavnom dva puta dnevno, u 00 i 12 UTC, upotrebljavaju se samo kao opće referentne vrijednosti AGS-a. Pozitivne karakteristike su njihova relativno dobra prostorna pokrivenost u Europi kao i raspoloživost, te kontroliranost podataka. U ovom radu korišteni su podaci sa 24 radiosondažne postaje Tablica 2.

2.4.3 Cabauw mjerenja

Cabauw toranj, Slika 3, se nalazi u zapadnom dijelu Nizozemske (51°58´N, 4°56´E) nad ravnim terenom (npr. van Ulden i Wieringa, 1995). Prosječne vrijednosti vjetra i temperature računaju se u 10 minutnim intervalima. Brzina i smjer vjetra mjere se na šest nivoa: 10, 20, 40, 80, 140 i 200 m, dok se temperatura mjeri dodatno i na 1.5 m gdje se mjeri i atmosferski tlak. Kako bi se dobila potencijalna temperatura na svim nivoima, potrebna za proračun Ri_B vrijednosti, pretpostavljena je hidrostatička ravnoteža. Tlak na višim nivoima dobiven je iz prizemnog tlaka trapezoidalnim numeričkim zakonom. Cabauw podaci se često koriste u raznim radovima npr. Beljaars i Bosveld (1997), Chen i sur. (1997) i Ek i Holtslag (2005).

2.4.4 Radon

Radon je radioaktivni plin koji se pojavljuje u 3 prirodna lanca radioaktivnog raspada sa početnim elementima: uranom-238, uranom-235 i torijem-232. U prirodi se ovi radionuklidi nalaze u tragovima u većini stijena i vrsta tla dok se najveći prirodni izvori urana-238 koji uključuje radon-222 (^{222}Rn). Visoka prisutnost ^{222}Rn kao i njegovo vrijeme poluraspada od 3.8 dana čini ga jednim od najvažnijih radioaktivnih elemenata koji ugrožavaju ljudsko zdravlje. Mjeri se u Becquerelima po kubnom metru (Bqm^{-3}). ^{222}Rn se emitira relativno jednoliko iz tla sa kontinenata, uglavnom je netopiv u vodi, inertan i kiša ga ne uklanja iz atmosfere procesom mokrog taloženja. Uzima se da je prosječni tok radona iz tla od 0.8 do 1 atom cm^{-2} s^{-1} (Dentener i sur. 1999). U EMEP modelu emisija ^{222}Rn je 1 atom cm^{-2}s^{-1} uniformno iznad kontinenta.

2.4.4.1 Mjerenja ^{222}Rn

U ovom redu korištena su satna mjerenja ^{222}Rn koncentracija sa četiri postaje u Europi: Freiburg (47°55´N, 7°54´E) i Schauinsland (47°59´, 7°51´) tijekom 2005., te podaci sa Cabauw tornja (opisan u potpoglavlju 2.4.3) u Nizozemskoj i Angus tornja (50 m) u Škotskoj tijekom 2006. godine. Freiburg (na 300 m nadmorske visine)i Schauinsland (na 1205 m nadmorske visine) su postaje u Njemačkoj. Schauinsland je planinska postaja 12 km južno od grada Freiburga koji se nalazi u njenom podnožju.

3. Metode

3.1 Opis $K(z)$ parametrizacijskih schema

U ovom radu testirane su i analizirane dvije metode za proračun koeficijenta vertikalne difuzije: O'Brienova (1970) metoda opisana u jednadžbi (1) kao i relativno nova metoda tzv. Grisogonova metoda u kojoj se $K(z)$ računa eksponencijalnom funkcijom opisanom u jednadžbi (4). Ulazni parametri u O'Brienov izraz su: K_H - koeficijent vertikalne difuzije na vrhu AGS-a, H-visina AGS-a, K_{H_S} - koeficijent vertikalne difuzije na visini prizemnog graničnog sloja i H_S-visina prizemnog graničnog sloja. Ulazni parametri u Grisogonov izraz (4) su $K_{\max}$ -maksimalna vrijednost koeficijenta vertikalne difuzije i h –visina maksimuma $K(z)$. Shematski prikaz svih ulaznih parametara dan je na Slici 5. Usporedbom jednadžbi (1) i (4) može se uočiti da je jedna od prednosti Grisogonove metode to što treba samo dva ulazna parametra umjesto prethodno četiri.

3.1.1 Praktično određivanje ulaznih parametara

Opis metoda proračuna svih ulaznih parametara korištenih za određivanje $K(z)$ profila dvjema metodama, O'Brienovom i Grisogonovom, iz FLOSSII, CASES-99, LES i EMEP podataka prikazan je u Tablici 3. Ulazni parametri za O'Brienovu mtodu (K_H, H, K_{H_S} i H_S) i za Grisogonovu metodu ($K_{\max}$, h) su određeni iz FLOSSII i CASES-99 podataka na temelju mjerenih profila (K_{meas}) prikazanim na Slikama 6 i 7 u radu Mahrt and Vickers (2006). Tako je K_{H_S} visina krajnje točke lineranog K_{meas} profila koji počinje od tla, dok je H određen kao $10K_{H_S}$ uz pretpostavku je visina PGS-a oko 10 % visine AGS-a (npr. Stull, 1988). U ovom radu K_H = 0.1 m ^{2} s $^{-1}$. Ulazni parametri u jednadžbu (4) $K_{\max}$ i h očitani su sa grafa.

Iz LES podataka vrijednost H je određena iz profila turbulentne kinetičke energije dok su vrijednosti K_{H_S} i K_H definirane na isti način kao i u FLOSSII i CASES-99 slučajevima. Vrijednost koeficijenta vertikalne difuzije na visini prizemnog graničnog sloja K_{H_S} određena je pomoću funkcija sličnosti jednadžbe (5), (6a) i (6b). Ulazni parametri za Grisogonov pristup parametrizirani su visinom graničnog sloja i brzinom trenja jednadžbe (7) i (8), te empirijskim koeficijentima $C(K)$ i $C(h)$ određenim iz LES podataka. Za svaku LES simulaciju određeni su $K(z)$ profili pomoću $K_{\max}$ i h vrijednosti dobivenih iz LES profila turbulentnih flukseva i $K(z)$

proračunatih Grisogonovom metodom pomoću predefiniranih inicijalnih emprijskih konstanti $C_0(K)$ i $C_0(h)$. Iz osrednjenih omjera $K_{\max}(LES)/K_{\max}(Grisogono)$, dobivaju se empirijski koeficijenti *C*(*K*) i *C*(*h*) čije su vrijednosti prikazane u Tablici 4. Može se uočiti de je koeficijent difuzije za količinu gibanja veći od toplinskog koeficijenta difuzije u stabilnim uvjetima za faktor 2. U EMEP modelu *K*(*z*) se inicijalno proračunava za cijelu domenu pomoću Blackadarove sheme (1979), jednadžba (10), a u nestabilnim uvjetima ti su koeficijenti u AGS-u zamijenjeni profilima dobivenim O'Brienovom metodom. Za primjenu Grisogonove sheme u EMEP modelu ulazni parametri su također proračunati jednadžbama (7) i (8) kao u LES-u uz empirijske konstante *C*(*K*)=0.1 i *C(h)*=3 dobivenih na temelju LES podataka (Jeričević i Večenaj, 2009).

Obje metode su nelokalnog tipa i uglavnom ovise o poziciji i intenzitetu od $K_{\max}$. U Grisogonovom pristupu vrijednost od $K_{\max}$ ekspilicitno uključuje u_* i *H*, koji se proračunavaju iz meteorološkog modela te je njihova točnost ograničena mogućnostima numeričkog prognostičkog modela. S druge strane, O'Brienov pristup ovisi o parametrima PGS-a, poput H_S, koje je izrazito teško razlučiti u statički stabilnim uvjetima (npr. Zilitinkevich i Calanca, 2000; Jeričević i Grisogono, 2006; Mahrt, 2007).

3.2 Opis parametrizacijskih shema atmosferskog graničnog sloja

Visina AGS-a, vrlo je važan parametar koji ograničava vertikalno miješanje u donjoj atmosferi. Operativna metoda za proračun *H* u EMEP modelu koristi izlazne podatke numeričkog prognostičkog modela PARLAM-PS (Jakobsen i sur., 1995). U stabilnim uvjetima *H* je ona visina na kojoj je $K(z)$ < 1 m ^{2} s $^{-1}$, a $K(z)$ profili su proračunati Blackadarovom metodom, jednadžba (10). U nestabilnim uvjetima satne vrijednosti toplinskog toka, Q_h, vertikalno se raspoređuju suho-adijabatičkom prilagodbom, te je *H* visina odgovarajućeg adijabatičkog sloja. Predložena Ri_B metoda, jednadžba (18), zasniva se na pretpostavci da kontinuirana turbulencija nestaje nakon neke određene, prethodno definirane kritične vrijednosti Ri_{BC}. Pretpostavljeno postojanje Ri_{BC} odnedavno prima znanstvene kritike (Zilitinkevich i Baklanov, 2002; Jeričević i Grisogono, 2006; Mauritsen i sur., 2007; Zilitinkevich i sur., 2008; Grisogono i Belušić, 2008), pa je razvoj shema višeg reda zatvaranja predmet novijih istraživanja. Osnovna prednost Ri_B metode nad operativnim pristupom je da uključuje dva osnovna izvora turbulencije u atmosferi:

toplinski i mehanički, te da je primjenjiva i u stabilnim jednako kao i u nestabilnim, atmosferskim uvjetima.

3.3 Opis sheme ukupne turbulentne energije i simulacije ^{222}Rn

U ovom dijelu prikazan je opis nove metode za proračun $K(z)$ tzv. metoda ukupne turbulentne energije koja se temelji na metodi zatvaranja parametrizacije turbulencije u neutralnim i stratificiranim atmosferskim uvjetima. Ukupna turbulentna energija je zbroj turbulentne kinetičke potencijalne energije (ova druga proporcionalna je varijanci potencijalne temperature). U nestabilnim uvjetima shema se temelji samo na turbulentnoj kinetičkoj energiji. Za detaljan izvod jednadžbi čitatelj se upućuje na engleski dio ove radnje kao i na originalni rad Mauritsen et al. (2007).

4. Rezultati

4.1 FLOSSII and CASES99

Proračunati su vertikalni profili koeficijenta vertikalne difuzije impulsa i topline, K_m i K_h, pomoću jednadžbi (1) i (4), i uspoređeni sa mjerenjima K_{meas}, Slika 6. O'Brienova metoda, jednadžba (1), precjenjuje visinu od K_m za FLOSSII (Slika 6a), kao i maksimalnu vrijednost od K_h za CASES-99 (Slika 6d), dok se rezultati dobiveni sa Grisogonovom metodom, jednadžba (4), dobro slažu sa K_{meas}. Visina maksimuma od K_m proračunata O'Brienovom metodom se dobro slaže s mjerenjima u CASES-99 (Slika 6c), ali iznos od K_m je precjenjen (Slika 6c). Za iste podatke maksimum od K_h je dobro uhvaćen O'Brienovom metodom, dok je visina od K_h nešto podcjenjena (Slika 6d). Precjenjivanje h i/ili $K_{\max}$ dobivenih sa jednadžbom (1), posljedica je pogrešne procjene parametara u PGS-u. Pogrešna procjena h i/ili $K_{\max}$ O'Brienovom metodom može voditi do precjenjivanja odnosno podcjenjivanja simuliranih koncentracija primjenom u raznim modelima kakvoće zraka.

4.2 LES

Oko 90 LES simulacija, uključujući širok spektar neutralnih i stabilno stratificiranih slučajeva, upotrebljeno je kako bi se evaluirale dvije metode za parametrizaciju vertikalne difuzije. Na Slici 7 prikazani su rezultati za konvencionalne neutralne uvjete, Slika 8 prikazuje noćne, a Slika 9 dugoživuće stabilne uvjete. Značajno bolji rezultati dobiveni su sa Grisogonovom metodom, posebno za vrijednosti od K_m. Obje metode precjenjuju K_h u dugoživućim stabilnim uvjetima (Slike 9d, 9e i 9f) vjerojatno stoga što su same vrijednosti od K_h vrlo male i ne mogu se opisati 'standardnim' nelokalnim parametrizacijskim metodama, štoviše karakteristično je jako raspršenje u podacima jer turbulencija ima povremeni karakter, izražene su vertikalne fluktuacije, te K_h nema kontinuiranu vertikalnu razdiobu. Slične rezultate dobili su Mahrt i Vickers (2006) u uvjetima ekstremno slabog atmosferskog miješanja u FLOSSII podacima. U ovakvim uvjetima tipična *K*-teorija ne daje zadovoljavajuće rezultate zbog povremenosti, nestacionarnosti i problema s mjerenjima.

4.3 Verifikacija *K*(*z*) shema u EMEP modelu

Proračunati su koeficijenti korelacije r i bias vrijednosti, $BIAS = \left(\frac{Model - Observation}{Observation}\right) \times 100\,\%$, između mjerenih dnevnih površinskih koncentracija NO_2, SO_2 i SO_4^{2-} ($c(NO_2)$, $c(SO_2)$, $c(SO_4^{2-})$) tijekom 2001. godine na raspoloživim EMEP postajama (Slika 2), i odgovarajućih modeliranih vrijednosti dobivenih operativnom verzijom EMEP modela. Rezultati evaluacije pokazuju dobro slaganje modela sa mjerenjima: $0.5 \le r\,(NO_2) \le 0.75$ na oko 56 % postaja, $0.5 \le r\,(SO_2) \le 0.77$ na 43 % postaje, i $0.5 \le r\,(SO_4^{2-}) \le 0.87$ na 86 % postaja. Ovdje je važno naglasiti da je $r\,(SO_4^{-2})$ najviši od svih analiziranih spojeva sa $r\,(SO_4^{2-}) > 0.7$ na oko 31 % postaja. Na temelju jedne godine podataka dobiveno je da EMEP model općenito podcjenjuje mjerene $c(NO_2)$ sa $BIAS\,(NO_2) \approx$ -20 %. Model precjenjuje SO_2 mjerenja na oko 71% postaja, $BIAS(SO_2) \approx 30\%$, dok je općenito sulfat podcjenjen $BIAS\,(SO_4^{2-}) \approx -12\%$. Rezultati dobiveni u analiziranoj 2001. godini u skladu su sa dosadašnjim rezultatima evaluacije EMEP modela (Fagerli i sur., 2003).

4.3.1 Nepouzdanosti u mjerenim podacima

Na temelju evaluacije operativne verzije EMEP modela tijekom 2001. godine ustanovljeno je da su određene postaje manje reprezentativne te da posjeduju određene nepouzdanosti u mjerenim podacima. Postaje sa odstupanjima faktora dva i više između mjerenih i modeliranih podataka mogu se kategorizirati u: (i) postaje pod utjecajem lokalnih izvora ili velikih emisijskih izvora i (ii) planinske postaje. Važno je analizirati rezultate postaja sa visokom nepouzdanošću u mjerenjima jer mogu ukazati na opće probleme u modeliranju kakvoće zraka, no ne mogu se koristiti u svrhu evaluacije turbulentnih parametrizacijskih shema meteoroloških modela.

4.3.1.1 Epizode

Na Slici 10 prikazan je godišnji hod mjerenih i modeliranih $c(NO_2)$ vrijednosti tijekom 2001. godine na dvjema odabranim postajama: a) Westerland/Wenningstedt (DE01) sa r > 0.7 i b) Svratouch (CZ01) sa r ≈ 0.1. Na postaji CZ01 zabilježene su epizodne situacije tijekom ljetnih mjeseci koje model nije adekvatno simulirao što je rezultiralo u nižoj r vijednosti. Važno je naglasiti da je model s različitim $K(z)$ shemama dao slične rezultate za vrijeme tih epizoda.

Slično je uočeno i u godišnjim hodovima $c(SO_2)$ i $c(SO_4^{2-})$. Na Slici 11 prikazan je godišnji hod $c(SO_2)$ za: a) Ilmitz (AT02) sa $r > 0.75$ i b) Vorhegg (AT05) sa $r = 0.25$, a na Slici 12 godišnji hod $c(SO_4^{2-})$ za: a) Neuglobsow (DE07) sa $r \approx 0.8$ i b) Peyrusse Vielle (FR13) sa $r \approx 0.25$.

4.3.1.2 Planinske postaje

Kao što je već spomenuto u potpoglavlju 2.4.1., planinske se postaje trebaju posebno tretirati. Ovdje su detaljnije analizirane dvije postaje sa najvišom nadmorskom visinom: CH01 i SK02. Godišnja srednja vrijednost na CH01 dobivena iz mjerenja je $\bar{c}(NO_2)$=0.11 μg(N)m $^{-3}$, dok je modelirana $\bar{c}(NO_2)$=0.33 μg(N)m $^{-3}$, nadalje za SO2 mjerenja daju $\bar{c}(SO_2)$= 0.08 μg(S)m^{-3} a modelirana $\bar{c}(SO_2)$= 0.27 μg(S)m^{-3} sa pripadajućim biasom *BIAS* (SO_2) > 200%. Slično je dobiveno i za SK02.

4.3.2 Grisogonova *K*(*z*) shema

Kako bi se ustanovilo eventualno poboljšanje u EMEP modelu s primjenom nove $K(z)$ sheme, proračunate su razlike, jednadžbe (44) i (45), između r i *BIAS* vrijednosti dobivene sa

O'Brienovom i Grisogonovom shemom. Slika 13 prikazuje relativne razlike između koeficijenata korelacije, $RD(r)$, proračunatih između modeliranih i mjerenih a) NO_2, b) SO_2 i c) SO_4^{2-} vrijednosti tijekom 2001. godine na raspoloživim postajama u EMEP domeni. Vrijednosti $RD(r)$ >0 označavaju bolju izvedbu proračuna Grisogonovom shemom. Slika 14 pokazuje isto što i Slika 13 samo za $RD(BIAS)$. Na slici 15 prikazane su prostorne interpolacije koeficijenata korelacije i njihovih razlika određenih dvjema rezličitim K(z) shemama tijekom 2001. godine. Slika 16 prikazuje godišnji hod od a) r, b) $BIAS$, c) $RMSE$ proračunatih između mjerenih i modeliranih $c(NO_2)$ kao i d) mjesečne srednjake u 2001. godini. Prikazani su rezultati dobiveni dvjema različitim shemama O'Brienovom (crvena krivulja) i Grisogonovom (plava) metodom, a zelena krivulja prikazuje mjesečne srednjake proračunate iz mjerenja. Na Slici 17 prikazani su godišnji prostorno-vremenski r i $BIAS$ na svim raspoloživim postajama između mjerenih i modeliranih $c(NO_2)$, $c(SO_2)$ and $c(SO_4^{2-})$ vrijednosti.

4.4 Verifikacija visine graničnog sloja

Uspoređene su dvije navedene sheme za proračun visine AGS-a u EMEP modelu: operativna i metoda temeljena na Ri_B broju. Verifikacija je obavljena pomoću dva skupa mjerenih podataka: (i) radiosondažna mjerenja na 24 različite mjerne postaje u Europi tijekom siječnja i srpnja 2001. i (ii) mjereni vertikalni profili temperature i vjetra tijekom 2001. godine na Cabauw tornju, Nizozemska.

4.4.1 Radiosondažna mjerenja

Visina graničnog sloja iz radiosondažnih mjerenja (H_{sond}) u siječnju i srpnju 2001. izračunata je iz raspoloživih UTC termina (Tablica 2) Ri_B metodom. Odgovarajuće visine u EMEP modelu (H_{EMEP}) proračunate su operativnom metodom (H_{old}), i Ri_B metodom (H_{new}). Slika 18a prikazuje koeficijente korelacije između H_{sond} i H_{EMEP} dok su na Slici 18b prikazane odgovarajuće $BIAS$ vrijednosti, a na Slici 18c srednje vrijednosti AGS-a proračunate iz mjerenja i modela. Na slici 18 dani su vremenski nizovi za četiri odabrane lokacije: Herstmonceux i Stavanger s višim koeficijentom korelacije, te Torshavn i Legionowo s nešto nižim r vrijednostima, kako bi se detaljnije proučile vremenske varijacije visine AGS-a. Slična analiza obavljena je za srpanj 2001. i rezultati su prikazani na Slikama 20 i 21.

4.4.2 Cabauw podaci

U ovom potpoglavlju opisana je procedura za proračun *H* metodom Ri_B broja iz Cabauw mjerenja (H_{tower}). Nakon toga analizirani su prosječni satni vertikalni profili Ri_B broja, ($\overline{Ri_B(z_j,t)}$), gdje su j = 10, 20,…, 200 m nivoi mjerenja; a odgovarajuća *H* analizirana je tijekom svakog mjeseca u 2001. godni (Slika 22). Vertikalni profili vjetra i temperature na Cabauw tornju mjereni su u vremenskim intervalima od Δt =10 minuta iz kojih su proračunati nizovi $Ri_B(z,t)$ vrijednosti za 2001. godinu i satno osrednjeni kako bi dobili dnevne hodove Ri_B vrijednosti, ($\overline{Ri_B(z_j,t)}$) za svaki mjesec tijekom 2001. godine (Slika 22). Relativno je jednostavno ustanoviti dnevne varijacije od *H* prateći liniju Ri_{BC} = 0.25 (tj. vrh plavog područja na Slici 22).

Analiza $\overline{Ri_B(z_j,t)}$ vrijednosti daje dobar uvid u procese razvoja i destrukcije KGS-a i SGS-a u raznim sezonama. Također se može uočiti jedna od manje istraživanih pojava a to je proces stvaranja i nestajanja prijelaznog AGS-a u jutarnjim i poslijepodnevnim satima.

Na Slici 23 prikazani su mjesečni koeficijenti korelacije proračunati između mjerenih (H_{tower}), i modeliranih vrijednosti; H_{old} (operativna metoda, crvena krivulja) i H_{new}(Ri_B metoda, plava krivulja). Očito je da nova shema daje bolje rezultate za sve mjesece osim u lipnju, srpnju i kolovozu u 2001 godini, kada su obje sheme dale slične rezultate. Budući da mjerenja na Cabauw tornju idu samo do visine od 200 m, nije bilo moguće procijeniti visinu KGS-a, već samo koliko model dobro simulira vremensku evoluciju KGS-a kao i intenzitet turbulencije uz površinu zemlje u konvektivnim uvjetima. Mjerenja na višim visinama svakako bi omogućila detaljniju evaluaciju metoda za proračun AGS-a za vrijeme toplijeg dijela godine. Svakako treba uočiti da su ovi rezulatati u skladu sa rezultatima dobivenim iz radiosondažnih mjerenja koja su također pokazala da metoda Ri_B broja daje bolje rezultate u stabilno stratificiranim uvjetima od operativne metode.

4.5. Test signifikantnosti

Primjenjen je standardni z-test (Pavlić, 1988) kako bi se ocijenila signifikantnost poboljšanja koeficijenta korelacije. Iako je formalni kriterij testa zadovoljen tek na nekoliko postaja, ustanovljeno je da je za NO_2 nivo signifikantnosti veći za postaje u Njemačkoj, Irskoj, Nizozemskoj, Norveškoj i Švedskoj, dok je za SO_2 to slučaj u Danskoj i Španjolskoj. Promjene u koeficijentu korelacije validirane na dnevnim koncentracijama sulfata ne pokazuju značajne promjene. Promjene u koeficijentu korelacije za *H* procijenjene iz Cabauw podataka su signifikantne u ožujku i travnju. Ipak primjenjivost z-testa na ovu vrstu podataka je upitna budući da inicijalni uvjeti nisu zadovoljeni a to su normalna razdioba mjernih podataka i međusobna nezavisnost varijabli. Svakako da ovaj postupak nije u potpunosti neutemeljen i promjene u koeficijentu korelacije se mogu komparativno promatrati, a informacija o nivou signifikantnosti je značajna.

4.6 Verifikacija $K(z)$ shema na temelju ^{222}Rn mjerenja

U ovom potpoglavlju dan je pregled svih prikazanih rezultata verifikacije modela na ^{222}Rn podacima.

Na Slici 26 prikazan je godišnji hod srednjih mjesečnih ^{222}Rn (Bqm^{-3}) koncentracija tijekom 2006. godine. Na slici 27 prikazani su vremenski nizovi satnih Rn vrijednosti na Angus tornju za sve mjesece u 2001. godini. Na slici 28 isto kao slika 26 samo za Cabauw toranj. Na Slici 29 su prosječne mjerene satne Rn koncentracije na dva nivoa 20 m i 200 m na Cabauw tornja tijekom 2006 i 2007 godine. Slike 30. i 31 su isto kao Slika 27 samo za mjerenja na Cabauw tornju na 20 m i na 200 m. Slika 32 je isto kao slika 26 samo za Schauinsland i Freiburg. Slike 33 i 34 su isto kao Slika 27 samo za Schauinsland i Freiburg. Slika 35 je isto kao Slika 26 za Krakow, Poljska, a Slika 36 je isto kao Slika 27 Samo za Krakow. Slika 37 prikazuje modelirane vertikalne profile K(z) sa a) operativnom, b)Grisogono i c)TTE shemom u razdoblju od 10 do 11 lipnja 2006 za Cabauw toranj. Slika 38 prikazuje isto što i slika 37 samo za Rn koncentracije Slika 39 isto što i Slika 37 samo za razdoblje 7-8 Studenog 2006. Slika 40 isto što i Slika 38 samo za razdoblje 7-8 Studenog 2006. Na slici 41 uspoređeni su prosječni satni mjereni i modelirani profili Rn koncentracija. Godišnji grafovi raspršenja po svim analiziranim postajama dani su na Slici 42, mjesečni grafovi koeficijenta korelacije su na slici 43, a kumulativne funkcije distribucije su na Slici 43. Nadalje, godišnje vrijednosti MAE, MSE i RMSE su na Slici 45, a mjesečne na Slikama od 46 do 50. U Tablicama 5 i 6 prikazane su sve proračunate statističke veličine.

5. Zaključci

Razvoj EMEP modela uključuje složene meteorološke efekte čija važnost progresivno raste sa horizontalnom rezolucijom modela. Jedan od tih složenih meteoroloških efekata je i turbulencija, a u ovom radu implementirana je i testirana shema za parametrizaciju vertikalne turbulentne difuzije, $K(z)$, kao i visine graničnog sloja u EMEP modelu. Budući da su procesi u atmosferskom kemijskom modelu nelinearni, bilo je nužno prethodno evaluirati $K(z)$ sheme na LES (DATABASE64; Esau i Zilitinkevich, 2006) i eksperimentalnim skupovima podataka (FLOSII i CASES99; Mahrt i Vickers, 2006). Kako ne postoji jedinstvena mjera za procjenu rada modela jednako kao ni najbolja evaluacijska metoda, preporuka je da se koristi čitav niz različitih mjera za ocjenu rada modela (Chang i Hanna, 2003).

Daljnja evaluacija temeljila se na r i *BIAS* vrijednostima proračunatih između modeliranih i mjerenih vrijednosti na svim raspoloživim EMEP postajama tijekom 2001. godine (Jeričević i sur., 2009). U obzir su uzete ustanovljene nepouzdanosti i nereprezentativnosti određenih mjerenja kako bi se mogle procijeniti mogućnosti modela da simulira transport i disperziju različitih kemijskih elemenata. Svakako treba napomenuti da je *BIAS* u modelu samo opća mjera budući da je vrlo osjetljiva na promjene u parametrizacijama te ne mora nužno odražavati poboljšanja kao posljedicu promjena u shemama parametrizacija. Stoga su glavni zaključci utemeljeni na promjenama u iznosu koeficijenta korelacije za NO_2, SO_2 i SO_4^{-2} koje su nastale kao rezultat promjena u parametrizacijskim shemama modela. Nadalje, modelirane visine AGS-a proračunate EMEP modelom uspoređene su sa visinama određenima iz radiosondažnih mjerenja sa 24 postaje u Europi (Tablica 2) tijekom siječnja i srpnja 2001. godine kao i sa satnim visinama AGS-a određenim iz satnih podataka sa Cabauw tornja. Primjenjen je standardni z-test (Pavlić, 1988) kako bi se ocijenila signifikantnost poboljšanja koeficijenta korelacije dobivenih implementacijom novih shema u model. Primjenjivost z-testa na ovu vrstu podataka je upitna budući da inicijalni uvjeti nisu zadovoljeni a to su da analizirani podaci podliježu normalnoj razdiobi te međusobna nezavisnost varijabli (Fox, 1980; Willmott, 1982). Svakako da ovaj postupak nije u potpunosti neutemeljen i promjene u koeficijentu korelacije se mogu komparativno promatrati, a informacija o nivou signifikantnosti je značajna. Daljnja evaluacija rađena je na raspoloživim mjerenjima ^{222}Rn u Europi budući da je ^{222}Rn kemijski nereaktivan i posjeduje relativno dugo vrijeme poluraspada od 3.8 dana odličan je element za analizu dinamičkih svojstava atmosfere. Simulacije ^{222}Rn EMEP modelom rađene su za 2005. i 2006. godinu i uspoređene sa odgovarajućim mjerenjima na postajama: Cabauw, Angus, Freiburg and Schauinsland u svrhu evaluacije vertikalnog miješanja u modelu. Također, nova shema višeg reda zatvaranja, tzv. lokalna shema, koja se temelji na ukupnoj turbulentnoj energiji (Mauritsen i sur., 2007) je implementirana i analizirana u EMEP modelu (Jeričević i sur., u pripremi). Nelokalne $K(z)$ sheme, O'Brienova i Grisogonova, evaluirane su na ^{222}Rn podacima pomoću: r, srednje apsolutne pogreške ili odstupanja (*MAE*), srednje kvadratne pogreške (*MSE*) i drugog korijena srednje kvadratne pogreške (*RMSE*).

Glavni zaključci su:

- EMEP model na većini analiziranih postaja pokazuje umjereno poboljšanje u $r(NO_2)$ i $r(SO_2)$ vrijednostima i manje poboljšanje za $r(SO_4^{2-})$ primjenom Grisogonove metode. Tako je $r(NO_2)$ povećan za oko 30% na 51% analiziranih postaja, dok $r(SO_2)$ s primjenjenom Grisogonove metode bilježi povećanje sa 10% sve do 50% na 54% postaja. Za sulfat zabilježen je manji porast u $r(SO_4^{2-})$ vrijednostima od 5 do 10%. Godišnji grafovi raspršenja između mjerenih i modeliranih dnevnih površinskih koncentracija na svim raspoloživim postajama, osim onih sa utvrđenom visokom nepouzdanosti, pokazuju poboljšanja u koeficijentu korelacije od 0.63 do 0.65 za NO_2, i od 0.55 do 0.57 za SO_2 sa Grisogonovom shemom. Za SO_4^{2-} koeficijent korelacije je oko 0.61 za obje sheme.
- Na temelju LES podataka utvrđeno je da je Grisogonova shema manje difuzivna što je važna karakteristika naročito u stabilnim atmosferskim uvjetima. Ustanovljeno je da Grisogonova shema daje bolje rezultate od O'Brienove sheme u stabilnim atmosferskim uvjetima (Jeričević and Večenaj, 2009). Predložena Grisogonova shema se preporučuje u daljnjim primjenama zbog svojih znanstvenih i tehničkih predosti (sve dok govorimo o nelokalnim shemama prvog reda zatvaranja parametrizacije turbulencije) budući da zahtjeva dvije ulazne varijable, umjesto četiri koje su potrebne kod O'Brienove metode. U praktičnoj primjeni npr. u modelima kakvoće zraka, obje metode ovise o kvaliteti ulaznih polja koja se dobivaju iz numeričkog prognostičkog meteorološkog modela kao i o prostorno-vremenskoj rezoluciji u modelu. Stoga će poboljšanja izvedbe samog numeričkog prognostičkog meteorološkog modela zasigurno rezultirati razlikama i vjerojatnim poboljšanjima u prostorno vremenskoj razdiobi onečišćenja.

- Postaje koje su pod utjecajem lokalnih emisijskih izvora, kao i planinske postaje, ne pokazuju značajnu osjetljivost na promjenu parametrizacijske sheme u modelu. Na tim je postajama iznos odstupanja od mjerenja, odnosno pogreške, mnogo veći od iznosa promjene nastale kao rezultat promjena u $K(z)$ shemi u modelu. Ovi rezultati upućuju na to da su bolja horizontalna rezolucija jednako kao i realnije emisije u modelu potrebne kako bi mogao uspješnije simulirati transport onečišćenja u uvjetima kompleksne orografije i pod utjecajem lokalnih izvora.
- Visina graničnog sloja, H, proračunata u EMEP modelu dobro se slaže s visinama procijenjenim iz radiosondažnih mjerenja iz različitih postaja u Europi. EMEP model dobro reproducira prostornu i vremensku varijabilnost od H, sa r od 0.7 do 0.9 u konvektivnim atmosferskim uvjeti ma, dok r varira od 0.4 do 0.6 u stabilnim uvjetima za obje sheme AGS-a. Nova shema koja se temelji na Ri_B broju postiže bolje rezultate u stabilnim uvjetima u usporedbi sa operativnom shemom utemeljenom na Blackadarovim $K(z)$ profilima na što ukazuju i značajno niže *BIAS* vrijednosti. Rezultati usporedbe između modeliranih i H procjenjenih iz mjerenja na Cabauw tornju ukazuju na sustavno poboljšanje novom AGS shemom, naročito u hladnijem dijelu godine (Slika 23).
- Srednje mjesečne ^{222}Rn vrijednosti ukazuju na značajne sezonske varijacije u koncentracijama ^{222}Rn, tijekom hladnijeg dijela godine od 2 do 3 puta većima od onih u toplijem dijelu godine. Najniže vrijednosti ^{222}Rn izmjerene su na Angus tornju dok su u Freiburgu u Njemačkoj ^{222}Rn koncentracije najviše.
- U stabilnim atmosferskim uvjetima vertikalno miješanje proračunato sa TTE shemom je bilo izrazito slabo, a rezultirajuće koncentracije ^{222}Rn su bile značajno više od onih dobivenih sa Grisogonovom i O'Brienovom metodom. Više koncentracije ^{222}Rn dobivene sa TTE shemom su se zadržale u plitkom sloju uz površinu zemlje, debljine oko 50 m dok je vertikalno miješanje sa druge dvije sheme bilo mnogo intenzivnije čime su se veće koncentracije transportirale na veće visine.
- Ustanovljeno je dobro slaganje mjerenih i modeliranih koncentracija ^{222}Rn naročito na Cabauw i Angus tornjevima. Na podacima Angus tornja u godini 2006. dobiveno je r = 0.4 - 0.72, a za Cabauw na 20 m r = 0.7 - 0.8, dok su na 200 m koeficijenti korelacije najviši među svim analiziranim postajama r = 0.6 - 0.8. Freiburg u 2005. godini ima r = 0.5 - 0.7 a Schauinsland, koji je planinska postaja, r = 0.2 - 0.6. Prema vrijednostima

koeficijenta korelacije utvrđeno je manje poboljšanje za Cabauw i Angus sa Grisogonovom metodom dok to nije bio slučaj na Njemačkim postajama.

Rezultati ovog rada na evaluaciji parametrizacijskih shema modeliranja turbulencije u atmosferskom kemijskom modelu EMEP predstavljaju temelj budućem razvoju hrvatskih kapaciteta u modeliranju kakvoće zraka.

9. Curriculum vitae

Name **Amela Jeričević**

Personal Information

Maiden Name:	Peljto
Date of Birth:	28 Jun 1973.
Place of Birth	Brčko, Bosnia and Herzegovina
Marital Status	Married, two children
Citizenship:	Croatian
Address:	HR – 10 000 Zagreb, Gruška 18, Croatia
e-mail:	jericevic@cirus.dhz.hr
Phone:	+385 1 4565 787
Fax:	+385 1 1 4565 630

Education

1993 – 1999:	University of Zagreb/ Faculty of natural Sciences/ Department of physic, /Meteorology
March 1999:	dipl. Ing, Physicist / Meteorologist Thesis: 'Trajectory computation with the method of Chen and Smith'
2002:	Postgraduate: field of study: modelling, trajectory studies, mixing height determination from NWP model in urban areas
2005:	Master of Sc. / Meteorologist Thesis: 'Atmospheric boundary layer in urban conditions'
2006:	started a PhD at the University of Zagreb/ Faculty of natural Sciences/ Department of physic, /Meteorology

Languages English (excellent), Italian (good)

Professional Experience

Meteorological and Hydrological Service-permanent position

2009- Head of Air Quality Research Department, Air Quality Service, Meteorological and Hydrological Service of Croatia, Zagreb, Croatia.

2008-2009 Senior Meteorologist Research Advisor, Air Quality Unit, Meteorological Research and Development Departement, Meteorological and Hydrological Service of Croatia, Zagreb, Croatia.

2005-2008 Meteorologist Research Advisor, Air Quality Unit, Meteorological Research and Development Departement, Meteorological and Hydrological Service of Croatia, Zagreb, Croatia.

2001-2005 Meteorologist Research Assistant, Air Quality Unit, Meteorological Research and Development Departement, Meteorological and Hydrological Service of Croatia, Zagreb, Croatia.

Andrija Mohorovičić Geophysical Institute-teaching experience

2006-: Meteorological Practicum I-WMO, WWW, meteorological data codes: SYNOP, TEMP, BUFFER etc. (100% of time)

Meteorological Practicum II – Introduction to numerical modeling, senior undergraduate level (30% of time)

Other

2008: Vice chair of the HARMO12 Organizing committee

2009: Member of the HARMO13 Scientific committee

2009: President of the Croatian Meteorological Society

Additional Qualifications

Courses on C/C++ programming, UNIX/Linux, Trainings on communication skills, human resource management, presentation, planning and organization

Projects:

National Department of science and technology.

2001-2005 Storms and natural disasters in Croatia -investigator

2006-2009 Storms and natural disasters in Croatia-ongoing project-investigator

2006-2009 Air quality over complex topography-investigator

International projects:

CARDS 2001 EU project : Public service reform program

2006-2009 High Resolution Environmental Modelling and Evaluation Programme for Croatia, EMEP4HR (2006-2009)-investigator

2009-2010 EU Phare 2006 Twinning Pr Establishment of Air Quality Monitoring and Management System in Croatia

Additional Professional Memberships

2001 - Croatian Meteorological Society

2007 – EURASAP

2009- Member of the HARMO13 scientific committee

Congress and Workshop Attendance

2002, ALATNET Seminar on the Numerical Methods and NWP applications, 27 May – 6 Jun, Kranjska Gora, Slovenia

2002, 12th ALADIN Workshop, 3-6 Jun, Medulin, Croatia

2002, VII'th International symposium in waste management, 13 -15 November Zagreb, Croatia

2003, Air Pollution Issues & Simulation Modeling, 13-17 September, Catania, Italy Organization: Wessex Institute of Technology, UK, Teacher: prof. Paolo Zannetti

2004, 9th International Conference on Harmonization within Atmospheric Dispersion Modelling for Regulatory purposes, 1-4 June, Garmisch-Partenkirchen,Germany.

2004, IPA Workshop: 'Introduction in management of human sources in public service', 13-14 July, Zagreb.

2004, IPA Workshop: 'Introduction in basic principles of public service management', 15-16 July, Zagreb.

2004, ECMWF Seminar. 'Recent developments in numerical methods for atmospheric and ocean modelling', 6-10 September, Reading, UK.

2004, Environmental Odour Management, European Conference, November 17-19, Cologne, Germany.

2006, NATO Security through Science Programme, Advanced Research Workshop on Atmospheric Boundary Layers: Modelling and Applications for Environmental Security, 18-22 April, Dubrovnik, Croatia.

2006, 2nd scientific symposium: Natural history researches of the Rijeka region, 14-17 Jun, Rijeka Croatia.

2007, 6'th International Conference on Urban Air Quality, 27-29 March, Limassol, Cyprus.

2007, AMGI/EURASAP workshop, Air quality Management, Monitoring, Modeling and Health Effects, 24-26, May, Zagreb, Croatia.

2007, International course of lectures 'Geophysical turbulence and boundary layers: nature, theory and role in Earth's systems', 27 May-1 Jun, Helsinki, Finland.

2007, 11th International Conference on Harmonisation within Atmospheric Dispersion Modelling for Regulatory Purposes, 2-5 July, Cambridge, United Kingdom

2007, Summer School: 'Transport and Chemistry in Air Pollution Modeling', 17-21 September, Castro Marina, Italy

2008, 9th meeting of the Task Force on Measurements and Modelling, Bordeaux, France, 23-25 April 2008.

2008, Task Force on Hemispheric Transport of Air Pollution under the LRTAP Convention, 7-11 April 2008, Rome, Italy

2008, Atmospheric Chemistry, Climate, and Transboundary Air Pollution Workshop',Washington, SAD, June, 2008

2008, 12th Conference on Harmonisation within Atmospheric Dispersion Modelling for Regulatory Purposes, 6.-9. October 2008, Cavtat, Croatia.

2008, Task Force on Measurements and Modelling: 1st Open source Unified EMEP model training course, 13th October 2008, Oslo, Norway.

2008, Task Force on Measurements and Modelling Workshop: Bridging the modelling scales for a better assessment of air pollution, 14-15th October 2008, Oslo, Norway.

2009, 7th International Conference on Air Quality - Science and Application (Air Quality 2009), Istanbul, 24-27 March 2009, Turkey.

10. List of publications

CC publiations

1. Jeričević, A., Fagerli, H., and Grisogono, B.: Local and non-local vertical diffusion schemes evaluation with simulation of ^{222}Rn regional transport, in preparation for Atmos. Chem. Phys., 2009.
2. Jeričević, A., Kraljević, L. Grisogono, B., Fagerli, H., and Večenaj, Ž.: Parameterization of vertical diffusion and the atmospheric boundary layer height determination in the EMEP model, Atmos. Chem. Phys. Discuss, 9, 9597-9645, 2009.(tentatively accepted)
3. Prtenjak, M. T., A. Jeričević, L. Kraljević, I. H. Bulić, T. Nitis, and Z. B. Klaić: Exploring atmospheric boundary layer characteristics in a severe SO_2 episode in the north-eastern Adriatic, Atmos. Chem. Phys., 9, 4467-4483, 2009.
4. Jeričević, A., and Večenaj, Ž.: Improvement of vertical diffusion analytic schemes under stable atmospheric conditions, Boundary- Layer Meteorol., 131, 293-307, 2009.
5. Grisogono, B., Kraljević, L., and Jeričević, A.: The low-level katabatic jet height versus Monin-Obukhov height, Quart. J. Roy. Met. Soc., 133, 2133-2136, 2008.
6. Jeričević, A. i Grisogono, B.: The critical bulk Richardson number in urban areas: verification and application in a NWP model, Tellus A 58, 19-27, 2006.

Publication in other journals with international review

1. Jeričević, A., Kraljević, L., Vidič, S., and Tarrason, L.: Project description: High Resolution Environmental Modelling and Evaluation Programme for Croatia (EMEP4HR), Geofizika, 24, 137-143, 2007.
2. Jeričević, A., Čanić, Š.K., Tomšić, D., Žibrat, Z., Kraljević L. and Grisogono B.: Sodar and radio sounding measurements at Zadar, Croatia, Croatian Meteorological Journal, 40, 312-315, 2005.
3. Kos, I., Belušić, D., Jeričević, A., Horvath, K., Koračin, D., and Telišman Prtenjak, M.: A Description of Atmospheric Lagrangian Particle Stochastic (ALPS) Dispersion Model, Geofizika, 21, 37-52, 2004.

4. Jeričević, A., Špoler Čanić, K., and Vidič, S.: The prediction of mixing height and stability in complex orography, Croatian Meteorological Journal, 39, 3-14, 2004.
5. Peljto (Jeričević) A., and Klaić B. Z: Accidental release of hydrogen sulphide in Nagilengel, Hungary on November 14, 1998- A trajectory study, Geofizika, 16-17, 43-51, 1999-2000.

Publication in Conference books

1. Jeričević, A., Grisogono, B., and Tarrason, L.: Implementation and verification of vertical diffusion scheme in the EMEP model, Proceedings of the 12th HARMO conference, Cavtat, Croatia, 6-9 October 2008.
2. Kraljević, L., Belušić, D., Bencetić Klaić, Z., Bennedictow, A., Fagerli, H., Grisogono, B., Jeričević, A., Mihajlović, D., Špoler Čanić, K., Tarrason, L., Valiyaveetil, S., Vešligaj, D., and Vidič, S.: Application of EMEP Unified model on regional scale – EMEP4HR, Proceedings of the 12th HARMO conference, Cavtat, Croatia, 6-9 October, 2008.
3. Bencetić Klaić, Z., Belušić, D., Jeričević, A., and Cvitaš, T.: High ozone episode at Zavižan, Croatia during 17 – 19 July 1998, Proceedings of the 12th HARMO conference, Cavtat, Croatia, 6-9 October, 2008.
4. Jeričević A., Kraljević, L., and Vidič, S.: High resolution environmental modelling and evaluation programme for Croatia (EMEP4HR) // Proceedings of the 11th International Conference on Harmonisation within Atmospheric Dispersion Modelling for Regulatory Purposes / Carruthers David J. and McHugh Christine A. (ur.). Cambridge: Suitable Design Limited, 83-87, 2007.
5. Jeričević A.: Developement of the atmospheric lagrangian particle stohastic (ALPS) dispersion model, AMGI/EURASAP Workshop on the Air Quality Management, Monitoring, Modeling, and Effects, Zagreb, May 24 - 26, 2007, Abstracts / Builtjes, Peter ; Bencetić Klaić, Zvjezdana 13-13, 2007.
6. Jeričević, A.: Vertical diffusion verification in the EMEP model, AMGI/EURASAP Workshop on the Air Quality Management, Monitoring, Modelling, and Effects, Zagreb, May 24 - 26, 2007, Abstracts / Builtjes, Peter ; Bencetić Klaić, Zvjezdana 13-13, 2007.
7. Jeričević, A.: Quasy-steady state equilibrium boundary layer height determination in urban conditions, Proceedings of abstracts of 6th International conference on Urban Air Quality,

Ranjeet S Sokhi and marins Neophytou (Ed),University of Hertfordshire (pub), Cyprus, 27-29 March 2007. (299186-Crosby), 2007.

8. Jeričević, A., and Špoler Čanić, K.: Pollution episodes prediction based on stability parameters in the Rijeka area, Book of Abstracts: Natural History Research of the Rijeka Region / Arko-Pijevac, Milvana; Kružić, Borut ; Kovačić, Maredo (ed.), Rijeka, 41-41, 2006.
9. Jeričević, A.: The possibility of urban mixing height estimations with the bulk Richardson method in stable boundary layer conditions, NATO Security through Science Programme, Advanced Research Workshop on Atmospheric Boundary Layers: Modelling and Applications for Environmental Security, Dubrovnik, Croatia 18-22 April 2006.
10. Špoler Čanić, K., and Jeričević, A.: Modelled concentrations of air pollutant depending on input data, Proceedings of the 10th International Conference on "Harmonization within Atmospheric Dispersion Modeling for Regulatory Purposes" / A. N. Skouloudis, P. Kassomenos, J. Bartzis (ed.), Heraklion, September, 255-259, 2005.
11. Belušić, D., Koračin, D., Kos, I., Jeričević, A., and Horvath, K.: Simulations of the turbulence and dispersion processes in a coastal region. 11th Conference on Mountain Meteorology and the Annual Mesoscale Alpine Program (MAP), Bartlett, NH, USA, 21-25 Jun, 2004.
12. Jeričević, A., and Grisogono, B.: Mixing height computation from a numerical weather prediction model. Proceedings form 9th Int. Conf. On Harmonization within Atmospheric Dispersion Modelling for Regulatory Purposes, Garmisch-Partenkirchen, Germany, 1-4 Jun 265-269, 2004.